

Stefanos Aretakis

# Dynamics of Extremal Black Holes

# **SpringerBriefs in Mathematical Physics**

Volume 33

## **Series editors**

Nathanaël Berestycki, Cambridge, UK

Mihalis Dafermos, Princeton, USA

Tohru Eguchi, Tokyo, Japan

Atsuo Kuniba, Tokyo, Japan

Matilde Marcolli, Pasadena, USA

Bruno Nachtergaele, Davis, USA

SpringerBriefs are characterized in general by their size (50–125 pages) and fast production time (2–3 months compared to 6 months for a monograph).

Briefs are available in print but are intended as a primarily electronic publication to be included in Springer's e-book package.

Typical works might include:

- An extended survey of a field
- A link between new research papers published in journal articles
- A presentation of core concepts that doctoral students must understand in order to make independent contributions
- Lecture notes making a specialist topic accessible for non-specialist readers.

**SpringerBriefs in Mathematical Physics** showcase, in a compact format, topics of current relevance in the field of mathematical physics. Published titles will encompass all areas of theoretical and mathematical physics. This series is intended for mathematicians, physicists, and other scientists, as well as doctoral students in related areas.

More information about this series at <http://www.springer.com/series/11953>

Stefanos Aretakis

# Dynamics of Extremal Black Holes

 Springer

Stefanos Aretakis  
University of Toronto  
Toronto, ON, Canada

ISSN 2197-1757 ISSN 2197-1765 (electronic)  
SpringerBriefs in Mathematical Physics  
ISBN 978-3-319-95182-9 ISBN 978-3-319-95183-6 (eBook)  
<https://doi.org/10.1007/978-3-319-95183-6>

Library of Congress Control Number: 2018948606

© The Author(s) 2018

This work is subject to copyright. All rights are reserved by the Publisher, whether the whole or part of the material is concerned, specifically the rights of translation, reprinting, reuse of illustrations, recitation, broadcasting, reproduction on microfilms or in any other physical way, and transmission or information storage and retrieval, electronic adaptation, computer software, or by similar or dissimilar methodology now known or hereafter developed.

The use of general descriptive names, registered names, trademarks, service marks, etc. in this publication does not imply, even in the absence of a specific statement, that such names are exempt from the relevant protective laws and regulations and therefore free for general use.

The publisher, the authors and the editors are safe to assume that the advice and information in this book are believed to be true and accurate at the date of publication. Neither the publisher nor the authors or the editors give a warranty, express or implied, with respect to the material contained herein or for any errors or omissions that may have been made. The publisher remains neutral with regard to jurisdictional claims in published maps and institutional affiliations.

This Springer imprint is published by the registered company Springer Nature Switzerland AG  
The registered company address is: Gewerbestrasse 11, 6330 Cham, Switzerland

*To my children*

# Preface

*Black holes* are one of the most celebrated predictions of general relativity. Understanding the dynamics of black holes is a problem of paramount importance in mathematical physics. A positive resolution of the *black hole stability conjecture* would establish the relevance of black holes from a theoretical point of view. For this reason, black hole dynamics have been intensively studied from a rigorous mathematical point of view during the past 15 years and significant progress has been made toward the full resolution.

The present Brief focuses on the dynamics of a special class of black holes, namely, *extremal black holes*. These are, roughly speaking, either maximally rotating or maximally charged. Astronomical observations suggest that nearly 70% of all stellar black holes are near extremal. Hence, even though extremal black holes are inherently nongeneric, a study of their dynamics is of great importance in advancing our knowledge of the structure of the universe.

The ultimate aim of this Brief is to introduce the reader to the fascinating world of extremal black holes. Specifically, the aim is to

1. present the main mathematical difficulties concerning the dynamics of extremal black holes,
2. present in a unified, nontechnical, and illustrative fashion the main recent results and techniques,
3. provide a discussion of the outstanding open problems and offer insights for potential resolutions, and
4. provide common ground for communication between different scientific communities including those of pure mathematicians, theoretical physicists, and astrophysicists.

Before we further discuss the dynamics of extremal black holes, let us summarize the reasons why extremal black holes are important in the following disciplines:

- *astronomy*: according to an abundance of astronomical observations, near-extremal black holes appear to be ubiquitous in the universe. Such observations concern stellar black holes and supermassive black holes in the center of galaxies;
- *high energy physics*: extremal black holes appear in the study of supersymmetric theories of gravity, black hole thermodynamics, and of quantum descriptions of gravity;
- *classical general relativity*: they saturate various geometric inequalities concerning the mass, angular momentum, and charge. Furthermore, they have very intriguing dynamical properties with no analog in sub-extremal black holes.

The latter intriguing dynamical properties of extremal black holes is the object of study of this Brief. It has been shown that scalar perturbations of extremal black holes decay slowly, whereas higher order derivatives grow in time. This scalar instability was first discovered by the author in 2010 and has since been investigated and extended by various research groups in recent years. We remark that this result is in stark contrast with the case of sub-extremal black holes for which it has been rigorously shown that scalar perturbations and their derivatives of all orders decay in time.

A synopsis of the brief is the following: Chap. 1 provides a self-contained introduction to Lorentzian geometry presenting topics such as the Einstein equations, trapped surfaces, and black holes. Chapters 2 and 3 present in a nontechnical language the state of the art for the dynamics of extremal Reissner–Nordström and extremal Kerr, respectively. Chapters 4 and 5 provide an overview of the main techniques and ideas of the proofs. The aim here is to prepare the reader for studying the papers where the complete proofs can be found. As we shall see, the asymptotic behavior of perturbations is governed by conservation laws on the event horizon and on null infinity. For this reason, the final chapter, Chap. 6, develops a unifying theory of conservation laws along null hypersurfaces in general Lorentzian manifolds.

Toronto, Canada

Stefanos Aretakis

# Acknowledgements

I would like to thank my wife Miji, my father Demetrios, and my mother Maria for their continuous support. I am eternally indebted to my mentor Mihalis Dafermos for all the help he has provided me during the last 10 years. I would like to cordially thank Sergiu Klainerman, Igor Rodnianski, Harvey Reall, and Spyros Alexakis for their support and interest in this work. This Brief would have not been possible without the help of my collaborators Dejan Gajic and Yannis Angelopoulos. Special thanks go to my friends and colleagues Georgios Moschidis, Gustav Holzegel, Yakov Shlapentokh-Rothman, Volker Schlue, Grigorios Fournodavlos, and Stefan Czimek. I would like to thank the four institutions that have hosted me since the beginning of my career as a mathematician: The University of Cambridge (UK), Princeton University (USA), the Institute for Advanced Study (USA), and currently the University of Toronto (CA). I would also like to thank my Professors at the University of Patras (GR) for guiding me during my undergraduate studies there. Finally, I would like to thank the National Science Foundation of USA, the Natural Sciences and Engineering Research Council of Canada, the Sloan Foundation, and the Government of Ontario for their generous support and funding.

# Contents

## Part I Stability and Instability of Extremal Black Holes

<b>1</b>	<b>Introduction to General Relativity and Black Hole Dynamics</b> . . . . .	3
1.1	Lorentzian Geometry and Causality . . . . .	3
1.1.1	Causal Theory . . . . .	3
1.1.2	Global Hyperbolicity . . . . .	8
1.1.3	Null Geometry . . . . .	10
1.1.4	Optical Functions . . . . .	13
1.2	The Einstein Field Equations . . . . .	14
1.3	Trapped Surfaces . . . . .	15
1.4	Null Infinity . . . . .	16
1.5	Black Holes . . . . .	18
1.5.1	Definitions, Diagrams and Examples . . . . .	18
1.5.2	The Surface Gravity of the Event Horizon . . . . .	21
1.5.3	Extremal Versus Sub-extremal Black Holes . . . . .	21
1.5.4	The Redshift Effect . . . . .	22
1.6	The Black Hole Stability Problem . . . . .	24
1.7	The Wave Equation on Black Hole Exteriors . . . . .	25
1.8	Price's Asymptotics for Sub-extremal Black Holes . . . . .	26
1.8.1	Price's Heuristics . . . . .	26
1.8.2	The Newman–Penrose Constants $I_0$ and $I_0^{(1)}$ . . . . .	27
1.8.3	The Precise Late-Time Asymptotics . . . . .	29
1.9	Physical Importance of Extremal Black Holes . . . . .	30
	References . . . . .	32
<b>2</b>	<b>Extremal Reissner–Nordström Black Holes</b> . . . . .	37
2.1	The Geometry of ERN . . . . .	37
2.1.1	The ERN Metric . . . . .	37
2.1.2	Penrose Diagrams . . . . .	40

2.1.3	Global Properties of ERN	45
2.1.4	The Couch–Torrence Conformal Inversion	46
2.2	The Horizon Instability of ERN	48
2.2.1	Conservation Laws Along the Event Horizon	49
2.2.2	Non-decay and Blow-up for Transversal Derivatives	50
2.3	The Precise Late-Time Asymptotics	51
2.3.1	Scalar Perturbations of Type <b>A</b> , <b>B</b> , <b>C</b> , and <b>D</b>	52
2.3.2	Review of Physics Literature	53
2.3.3	The New Horizon Charge $H_0^{(1)}[\psi]$	55
2.3.4	Asymptotics for Type <b>C</b> Perturbations	56
2.3.5	Asymptotics for Type <b>A</b> Perturbations	57
2.3.6	Asymptotics for Type <b>B</b> Perturbations	57
2.3.7	Asymptotics for Type <b>D</b> Perturbations	58
2.3.8	Asymptotics for Higher Order Derivatives	59
2.3.9	Summary of the Precise Asymptotics	60
2.4	Applications and Additional Remarks	62
2.4.1	Measuring the Horizon Hair from Null Infinity	62
2.4.2	Singular Time Inversion and the New Horizon Charge	63
2.5	The Murata–Reall–Tanahashi Spacetimes	64
2.6	The Interior of ERN and Strong Cosmic Censorship	66
	References	68
<b>3</b>	<b>Extremal Kerr Black Holes</b>	71
3.1	The Geometry of EK	71
3.2	Stability and Instability of EK for Scalar Perturbations	74
3.3	The Lucietti–Reall Gravitational Instability of EK	76
3.4	The Casals–Gralla–Zimmerman Work on EK	78
3.5	Open Problems	79
	References	80
<b>Part II An Overview of the Proofs</b>		
<b>4</b>	<b>Asymptotics for Extremal Reissner–Nordström</b>	85
4.1	Introduction to the Vector Field Method	85
4.2	Conservation of the $J^T$ -Flux	86
4.3	The Morawetz Estimate	87
4.4	The $T$ , $P$ , $N$ Hierarchical Vector Fields	87
4.5	The Trapping Effect on the Event Horizon	90
4.6	Horizon Localized and Infinity Localized Hierarchies	91
4.6.1	The Conformal Fluxes $C_{N_r^{\mathcal{H}}}$ and $C_{N_r^{\mathcal{I}}}$	91
4.6.2	Commutated Hierarchies in the Regions $\mathcal{A}^{\mathcal{H}}$ and $\mathcal{A}^{\mathcal{I}}$	93
4.6.3	Improved Hierarchies for $\ell = 0, 1$	95

- 4.7 Energy and Pointwise Decay . . . . . 98
  - 4.7.1 Decay for the Fluxes  $J_{\Sigma_r}^T$ ,  $C_{N_r^+}$  and  $C_{N_r^-}$  . . . . . 98
  - 4.7.2 Hardy Inequalities . . . . . 100
  - 4.7.3 An Elliptic Estimate for  $\ell \geq 1$  and Improved Decay . . . . . 101
  - 4.7.4 Summary of Energy and Pointwise Decay Rates . . . . . 102
- 4.8 Late-Time Asymptotics . . . . . 103
  - 4.8.1 A Priori Remarks . . . . . 103
  - 4.8.2 The Main Difficulties . . . . . 104
  - 4.8.3 Asymptotics for Type **C** Perturbations . . . . . 105
  - 4.8.4 Asymptotics for Type **A** Perturbations . . . . . 108
  - 4.8.5 Asymptotics for Type **B** Perturbations . . . . . 111
  - 4.8.6 Asymptotics for Type **D** Perturbations . . . . . 111
  - 4.8.7 Asymptotics for Higher Order Derivatives . . . . . 112
- References . . . . . 113
- 5 Decay Estimates for Extremal Kerr . . . . . 115**
  - 5.1 Axisymmetry Versus Superradiance . . . . . 115
  - 5.2 The Carter Separation and Frequency Localization . . . . . 116
    - 5.2.1 The Killing Tensor  $K$  and the Symmetry Operator  $Q$  . . . . . 116
    - 5.2.2 Carter’s Separability for the Wave Equation . . . . . 116
    - 5.2.3 The Cut-off  $\xi_\tau$  and the Renormalized Carter Equation . . . . . 119
    - 5.2.4 Properties of the Potential  $V$  . . . . . 120
  - 5.3 Physical Space–Fourier Space Correspondence . . . . . 121
  - 5.4 Frequency Localized Morawetz Estimates . . . . . 121
  - 5.5 Energy and Pointwise Decay in Time . . . . . 123
- References . . . . . 124
- 6 A Theory of Conservation Laws on Null Hypersurfaces . . . . . 125**
  - 6.1 The Geometry of Null Foliations . . . . . 125
  - 6.2 Conservation Laws for the Wave Equation . . . . . 127
  - 6.3 The Characteristic Gluing Problem . . . . . 128
  - 6.4 Necessary and Sufficient Conditions . . . . . 129
  - 6.5 Conservation Laws on Extremal Black Holes . . . . . 130
- References . . . . . 131

**Part I**  
**Stability and Instability of Extremal**  
**Black Holes**

# Chapter 1

## Introduction to General Relativity and Black Hole Dynamics



In this chapter we provide the general framework for curved spaces and introduce the notions of Lorentzian geometry which are necessary for understanding the mathematical aspects of general relativity and black hole dynamics. For exhaustive presentations we refer to [1–3].

### 1.1 Lorentzian Geometry and Causality

General relativity postulates that space and time are combined to form unified entities known as Lorentzian manifolds.

- A *Lorentzian manifold*  $(\mathcal{M}, g)$  is a differentiable manifold of dimension  $n + 1$ , endowed with a *Lorentzian metric*  $g$ , namely a differentiable assignment of a symmetric, non-degenerate bilinear form  $g_x$  with signature  $(-, +, \dots, +)$  in  $T_x\mathcal{M}$  at each  $x \in \mathcal{M}$ .

The theory of Lorentzian manifolds is known as *Lorentzian geometry*. The formulas in Riemannian geometry for geodesics, parallel transport, curvatures etc. carry over to Lorentzian geometry. We will mostly consider the case of four dimensions (that is,  $n = 3$ ) and we will assume that  $(\mathcal{M}, g)$  is *orientable*.

#### 1.1.1 Causal Theory

##### Basic Notions and Trichotomy of Directions

The fundamental aspect of Lorentzian metrics  $g$  is that, for each  $x \in \mathcal{M}$ ,  $g_x$  is not positive-definite on  $T_x\mathcal{M}$ . In fact, for each  $x \in \mathcal{M}$ , the linear space  $(T_x\mathcal{M}, g)$ <sup>1</sup> is

---

<sup>1</sup>For simplicity, we will drop the index and thus by  $g$  we will also mean  $g_x$ .

isometric to the Minkowski spacetime  $(\mathbb{R}^{3+1}, m)$  and therefore there exists a basis  $(E_0, E_1, E_2, E_3)$  of  $T_x\mathcal{M}$  such that

$$g(E_\alpha, E_\beta) = m_{\alpha\beta},$$

where  $m_{\alpha\beta}$  is the Minkowski diagonal matrix

$$m = \begin{pmatrix} -1 & 0 & 0 & 0 \\ 0 & +1 & 0 & 0 \\ 0 & 0 & +1 & 0 \\ 0 & 0 & 0 & +1 \end{pmatrix}.$$

Then, for any vector  $X \in T_x\mathcal{M}$  we have  $X = \sum_\alpha X^\alpha E_\alpha$  and thus

$$g(X, X) = -(X^0)^2 + (X^1)^2 + (X^2)^2 + (X^3)^2. \tag{1.1.1}$$

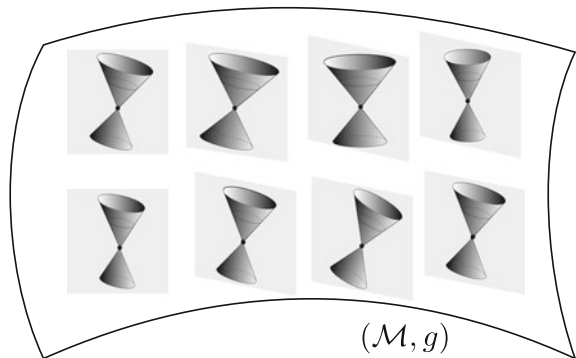
Note that unless  $(\mathcal{M}, g)$  is locally isometric to Minkowski space the frame  $(E_\alpha, \alpha = 0, 1, 2, 3)$  does not correspond to a coordinate frame. In view of (1.1.1), the Lorentzian metric  $g$  imposes a *trichotomy* on  $T_x\mathcal{M}$  as follows (Table 1.1):

**Table 1.1** Trichotomy of vectors in Lorentzian manifolds

$X \in T_x\mathcal{M}$	$g(X, X)$
<i>spacelike</i>	$>0$
<i>timelike</i>	$<0$
<i>null</i>	$=0$

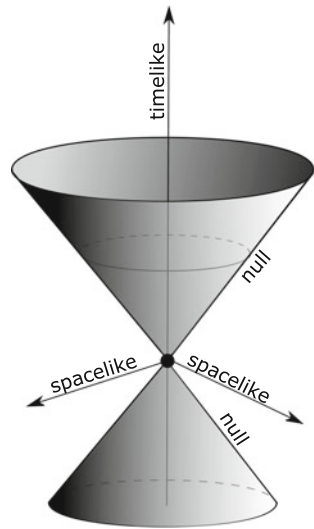
If  $X$  is either timelike or null, then it is called *causal*. By virtue of (1.1.1), all null vectors span a *double cone*  $C_x$  in  $T_x\mathcal{M}$  (with vertex at  $x$ ) the exact shape of which depends on the basis  $E_\alpha$  (Fig. 1.1).

**Fig. 1.1** The double null cone at each point in  $\mathcal{M}$



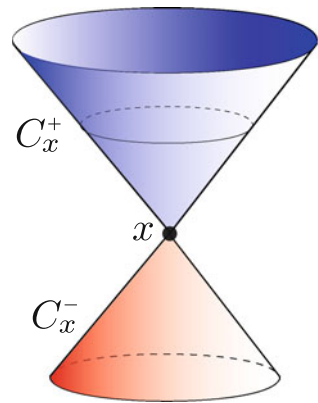
The interior  $\mathcal{I}_x$  of  $C_x$  consists of all timelike vectors at  $x$  and the exterior  $\mathcal{S}_x$  of  $C_x$  consists of all spacelike vectors at  $x$  (Fig. 1.2).

**Fig. 1.2** Timelike, null and spacelike vectors



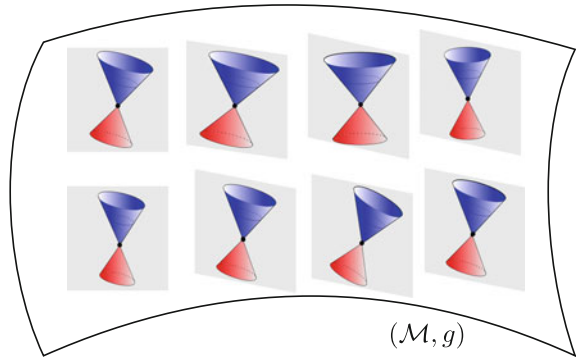
Note that  $\mathcal{S}_x$  is connected whereas  $\mathcal{I}_x$  has two connected components which we denote by  $\mathcal{I}_x^+$  and  $\mathcal{I}_x^-$ . Similarly, we can decompose  $C_x = C_x^+ \cup C_x^-$ , where  $C_x^+ = \partial\mathcal{I}_x^+$  and  $C_x^- = \partial\mathcal{I}_x^-$  (Fig. 1.3).

**Fig. 1.3** The future (blue) and the past (red) light cone at  $x$



- A *time-orientation* of  $(M, g)$  is a continuous choice of a positive component  $\mathcal{I}_x^+$  at each point in  $M$  (Fig. 1.4).

**Fig. 1.4** Time-orientation of  $(\mathcal{M}, g)$



From now on, we will only consider time-orientable Lorentzian manifolds. We define  $\mathcal{I}_x^+$  (resp.  $\mathcal{I}_x^-$ ) to be the set of *future-directed* (resp. *past-directed*) timelike (resp. *past-directed*) vectors at  $x$ . Similarly, we define  $C_x^+$  (resp.  $C_x^-$ ) to be the set of *future-directed* (resp. *past-directed*) null vectors at  $x$ .

### Causal Curves, Observers and Photons, Proper Time

We have so far provided causal characterizations of directions at each point. We will next provide causal characterizations of curves. We have the following definition

- A curve  $\alpha : I \rightarrow \mathcal{M}$  is called future-directed (resp. past-directed) timelike (resp. null) if the tangential vector  $\dot{\alpha}(t) \in T_{\alpha(t)}\mathcal{M}$  is future-directed (resp. past-directed) timelike (resp. null) at  $\alpha(t) \in \mathcal{M}$  for all  $t \in I$  (Fig. 1.5).

**Fig. 1.5** A future-directed timelike curve



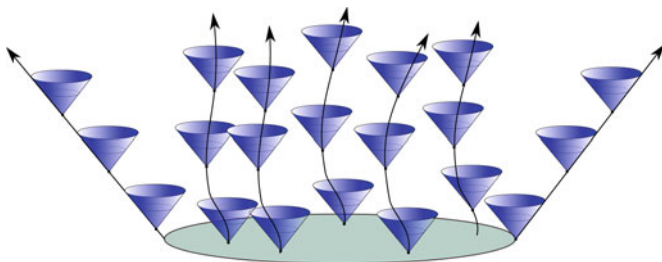
The worldline of an observer (resp. a light particle) is represented by a timelike (resp. null) curve. Freely falling observers (resp. photons) move on timelike (resp. null) geodesics.

The *proper time*  $\tau$  of an observer is defined to be the parametrization of its world-line  $\alpha$  such that  $g(\dot{\alpha}(\tau), \dot{\alpha}(\tau)) = -1$ . Null curves, on the other hand, by definition satisfy  $g(\dot{\alpha}(\tau), \dot{\alpha}(\tau)) = 0$  for all parametrizations. Nonetheless, we can still obtain distinguished parametrizations for null geodesics; indeed, we define the affine parametrization of a null geodesic  $\alpha$  to be such  $\nabla_{\dot{\alpha}}\dot{\alpha} = 0$ .

### Causal Future and Past of a Set

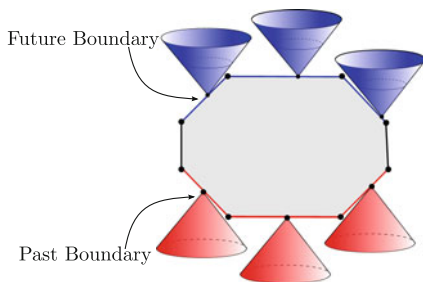
Let  $S \subset \mathcal{M}$  be a region in spacetime. We have the following definitions:

- The *causal future*  $\mathcal{J}^+(S)$  (resp. *causal past*  $\mathcal{J}^-(S)$ ) of  $S$  is defined to be the set of all points in  $\mathcal{M}$  which can be connected with a point of  $S$  through a future-directed (resp. past-directed) causal curve.
- The *chronological future*  $\mathcal{I}^+(S)$  (resp. *chronological past*  $\mathcal{I}^-(S)$ ) of  $S$  is defined to be the set of all points which can be connected with a point of  $S$  through a future-directed (resp. past-directed) timelike curve.<sup>2</sup>



### Causal Boundaries

Recall that the (topological) boundary  $\partial S$  of  $S$  is defined as follows  $\partial S = \overline{S} \cap \overline{\mathcal{M}/S}$ . We define the *future boundary*  $\partial^+ S$  (resp. *past boundary*  $\partial^- S$ ) of  $S$  to be the subset of  $\partial S$  which has the property that for all  $x \in \partial^+ S$  we have  $\mathcal{I}^+(x) \cap S = \emptyset$  (resp.  $\mathcal{I}^-(x) \cap S = \emptyset$ ).



Note that  $\partial^+(\mathcal{J}^+(S)) = \emptyset$  and  $\partial^-(\mathcal{J}^-(S)) = \emptyset$ .

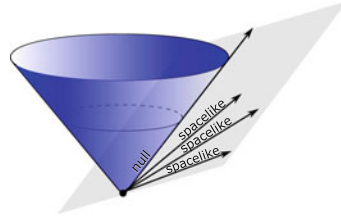
---

<sup>2</sup>Note that  $\mathcal{I}^+(x) \subset \mathcal{M}$  denotes the chronological future of  $x$  whereas  $\mathcal{I}_x^+ \subset T_x\mathcal{M}$  denotes the set of all future-directed timelike vectors in  $T_x\mathcal{M}$ .

## Causality and Orthogonality

Let  $x \in \mathcal{M}$ . Then we have the following orthogonality properties for causal vectors:

- If  $X \in T_x\mathcal{M}$  is timelike, then  $\langle X \rangle^\perp \subset T_x\mathcal{M}$  consists of spacelike vectors.



- If  $X \in T_x\mathcal{M}$  is null, then  $\langle X \rangle^\perp \subset T_x\mathcal{M}$  consists of spacelike vectors and the null line  $\langle X \rangle$ .

Here  $\langle X \rangle$  denotes the line spanned by the vector  $X$  and  $\langle X \rangle^\perp$  the orthogonal complement of  $\langle X \rangle$ . Note that two causal vectors are never orthogonal unless they are parallel and null.

## Submanifolds

Let  $\mathcal{N}$  be a submanifold of  $\mathcal{M}$ . Then  $\mathcal{N}$  is called:

- *spacelike*, if the induced metric  $g|_{T_x\mathcal{N}}$  is positive-definite for all  $x \in \mathcal{N}$ .
- *timelike*, if the induced metric  $g|_{T_x\mathcal{N}}$  has signature  $(-, +, +)$  for all  $x \in \mathcal{N}$ .
- *null*, if the induced metric  $g|_{T_x\mathcal{N}}$  is degenerate for all  $x \in \mathcal{N}$ .

Recall that a symmetric bilinear form  $g$  on a linear space  $V$  is called degenerate if there exists a vector  $X \in V$  such that  $g(X, Y) = 0$  for all  $Y \in V$ . By Sylvester's law of inertia, hypersurfaces  $(\mathcal{N}, g|_{\mathcal{N}})$  of co-dimension 1 can be characterized in terms of their normal (in  $\mathcal{M}$ ) vector field  $N$ . Indeed:

- A hypersurface  $\mathcal{N}$  is called spacelike, if the normal  $N_x$  at each point  $x \in \mathcal{N}$  is timelike.
- A hypersurface  $\mathcal{N}$  is called timelike, if the normal  $N_x$  at each point  $x \in \mathcal{N}$  is spacelike.
- A hypersurface  $\mathcal{N}$  is called null, if the normal  $N_x$  at each point  $x \in \mathcal{N}$  is null.

Note the normal  $N_x$  of null hypersurface, being orthogonal to itself, is also tangential to  $\mathcal{N}$ . This leads to very interesting properties of null hypersurfaces; see Sect. 1.1.3.

### 1.1.2 Global Hyperbolicity

The causal structure of Lorentzian manifolds might in some cases exhibit unphysical behavior. For example, there are Lorentzian manifolds with closed timelike curves. This kind of behavior is very pathological and so we want to impose conditions on the

spacetimes in order to preclude it. The main condition is that of *global hyperbolicity*. First we need the following definition

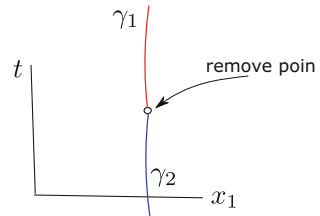
- An spacelike hypersurface  $H$  is a *Cauchy hypersurface* if every inextendible causal curve intersects  $\Sigma$  **exactly once**.

We next provide the definition of global hyperbolicity:

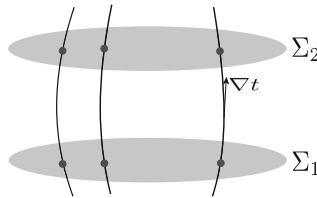
- A spacetime  $(\mathcal{M}, g)$  which possesses a Cauchy hypersurface is called *globally hyperbolic*.

The spacetime  $\mathbb{R}^{1+1}$  minus a point is not globally hyperbolic (Fig. 1.6)

**Fig. 1.6** The spacetime  $\mathbb{R}^{1+1}$  minus a point is not globally hyperbolic



The existence of a Cauchy hypersurface  $\Sigma$  is a global causal property. Any two Cauchy hypersurfaces  $\Sigma_1, \Sigma_2$  are homeomorphic.



- A globally hyperbolic spacetime  $\mathcal{M}$  with Cauchy hypersurface  $\Sigma$  is homeomorphic to  $\Sigma \times \mathbb{R}$ . In particular, there exists a global ‘time’ function  $t : \mathcal{M} \rightarrow \mathbb{R}$  such that the level sets  $\Sigma_\tau = \{t = \tau\}$  are Cauchy hypersurfaces and the vector field  $\nabla t$  is everywhere timelike. Furthermore, the hypersurfaces  $\Sigma_\tau$  foliate  $\mathcal{M}$ .

Global hyperbolicity plays a role similar to that of completeness of Riemannian manifolds.

- Let  $(\mathcal{M}, g)$  be a globally hyperbolic spacetime. Let also  $x, y \in \mathcal{M}$  with  $y \in \mathcal{I}^+(x)$ . Then there exists a timelike geodesic  $\gamma$  which connects  $x, y$  and maximizes the length function defined by the following formula

$$L(\gamma) = \int_0^s \left( -g(\dot{\gamma}(t), \dot{\gamma}(t)) \right)^{\frac{1}{2}} dt.$$

As we shall see, global hyperbolicity is a natural condition for studying hyperbolic partial differential equations. A spacetime may not be globally hyperbolic; however there may exist subsets of such spacetimes which are globally hyperbolic.

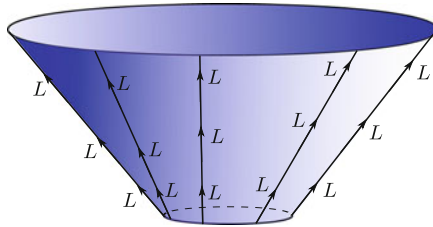
- Let  $\Sigma$  be a spacelike hypersurface of a spacetime  $(\mathcal{M}, g)$ . Then the *Cauchy development*  $D(\Sigma)$  of  $\Sigma$  is defined to be the biggest globally hyperbolic subset of  $\mathcal{M}$  which admits  $\Sigma$  as a Cauchy hypersurface.

The Cauchy development can be split as follows  $D(\Sigma) = D^+(\Sigma) \cup D^-(\Sigma)$  into the *future Cauchy development*  $D^+(\Sigma) = \mathcal{J}^+(\Sigma) \cap D(\Sigma)$  and the *past Cauchy development*  $D^-(\Sigma) = \mathcal{J}^-(\Sigma) \cap D(\Sigma)$ . A very important definition that concerns the global problem is the following

- The boundary  $\mathcal{CH}$  of the Cauchy development  $D(\Sigma)$  of an **inextendible** spacelike hypersurface  $\Sigma$  in a Lorentzian manifold  $\mathcal{M}$  is called the *Cauchy horizon* of  $D(\Sigma)$ .

### 1.1.3 Null Geometry

Null geometry concerns the study of null hypersurfaces. Recall that a hypersurface  $\mathcal{H}$  of a Lorentzian manifold  $(\mathcal{M}, g)$  is called null if at each point  $x \in \mathcal{H}$  the normal  $L_x$  to  $T_x\mathcal{H}$  is a null vector. This implies that the normal  $L_x$  is tangential to  $\mathcal{H}$ . In fact, for each  $x \in \mathcal{H}$ ,  $T_x\mathcal{H}$  contains a unique null line  $\langle L_x \rangle$  and every other direction in  $T_x\mathcal{H} - \langle L_x \rangle$  is spacelike (and orthogonal to  $\langle L_x \rangle$ ).



#### Null Generators

We have established that null hypersurfaces admit a distinguished *null line bundle* on  $H$ , namely the line bundle spanned by the normal lines  $\langle L_x \rangle$ ,  $x \in \mathcal{H}$ . We have the following

- *The integral curves of the null line bundle of a null hypersurface  $\mathcal{H}$  are null geodesics and are called the null generators of  $\mathcal{H}$ .*

Indeed, it suffices to show that  $\nabla_L L$  is normal to  $\mathcal{H}$  and hence parallel to  $L$ : If  $X \in T\mathcal{H}$ , then

$$g(\nabla_L L, X) = -g(L, \nabla_L X) = -g(L, \nabla_X L) = -\frac{1}{2}X(g(L, L)) = 0, \quad (1.1.2)$$

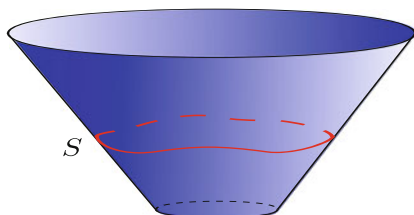
since  $[L, X] \in T\mathcal{H}$  and hence  $g(L, [L, X]) = 0$ . In other words, there is a function  $f : \mathcal{H} \rightarrow \mathbb{R}$  such that

$$\nabla_L L = f \cdot L \quad \text{on } \mathcal{H}. \quad (1.1.3)$$

### Sections of Null Hypersurfaces

- A *section*  $S$  of a null hypersurface  $\mathcal{H}$  is a two-dimensional submanifold of  $\mathcal{H}$  which intersects each null generator of  $\mathcal{H}$  transversally.

In view of the properties of  $\mathcal{H}$  we conclude that every section  $S$  is a two-dimensional Riemannian manifold. Furthermore, all null generators intersect  $S$  orthogonally.



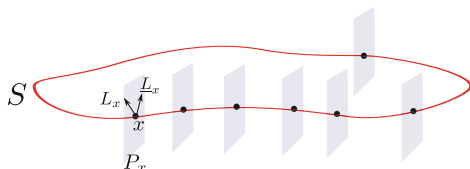
We will mainly be interested in the case where  $S$  is topologically homeomorphic to the two-dimensional sphere  $\mathbb{S}^2$ .

### Null Normal Geodesic Congruences

Let us now start with a surface  $S$ , namely a two-dimensional Riemannian manifold (homeomorphic to  $\mathbb{S}^2$ ). For every point  $x \in S$  we have that  $\dim(T_x S) = 2$  and  $g|_{T_x S}$  is positive definite. Hence, by Sylvester’s law of inertia we have that the orthogonal complement  $P_x = (T_x S)^\perp$  of  $T_x S$  in  $T_x \mathcal{M}$  is a two-dimensional Lorentzian plane and hence isometric to the two-dimensional Minkowski spacetime  $\mathbb{R}^{1+1}$ . The vector bundle

$$\mathcal{P} = \bigcup_{x \in S} P_x$$

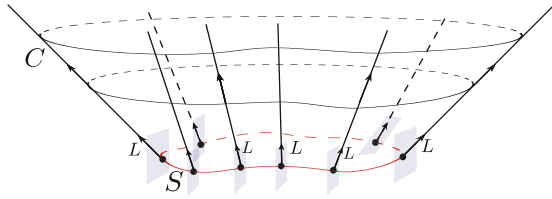
is called the normal bundle of  $S$  in  $\mathcal{M}$ . Note that  $P_x = \langle L_x, \underline{L}_x \rangle$ .



Hence, for each  $x \in S$  there are exactly two null lines orthogonal to  $S$ . Let  $L_x$  and  $\underline{L}_x$  be two future-directed null vectors in  $P_x$  such that  $L_x$  projects to the exterior of  $S$  and  $\underline{L}_x$  projects to the interior of  $S$ . We will call  $L_x$  the *outer null normal* to  $S$  at  $x$  and  $\underline{L}_x$  the *inner null normal* to  $S$  at  $x$ . We will require that  $L_x$  and  $\underline{L}_x$  depend differentiably on  $x$  so the resulting vector fields  $L$  and  $\underline{L}$  along  $S$  are differentiable.

For each  $x \in S$  there is a unique affinely parametrized null geodesic  $G_x$  with initial conditions  $(x, L_x)$ , that is to say  $G_x(0) = x$  and  $\dot{G}_x(0) = L_x$ . Similarly, there is a unique affinely parametrized null geodesic  $\underline{G}_x$  with initial conditions  $(x, \underline{L}_x)$ . We consider the sets in  $\mathcal{M}$  foliated by these geodesics:

$$C = \bigcup_{x \in S} G_x, \quad \underline{C} = \bigcup_{x \in S} \underline{G}_x. \tag{1.1.4}$$



- The regular parts of  $C$  and  $\underline{C}$  are null hypersurfaces known as *the outgoing and the incoming null normal geodesic congruences*, respectively, emanating from  $S$ .

**Affine Foliations**

Let  $\tau$  and  $\underline{\tau}$  be the affine parameters of the affinely parametrized null generators  $G_x$  and  $\underline{G}_x$  normalized such that  $S = \{\tau = 0\} = \{\underline{\tau} = 0\}$ . Then, the level sets  $S_\tau$  and  $\underline{S}_{\underline{\tau}}$  of  $\tau$  and  $\underline{\tau}$  are sections of  $C$  and  $\underline{C}$ , respectively. The following foliations

$$C = \bigcup_{\tau \geq 0} S_\tau, \quad \underline{C} = \bigcup_{\underline{\tau} \geq 0} \underline{S}_{\underline{\tau}}$$

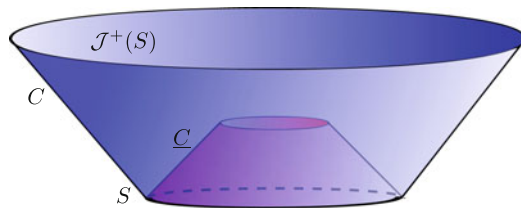
are called affine foliations of the null hypersurfaces  $C$  and  $\underline{C}$ , respectively.

**Null Normal Congruences and Causality Theory**

The importance of the null normal geodesic congruences lies in the following property:

- Let  $S$  be a two-dimensional surface in a globally hyperbolic spacetime  $(\mathcal{M}, g)$ . Let  $C$  and  $\underline{C}$  denote the (future) outgoing and incoming null geodesic congruences normal to  $S$ , respectively. Then,

$$\partial \mathcal{J}^+(S) \subseteq C \cup \underline{C}.$$



### 1.1.4 Optical Functions

Optical functions provide a level set approach to studying families of null hypersurfaces. We have the following definition

- A differentiable function  $u : \mathcal{M} \rightarrow \mathbb{R}$  is called *optical* if its level sets  $\mathcal{H}_c = \{u = c\}$  are null hypersurfaces.

Since the gradient vector field  $\nabla u$  is normal to the level sets  $\mathcal{H}_c$  of  $u$  we conclude that  $u$  is optical if only if  $\nabla u$  is null. In other words,

- A differentiable function  $u : \mathcal{M} \rightarrow \mathbb{R}$  is called *optical* if it satisfies the *eikonal equation*

$$g(\nabla u, \nabla u) = g^{\mu\nu}(\partial_\mu u)(\partial_\nu u) = 0. \tag{1.1.5}$$

Let us denote  $L = \nabla u$ . Then for any vector field  $X \in \mathcal{M}$  we have:

$$\begin{aligned} g(\nabla_L L, X) &= (\nabla_L L)_b(X) = (\nabla_L L_b)(X) = \nabla_L(du)(X) \\ &= \nabla^2 u(L, X) = \nabla^2 u(X, L) = \nabla_X(du)(L) = g(\nabla_X L, L) \\ &= \frac{1}{2} \nabla_X(g(L, L)), \end{aligned}$$

where we used the symmetry of the Hessian  $\nabla^2 u$  and the standard metric index-lowering musical isomorphism  $\flat : T\mathcal{M} \rightarrow T^*\mathcal{M}$ . Note that the above equation extends (1.1.2) since it holds for all vector field  $X$  (and not just the ones tangential to  $\mathcal{H}$ ). In other words, if  $L = \nabla u$  then

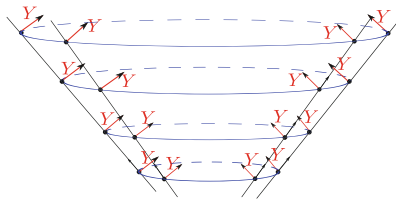
$$\nabla_L L = \frac{1}{2} \nabla(g(L, L)). \tag{1.1.6}$$

If  $u$  is an optical function, and  $L = \nabla u$ , then  $g(L, L) = 0$  everywhere which, in view of (1.1.6), yields the following

- If  $u$  is an optical function then the gradient vector field  $L = \nabla u$  is normal to the null hypersurfaces  $\mathcal{H}_c$  and is affinely parametrized, that is  $\nabla_L L = 0$ .

Let's finally consider a vector field  $Y$  transversal to the null hypersurfaces  $\mathcal{H}_c$  such that

$$g(L, Y) = 1. \tag{1.1.7}$$



Then, since  $L = \nabla u$ , we have that

$$Yu = 1 \tag{1.1.8}$$

and hence  $Y$  can be viewed as a “generator” of the optical function  $u$ .

## 1.2 The Einstein Field Equations

The Einstein field equations are the following

$$R_{\mu\nu}(g) - \frac{1}{2}R(g)g_{\mu\nu} = 2\mathbf{T}_{\mu\nu} \tag{1.2.1}$$

where  $R_{\mu\nu}(g)$ ,  $R(g)$  denote the Ricci and scalar curvature, respectively, and  $\mathbf{T}_{\mu\nu}$  denotes the energy-momentum tensor of matter fields. Note that  $\mathbf{T}$  is a  $(0, 2)$  symmetric divergence free tensor field.

### Einstein-Vacuum Equations

If no matter field is present then  $\mathbf{T} = 0$  and the field equations (1.2.1) reduce to the (still highly non-trivial) vacuum equations

$$R_{\mu\nu}(g) = 0. \tag{1.2.2}$$

which model the evolution of pure gravity. Minkowski spacetime is the trivial solution of the vacuum equations.

### Einstein–Maxwell Equations

The coupled Einstein–Maxwell equations consist of the system

$$\begin{aligned} R_{\mu\nu}(g) - \frac{1}{2}R(g)g_{\mu\nu} &= 2\mathbf{T}_{\mu\nu}^{\mathbf{M}}(F), \\ \nabla^\mu F_{\mu\nu} &= 0, \\ dF &= 0. \end{aligned} \tag{1.2.3}$$

Here  $F$  is a electromagnetic 2-form on  $\mathcal{M}$  and  $\mathbf{T}_{\mu\nu}^{\mathbf{M}}(F)$  is the electromagnetic energy momentum tensor of  $F$

$$\mathbf{T}_{\mu\nu}^{\mathbf{M}}(F) = F_\mu^\rho F_{\nu\rho} - \frac{1}{4}g_{\mu\nu}F^{ab}F_{ab}. \tag{1.2.4}$$

### Einstein–Maxwell–Scalar Field Equations

The coupled Einstein–Maxwell–scalar field equations consist of the system

$$\begin{aligned}
 R_{\mu\nu}(g) - \frac{1}{2}R(g)g_{\mu\nu} &= 2\mathbf{T}_{\mu\nu}(F, \psi), \\
 \mathbf{T}_{\mu\nu}(F, \psi) &= \mathbf{T}_{\mu\nu}^M(F) + \mathbf{T}_{\mu\nu}^{\text{sf}}(\psi), \\
 \nabla^\mu F_{\mu\nu} &= 0, \\
 dF &= 0, \\
 \square_g \psi &= 0.
 \end{aligned} \tag{1.2.5}$$

Here  $\psi$  is a massless scalar field on  $\mathcal{M}$  and  $\mathbf{T}_{\mu\nu}^{\text{sf}}(\psi)$  its energy-momentum tensor

$$\mathbf{T}_{\mu\nu}^{\text{sf}}(\psi) = \partial_\mu \psi \partial_\nu \psi - \frac{1}{2}g_{\mu\nu} \partial^\rho \psi \partial_\rho \psi. \tag{1.2.6}$$

### Maximal Globally Hyperbolic Developments

The local well-posedness of the Einstein–vacuum equations was established by Choquet-Bruhat in 1952 in her seminal paper [4]. Subsequently, Choquet-Bruhat and Geroch showed in [5] the following

- *Given initial data for the Einstein–vacuum equation on a 3-dimensional Riemannian manifold  $\Sigma$  there is a unique maximal globally hyperbolic spacetime which solves the Einstein equations and admits  $\Sigma$  as a Cauchy hypersurface.*

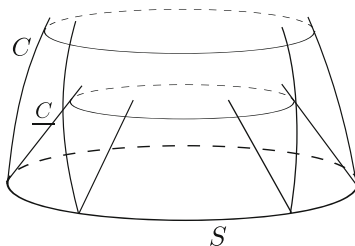
By maximal we mean that any other globally hyperbolic development of  $\Sigma$  can be isometrically embedded in the (unique) maximal development (in fact, for this reason, one should think of the maximal development as the “maximum” development). This theorem, which can be extended to the Einstein field equations, provides the main object of study in general relativity. For a detailed treatment see [6]. For recent refinements we refer to the work of Sbierski [7].

## 1.3 Trapped Surfaces

Let  $S$  be a closed surface and  $C \cup \underline{C}$  the null geodesic congruences normal to  $S$ . We have the following definition

- *A trapped surface is a closed two-dimensional surface  $S$  in  $(\mathcal{M}, g)$  for which the area decreases under arbitrary (infinitesimal) displacements along the null generators of both null geodesic congruences  $C \cup \underline{C}$  normal to  $S$ .*

If  $(\mathcal{M}, g)$  is globally hyperbolic, then since  $C \cup \underline{C}$  bounds the future of  $S$ , we obtain that a trapped surface cannot expand towards the future (hence the term trapped).



An alternative characterization is the following: A surface  $S$  is a trapped if the null mean curvatures along  $C$  and  $\underline{C}$  are everywhere negative on  $S$ .

### 1.4 Null Infinity

In order to study isolated systems in the universe we need to investigate the radiation that is emitted from these systems and reaches far away observers (such as ourselves). We therefore need a notion that models the region where radiation scatters. This gives rise to a concept known as future null infinity, an ideal incoming null hypersurface “at infinity”, traditionally denoted by  $\mathcal{I}^+$ . Even though there is not a single universally adopted definition for  $\mathcal{I}^+$ , we will here present a useful way to think of  $\mathcal{I}^+$ . Heuristically,

- *future null infinity  $\mathcal{I}^+$  consists of all limit points of future-directed null geodesics which reach arbitrarily large spatial distances.*

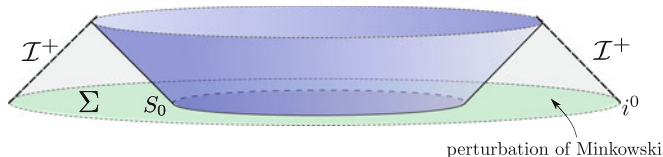


A similar construction can be considered for the past: *Past null infinity  $\mathcal{I}^-$*  consists of all limit points of past-directed null geodesics which reach arbitrarily large spatial distances. In the same spirit, we can think of *future timelike infinity  $i^+$*  as the limit point of future-directed timelike geodesics and *past timelike infinity  $i^-$*  as the limit point of past-directed timelike geodesics. There are various ways to implement the above naive definitions more precisely and concretely. One way is in terms of conformal transformations (see [1]). Another way is in terms of null foliations and the range of optical functions (see [8]). Later, in Chap. 2, we will present a more concrete realization of  $\mathcal{I}^+$  for ERN spacetimes that uses the latter approach.

#### Asymptotical Flatness and Null Infinity

We are mostly interested in studying isolated systems (such as solar systems, black holes and galaxies) in the universe. Hence, we can assume that far away from these

systems the spacetime approaches the flat Minkowski spacetime. Such a condition can a priori only be imposed on the initial Cauchy hypersurface  $\Sigma$ . Hence, let us assume that the data on  $\Sigma$  are asymptotically flat, i.e. approach Minkowskean data at infinity. We assume that  $\Sigma$  terminates at *spacelike infinity*  $i^0$ , the limit point of spacelike geodesics. Then, there exists a sphere  $S_0$  in  $\Sigma$  such that the data on the exterior of  $S_0$  in  $\Sigma$  is a small perturbation of the flat Minkowski data. Then it follows by the stability of Minkowski theorem, proved by Christodoulou–Klainerman [8] and Klainerman–Nicolò [9], that one can attach a piece of future null infinity at the Cauchy development  $D^+(\Sigma)$  of  $\Sigma$ :



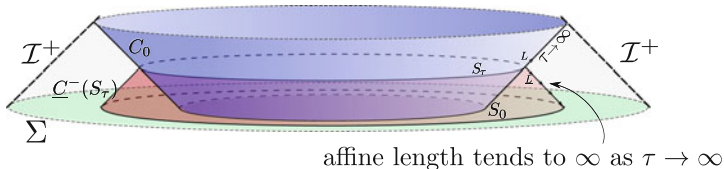
### Completeness of Null Infinity

An important concept is that of *future and past completeness of null infinity*. Roughly speaking, completeness of null infinity implies that observers on null infinity can receive radiation (for example from isolated systems) for infinite proper time. Thinking of  $\mathcal{I}^+$  as an null hypersurface, its completeness simply corresponds to future and past completeness of its null generators. Another way to think of the completeness of  $\mathcal{I}^+$ , in a *limiting* sense, without referring to  $\mathcal{I}^+$  as a concrete entity, is due to Christodoulou [10]. We briefly review Christodoulou’s approach below.

The past-completeness of future null infinity is defined *in a limiting* sense as follows: Let  $C_0$  be the outgoing null geodesic congruence normal to  $S_0$ . Let  $L$  be a geodesic null vector field along  $C_0$  with affine parameter  $\tau$ . We assume that we can take  $\tau \rightarrow \infty$  along  $C_0$ . For each section  $S_\tau$ , given by the level sets of  $\tau$  on  $C_0$ , we consider the (conjugate) incoming null normal geodesic congruence  $\underline{C}^-(S_\tau)$ . Let  $\underline{L}$  be the past-directed null geodesic vector field on  $\underline{C}^-(S_\tau)$  normalized at  $S_\tau$  such that

$$g(L, \underline{L}) = +1 \text{ at } S_\tau.$$

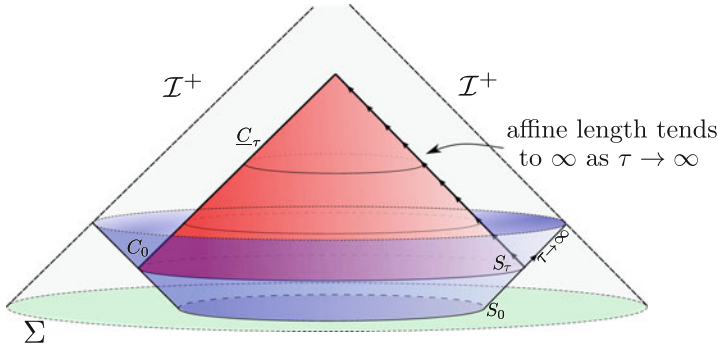
The past-directed null generators of  $\underline{C}^-(S_\tau)$  are generated by the vector field  $\underline{L}$ . Future null infinity is said to be past complete if the affine time it takes the null generators of  $\underline{C}^-(S_\tau)$  to intersect  $\Sigma$ , starting from  $S_\tau$ , tends to infinity as  $\tau \rightarrow \infty$ .



The works [8, 9] on the stability of Minkowski showed, in particular, that

- *Future null infinity of asymptotically flat spacetimes is past complete.*

Future completeness of future null infinity is defined in a similar way: Consider the null geodesic vector field  $\underline{L}$  along  $\underline{C}_\tau$  as above. The future-directed null generators of  $\underline{C}_\tau$  (spanning the red cone in the figure below) are generated by  $-\underline{L}$ . Future null infinity is said to be future complete if the affine time of the future-directed null generators of  $\underline{C}_\tau$  starting from  $S_\tau$  tends to infinity as  $\tau \rightarrow \infty$  while remaining in the Cauchy development of the interior of  $S_\tau$ .



### Weak Cosmic Censorship

Unlike past completeness, it is not known if “generic” asymptotically flat spacetimes admit a future complete  $\mathcal{I}^+$ . In fact, this is one of the most outstanding open problems in general relativity and is known as the *weak cosmic censorship conjecture*. A more accurate formulation of the conjecture can be found in [10].

## 1.5 Black Holes

In this Brief we focus on two specific families of spacetimes, namely the extremal Reissner–Nordström (ERN) family and the extremal Kerr (EK) family. These spacetimes contain black hole regions. The concrete definition for the black hole region in ERN and in EK is given in Chaps. 2 and 3, respectively. In this section, we will attempt to provide an informal account of the notion of black hole in general.

### 1.5.1 Definitions, Diagrams and Examples

Black holes are one of the most celebrated predictions of general relativity. They are regions which cannot communicate with far-away observers (to whom they appear “black”). Since far-away observers are heuristically modeled by future null infinity  $\mathcal{I}^+$ , we say that black holes cannot “communicate” with future null infinity  $\mathcal{I}^+$ .

Extending causal relations to null infinity, and referring to the set of all points in  $\mathcal{M}$  from which null geodesics can “reach” (and hence can “communicate” with)  $\mathcal{I}^+$  as the past  $\mathcal{J}^-(\mathcal{I}^+)$  of  $\mathcal{I}^+$ , we arrive at the following somewhat informal definition

- The black hole region  $\mathcal{BH}$  is the complement of the past  $\mathcal{J}^-(\mathcal{I}^+)$  of future null infinity. Symbolically,

$$\mathcal{BH} = \mathcal{M} - \mathcal{J}^-(\mathcal{I}^+).$$

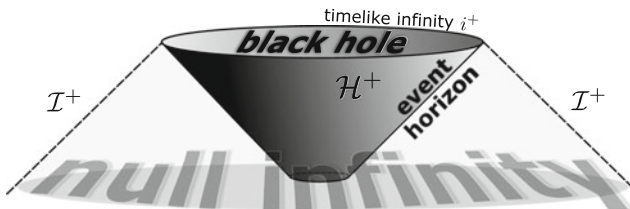
There is a close connection of black holes and the weak cosmic censorship. Indeed, black hole spacetimes with a complete future null infinity  $\mathcal{I}^+$  have the property that even though observers on  $\mathcal{I}^+$  *live forever* (in view of the future completeness of  $\mathcal{I}^+$ ) they never receive radiation from the black hole region. We have the following important definitions

- The exterior of the black hole region is known as the *domain of outer communications*.
- The boundary of the black hole region (that is, the boundary of the past of  $\mathcal{I}^+$ ) is known as the *future event horizon*.

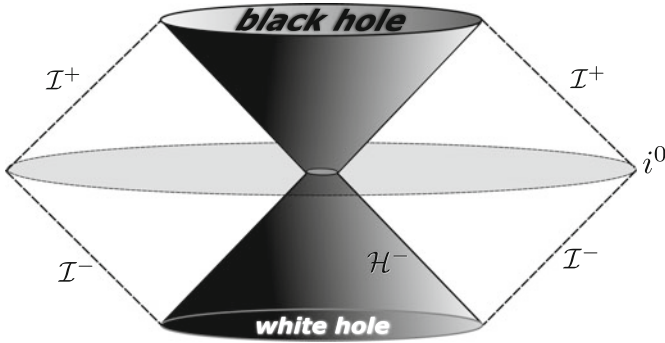
The future event horizon is an outgoing null hypersurface usually denoted by  $\mathcal{H}^+$ . Observers in the domain of outer communication can cross the event horizon but once they enter the black hole region they cannot escape it. We can also define the dual (past) notion of a black hole, namely the *white hole*. This is the complement of the future of past null infinity  $\mathcal{I}^-$  (that is, the set of all points in  $\mathcal{M}$  from which past-directed null geodesics cannot “reach”  $\mathcal{I}^-$ ) and cannot be entered from the outside. The boundary of the white hole is known as the past event horizon and denoted by  $\mathcal{H}^-$ . Of course, there are spacetimes without any black hole or white hole regions, for example Minkowski spacetime (and small perturbations of it).

### Heuristic and Penrose Diagrams

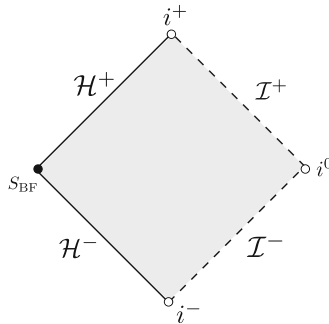
We will make use of the following heuristic (informal) picture to represent the black hole region, the domain of outer communications and future null infinity.



The heuristic picture depicting the black hole and the white hole regions is the following:



Another representation of (black hole) spacetimes is given by the so-called *Penrose diagrams*. They represent the domain on  $\mathbb{R}^2$  of a pair of conjugate optical functions forming a double null coordinate system and are very useful because they provide a means to read off the causal structure of spacetimes (see [3] for more details). Informally, the Penrose diagram of the domain of outer communications can be obtained by restricting to an angular slice of the above heuristic diagram as follows



In this Brief we will make use of both the heuristic pictures and Penrose diagrams.

**The Kerr–Newman Family of Black Holes**

Let us now consider explicit solutions to the Einstein field equations which contain black hole regions. We will consider the Einstein–Maxwell system (1.2.5). There is a (unique) family of analytic, stationary and asymptotically flat solutions to the Einstein–Maxwell system with black hole regions. This family is known as the *Kerr–Newmann* family and is parametrized by three parameters, namely the mass  $M$ , the charge  $e$  and the angular momentum  $a$  which satisfy  $M^2 \geq e^2 + a^2$ . Details about this family can be found in any standard textbook. If  $a = 0$  then the family reduces to the *Reissner–Nordström* family and if  $e = 0$  then it reduces to the *Kerr* family. Furthermore, if  $a = e = 0$  then the family reduces to the *Schwarzschild* 1-parameter family of black hole spacetimes.

### 1.5.2 The Surface Gravity of the Event Horizon

Let  $\mathcal{H}$  be a null hypersurface which admits a Killing normal vector field  $V$ . Then, in view of (1.1.3) there is a function  $\kappa : \mathcal{H} \rightarrow \mathbb{R}$  such that

$$\nabla_V V = \kappa \cdot V. \quad (1.5.1)$$

Since  $V$  is Killing we can easily see that  $\kappa$  has to be conserved along the null generators of  $\mathcal{H}$ , that is  $V\kappa = 0$ . Indeed, we can see that  $\kappa = g(\nabla_V V, Y)$  where  $Y$  is such that  $g(V, Y) = 1$  and  $[V, Y] = 0$ . The relation  $V\kappa = 0$  then follows from the fact that since  $V$  is Killing we have  $[V, \nabla_V V] = 0$ . Note however that  $\kappa$  depends on the normalization of the vector field  $V$  and hence  $\kappa$  is uniquely defined if and only if there is a distinguished Killing normal to  $\mathcal{H}$ . Such a distinguished normal exists for stationary, asymptotically flat spacetimes (such as the Kerr–Newman family of spacetimes). In this case, we require the normal  $V$  to be Killing and normalized at infinity in sense that it projects on the stationary Killing field  $T$  for which  $g(T, T) \rightarrow -1$  at infinity. For the Schwarzschild, and more generally the Reissner–Norström, family we simply take  $V = T$  on the event horizon.

- The *surface gravity* of the event horizon  $\mathcal{H}$  is given by (1.5.1) where  $V$  is the null normal to  $\mathcal{H}$  Killing vector field normalized at infinity.

Physically,  $\kappa$  measures the force needed to hold something on the event horizon from infinity. For the Kerr–Newman family (and more general stationary solutions to the Einstein equations) *the surface gravity  $\kappa$  is constant on the event horizon* (and not just conserved along the null generators). The surface gravity is related to the entropy of the black hole and hence is important in black hole thermodynamics.

### 1.5.3 Extremal Versus Sub-extremal Black Holes

Stationary black holes, such as the Kerr–Newman black holes, are partitioned in two classes

- *Sub-extremal black holes have strictly positive surface gravity on the event horizon.*
- *Extremal black holes have vanishing surface gravity on the event horizon.*

The *sub-extremal Kerr–Newman* family corresponds to the values of the parameters for which  $M^2 > a^2 + e^2$ . The *extremal Kerr–Newman* corresponds to the case where  $M^2 = a^2 + e^2$ . The case  $M = e$  (and hence  $a = 0$ ) corresponds to *extremal Reissner–Nordström* (ERN) and the case where  $M = a$  (and hence  $e = 0$ ) corresponds to *extremal Kerr* (EK).

There are various definitions of extremality (and resp. of sub-extremality) for dynamical black holes. These definitions involve bounds on the limiting area of the event horizon relative to the limiting mass along the horizon or the non-existence of

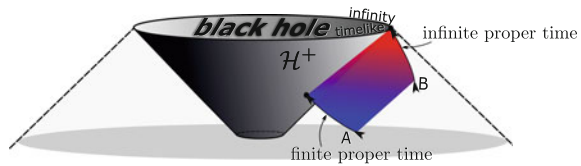
trapped surfaces. We will not pursue this here further (see, however, the discussion for the dynamically extremal Murata–Reall–Tanahashi spacetimes in Sect. 2.5).

### 1.5.4 The Redshift Effect

#### The Global Redshift Effect

Let us consider two observers A, B in the domain of outer communications. Observer A crosses the event horizon in finite proper time (and hence enters the black hole region) whereas observer B lives forever in the domain of outer communications and specifically on a timelike geodesic with infinite affine time terminating at the future timelike infinity  $i^+$ . Suppose that A emits a light signal that travels along outgoing null geodesics and is intercepted by B. Then, the frequency of this signal as measured by B will be “shifted to the red” when compared to the frequency measured by A. Intuitively, this is related to the fact that the signal, which was emitted in a finite proper time interval for A, is received by B for an infinite proper time. This means that the peak of the signal must be intercepted by B less frequently as the proper time of B progresses. Hence, the frequency as measured by B gets lower. This is precisely the content of the *global redshift effect* (see Fig. 1.7).

**Fig. 1.7** The global redshift effect. A crosses the event horizon. B remains in the domain of outer communications forever



The global redshift effect simply relies on the causal properties of the domain of outer communications and as such it holds for both extremal and sub-extremal black holes.

#### The Local Redshift Effect

There is nonetheless a *local* version of the redshift effect, which depends on the geometric properties of the event horizon and can be illustrated as follows (see also [3]): Consider two observers A and B entering the black hole region such that A crosses the event horizon  $\mathcal{H}^+$  first. Suppose A emits a light signal that travels along the event horizon and is intercepted by B. Then, *as long as the event horizon  $\mathcal{H}^+$  is sub-extremal*, the frequency of this signal as measured by B will be “shifted to the red” when compared to the frequency measured by A as in the Fig. 1.8.

**Fig. 1.8** The local redshift effect for sub-extremal horizons



*The local redshift effect degenerates for extremal black holes (Fig. 1.9):*

**Fig. 1.9** The degenerate local redshift effect for extremal horizons



**Capturing the Local Redshift Effect via the Surface Gravity**

The local redshift effect can be quantitatively captured via the positivity of the surface gravity on the event horizon. First note that the signal is emitted from the points of the worldline of A and then propagated along future-directed null geodesics (which emanate from those points). Then B receives the signal as long as B’s trajectory intersects these null geodesic. A change in the frequency of the signal as received by B would be due to an increase (or decrease) of the separation of nearby null geodesics. Specifically, the received frequency would be lower if the null geodesics are further apart when they reach B than when they started from the worldline of A. Indeed, this would force B to see the wavefronts of the signal be further apart resulting in measuring a lower frequency of the received signal.

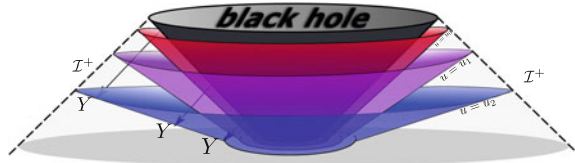
Instead of studying the dynamic separation of null geodesics, we can study the dynamic separation of null hypersurfaces (which are ruled by null geodesics) in a neighborhood of the event horizon. This is slightly more convenient since it allows us to work with optical functions. Consider an optical function  $u$  such that  $\mathcal{H}^+ = \{u = 0\}$ . We would like to study the separation of the level sets of  $u$  along the event horizon  $\mathcal{H}^+$ . Consider  $L = \nabla u$ . Then  $L$  is normal to  $\mathcal{H}^+$  and satisfies  $\nabla_L L = 0$ . Moreover, if  $Y$  is a transversal to  $\mathcal{H}^+$  vector field such that  $g(L, Y) = 1$  then  $Y u = 1$  (see Sect. 1.1.4). Hence, the size of  $Y$  along  $\mathcal{H}^+$  gives us the dynamic separation of the null hypersurfaces (the level sets of  $u$ ) along which the signal propagates. In order to measure  $Y$  along  $\mathcal{H}^+$  we need to compare it with vector fields defined in terms of the symmetry generating Killing normal  $V$ . Specifically, we will compare  $Y$  with the vector field  $Y^V$  normalized such that  $g(V, Y^V) = 1$ . We should think that  $Y^V$  carries no weights in time and hence can be used to measure the size of  $Y$ . Let us consider the *advanced time*  $v$  along the event horizon such that  $V v = 1$ . Then, since  $V$  solves (1.5.1) we obtain  $L = e^{-\kappa v} \cdot V$ . This immediately yields

$$Y = e^{\kappa v} \cdot Y^V$$

which proves that  $Y$  increases exponentially in  $v$ . Hence

- *outgoing null hypersurfaces in a neighborhood of  $\mathcal{H}^+$  diverge with an exponentially increasing factor that depends on the surface gravity  $\kappa$  (Fig. 1.10).*

**Fig. 1.10** Divergence of null hypersurfaces on sub-extremal black holes



The importance of the redshift effect for the dynamics of black hole spacetimes was first demonstrated by Dafermos and Rodnianski in [11]. The above discussion confirms our previous claim for extremal black holes:

- *the local redshift effect degenerates for extremal black holes. Outgoing null hypersurfaces do not diverge (Fig. 1.11).*

**Fig. 1.11** Outgoing null hypersurface on extremal black holes



This property of extremal black holes will play a crucial role in this brief.

## 1.6 The Black Hole Stability Problem

A rigorous understanding of black hole dynamics is of fundamental importance for addressing several conjectures in general relativity such as *the weak and strong cosmic censorship conjectures* as well as for investigating *the propagation of gravitational waves*. We provide here a rough formulation of the stability problem from the Kerr–Newman family. For details we refer to the lecture notes [3].

- **The black hole stability conjecture:** *Consider initial data sufficiently close to the initial data on a Cauchy hypersurface in the Kerr–Newman solution with parameters  $(M_0, a_0, e_0)$ . Then, the maximal Cauchy development satisfying the Einstein–Maxwell equations possesses a complete null infinity such that the metric*

restricted to the domain of outer communications approaches a Kerr–Newman solution  $(M_\epsilon, a_\epsilon, e_\epsilon)$  in a uniform way, where  $(M_\epsilon, a_\epsilon, e_\epsilon)$  are close to  $(M_0, a_0, e_0)$ .

The special case for the vacuum equations, starting with  $e_0 = 0$ , is known as the stability conjecture of the Kerr family. Note that we can study the dynamics of Schwarzschild by restricting further to initial data for which  $a_0 = 0$ , but unless we impose symmetry assumptions, the final  $a_\epsilon$  will be non-zero.

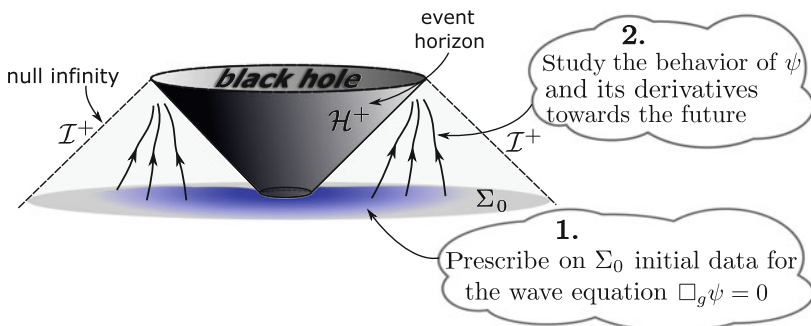
As we shall see, the results presented in this book strongly suggest that this conjecture is false of for a neighborhood of extremal black holes (with  $M^2 = a^2 + e^2$ ).

## 1.7 The Wave Equation on Black Hole Exteriors

Important aspects of the black hole dynamics are captured by the evolution of solutions to the *wave equation*

$$\square_g \psi = 0 \tag{1.7.1}$$

on black hole backgrounds. Initial data are prescribed on a Cauchy hypersurface  $\Sigma_0$  which intersects the event horizon  $\mathcal{H}^+$  and terminates at null infinity  $\mathcal{I}^+$ , as in the figure below. A first step towards the non-linear stability of black hole backgrounds is to establish quantitative *dispersive* estimates for (1.7.1) in the domain of outer communications up to and including the event horizon.



The initial value problem for the wave equation on black hole backgrounds has been extensively studied in both the mathematics and the physics communities. The main difficulties include the trapping effect at the photon sphere, the redshift effect at the horizon, dispersion at the near-infinity region and superradiance. We again refer to [3] for details of these difficulties in general spacetimes.

**Quantitative decay rates** for scalar fields satisfying (1.7.1) and all their higher-order derivatives have been obtained for the *general sub-extremal Kerr* family of black hole spacetimes by Dafermos, Rodnianski and Shlapentokh-Rothman in [12]. Similar decay estimates hold for the *general sub-extremal Reissner–Nordström* family (see, for example, [11]). We refer to [13–23] for additional results in the asymptotically flat setting and to [24–28] for results in the asymptotically de Sitter and anti

de Sitter setting. See also [29–32] for recent breakthroughs in the understanding of nonlinear stability problems in the context of the Einstein equations.

In this brief we will be largely occupied with presenting asymptotic results for scalar perturbations on extremal black holes. For comparison and completeness, we devote the rest of this section to a discussion on asymptotics of scalar perturbations on sub-extremal black holes, and mainly for Schwarzschild and Reissner–Nordström spacetimes.

## 1.8 Price’s Asymptotics for Sub-extremal Black Holes

A definitive proof of the **precise late-time asymptotics** of solutions to the wave equation on the general sub-extremal Reissner–Nordström backgrounds, including the Schwarzschild family of black holes, was obtained in the recent series of papers [33–35] confirming, in particular, Price’s heuristics. Let’s first present a discussion of Price’s asymptotics.

### 1.8.1 Price’s Heuristics

The following late-time *polynomial* tail for solutions to the wave equation with smooth, *compactly supported* initial data on Schwarzschild spacetimes was heuristically obtained by Price [36] in 1972 along hypersurfaces with constant radius  $r = r_0 > 2M$  away from the event horizon  $\mathcal{H}^+ = \{r = 2M\}$ :

$$\psi|_{r=r_0}(\tau, r = r_0, \Omega) \sim \frac{1}{\tau^3}. \quad (1.8.1)$$

Subsequent heuristic and numerical works [37–39] suggested the following asymptotics on the event horizon  $\mathcal{H}^+$ :

$$\psi|_{\mathcal{H}^+}(\tau, r = 2M, \Omega) \sim \frac{1}{\tau^3}, \quad (1.8.2)$$

and along the null infinity  $\mathcal{I}^+$ :

$$r\psi|_{\mathcal{I}^+}(\tau, r = \infty, \Omega) \sim \frac{1}{\tau^2}. \quad (1.8.3)$$

Here  $\Omega = (\theta, \varphi) \in \mathbb{S}^2$ . Moreover,  $\tau$  denotes a global time parameter such that its level sets are the hypersurfaces  $\Sigma_\tau = F_\tau^T(\Sigma_0)$ , where  $F_\tau^T$  is the flow of the stationary vector field  $T = \partial_t$  of Schwarzschild.

### 1.8.2 The Newman–Penrose Constants $I_0$ and $I_0^{(1)}$

The heuristic work of Leaver [37] related the late-time power law to the branch cut at temporal frequency  $\omega = 0$  in the Laplace transform of Green’s function for each fixed angular frequency. On the other hand, the approach of [34, 35] relied on purely physical space techniques and in particular related the late-time power law to *an obstruction to the invertibility of the time operator  $T = \partial_t$*  in a suitable functional space (and hence is related to the  $\omega = 0$  frequency in the Fourier space). Restricting (strictly) to the future of the bifurcation sphere where  $T \neq 0$ , we have that **an obstruction to the invertibility of the operator  $T$  is the existence of a conservation law along the null infinity  $\mathcal{I}^+$** : For solutions  $\psi$  to the wave equation (1.7.1) on R–N spacetimes, the limits

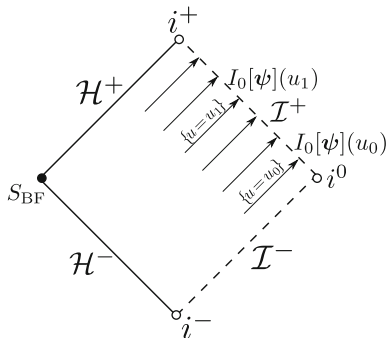
$$I_0[\psi](u) := \frac{1}{4\pi} \lim_{r \rightarrow \infty} \int_{\mathbb{S}^2} r^2 \partial_r(r\psi)(u, r, \Omega) d\Omega$$

are **independent** of the retarded time  $u$ . Here, we consider the standard outgoing Eddington–Finkelstein coordinates  $(u, r, \Omega)$  where  $u$  is an optical function whose level sets are the standard spherically symmetric outgoing null hypersurfaces,  $r$  is the area-radius of the spheres of symmetry,  $\Omega = (\theta, \varphi) \in \mathbb{S}^2$  and  $d\Omega = \sin \theta d\theta d\varphi$ . See Fig. 1.12 and also Sect. 2.1.1. The associated constant

$$I_0[\psi] := I_0[\psi](u) \tag{1.8.4}$$

is called the *Newman–Penrose constant* of  $\psi$  (see [40, 41]).

**Fig. 1.12** The Newman–Penrose constant on  $\mathcal{I}^+$



The existence of this asymptotic conservation law is an obstruction to inverting the time operator  $T$  if the domain of  $T$  is taken to be the set of all smooth solutions  $\psi$  to the wave equation which satisfy the condition  $|r^2 \partial_r(r\psi)| \in O_1(1)$  on the initial hypersurface  $\Sigma_0$ . Indeed, if there is a regular solution  $\psi^{(1)}$  to (1.7.1) in the domain of  $T$  such that

$$T\psi^{(1)} = \psi$$

then we must necessarily have that

$$I_0[\psi] = I_0[T\psi^{(1)}] = 0.$$

On the other hand, if we consider smooth initial data on a Cauchy hypersurface  $\Sigma_0$  which crosses the event horizon to the future of the bifurcation sphere (see Fig. 1.13) such that  $I_0[\psi] = 0$  and

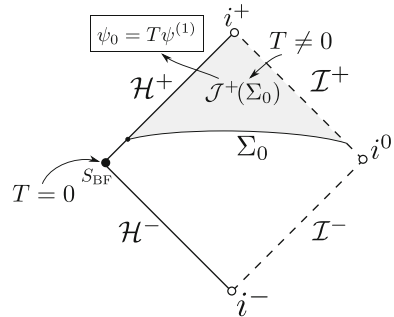
$$\lim_{r \rightarrow \infty} \int_{\mathbb{S}^2} r^3 \partial_r (r\psi)|_{\Sigma_0} d\Omega < \infty \tag{1.8.5}$$

then, by the results in [34], there is a unique smooth spherically symmetric solution  $\psi^{(1)}$  to (1.7.1) in the domain of  $T$  such that

$$T\psi^{(1)} = \frac{1}{4\pi} \int_{\mathbb{S}^2} \psi d\Omega \tag{1.8.6}$$

in  $\mathcal{J}^+(\Sigma_0)$ .

**Fig. 1.13** Time inversion for the spherical mean  $\psi_0$  of  $\psi$



Hence,  $I_0[\psi]$  appears as the unique obstruction to inverting the time operator  $T$  on the projection to the spherical mean of  $\psi$ . If (1.8.5) holds (and hence  $I_0[\psi] = 0$ ), then, as we just mentioned,  $T$  can be inverted to produce the time integral  $\psi^{(1)}$ . In this case, the Newman–Penrose constant  $I_0[\psi^{(1)}]$  of  $\psi^{(1)}$  is an obstruction to acting with  $T^{-1}$  on  $\psi^{(1)}$ , or equivalently, an obstruction to acting with  $T^{-2}$  on  $\frac{1}{4\pi} \int_{\mathbb{S}^2} \psi d\Omega$ . We call  $I_0[\psi^{(1)}]$  the *time-inverted Newman–Penrose constant* of  $\psi$  and we use the notation

$$I_0^{(1)}[\psi] = I_0[\psi^{(1)}].$$

Note that  $I_0^{(1)}[\psi]$  is given in terms of the initial data of  $\psi$  by

$$\begin{aligned}
I_0^{(1)}[\psi] &= \frac{M^3}{4\pi} \int_{\Sigma_0 \cap \mathcal{H}^+} \psi \, d\Omega \\
&+ \lim_{r_0 \rightarrow \infty} \left( \frac{M}{4\pi} \int_{\Sigma_0 \cap \{r \leq r_0\}} n_{\Sigma_0}(\psi) \, d\mu_{\Sigma_0} + \frac{M}{4\pi} \int_{\Sigma_0 \cap \{r=r_0\}} \left( \psi - \frac{2}{M} r L(r\psi) \right) r_0^2 \, d\Omega \right),
\end{aligned} \tag{1.8.7}$$

where  $L = \partial_v$  is the outgoing null derivative with respect to the double null coordinate system  $(u, v)$ ,  $n_{\Sigma_0}$  is the normal of  $\Sigma_0$  and  $d\mu_{\Sigma_0}$  is the induced volume form on  $\Sigma_0$ . For compactly supported initial data on the maximal hypersurface  $\{t = 0\}$ , the above expression for the coefficient  $I_0^{(1)}[\psi]$  reduces to

$$I_0^{(1)}[\psi] = \frac{M}{4\pi} \int_{S_{\text{BF}}} \psi \, r^2 \, d\Omega + \frac{M}{4\pi} \int_{\{t=0\}} \frac{1}{1 - \frac{2M}{r}} \partial_t \psi \, r^2 \, dr \, d\Omega,$$

where  $S_{\text{BF}}$  denotes the bifurcation sphere, that is the intersection of the future event horizon  $\mathcal{H}^+$  with the past event horizon  $\mathcal{H}^-$ .

### 1.8.3 The Precise Late-Time Asymptotics

The following global quantitative estimates were obtained for general sub-extremal Reissner–Nordström spacetimes in [34, 35]: If the Newman–Penrose constant  $I_0[\psi] \neq 0$  then

$$\left| \frac{1}{4\pi} \int_{\mathbb{S}^2} \psi(\tau, r_0, \Omega) - 4I_0[\psi] \cdot \frac{1}{\tau^2} \right| \leq C_{r_0} \cdot \sqrt{E_{\Sigma_0}[\psi]} \cdot \frac{1}{\tau^{2+\epsilon}}, \tag{1.8.8}$$

up to and including the event horizon (Fig. 1.14). On the other hand, if  $I_0[\psi] = 0$  (as in the case of compactly supported initial data) then we have the following estimates

$$\left| \psi(\tau, r_0, \Omega) + 8I_0^{(1)}[\psi] \cdot \frac{1}{\tau^3} \right| \leq C_{r_0} \cdot \sqrt{E_{\Sigma_0}[\psi]} \cdot \frac{1}{\tau^{3+\epsilon}}, \tag{1.8.9}$$

$$\left| r\psi|_{\mathcal{I}^+}(\tau, \Omega) + 2I_0^{(1)}[\psi] \cdot \frac{1}{\tau^2} \right| \leq C \cdot \sqrt{E_{\Sigma_0}[\psi]} \cdot \frac{1}{\tau^{2+\epsilon}}, \tag{1.8.10}$$

where  $\Omega = (\theta, \varphi)$ ,  $\sqrt{E_{\Sigma_0}[\psi]}$  are weighted norms of the initial data and the constant  $I_0^{(1)}$  is given explicitly in terms of the initial data of  $\psi$  by (1.8.7). We emphasize that (1.8.9) holds up to and including the event horizon (Fig. 1.14).

**Fig. 1.14** Price’s asymptotics for sub-extremal RN backgrounds



Generic compactly supported initial data satisfy  $I_0^{(1)}[\psi] \neq 0$  and hence give rise to solutions to the wave equation which decay exactly like  $\frac{1}{r^3}$ . This result yielded the first *pointwise lower bounds* for solutions to the wave equation on Schwarzschild backgrounds.<sup>3</sup> In other words, (1.8.9), (1.8.10) and (1.8.7) provide a complete characterization of all solutions to (1.7.1) which satisfy Price’s law as a lower bound. We remark that the study of lower bounds and late-time asymptotics is very important in issues related to the black hole interior regions and, in particular, in addressing the strong cosmic censorship conjecture [42–51].

Summarizing, we have:

asymptotics for $\psi$	origin of the coefficient
$-4I_0[\psi] \cdot \frac{1}{r^2}$	$I_0[\psi] \neq 0$ unique obstruction to inverting $T$
$8I_0^{(1)}[\psi] \cdot \frac{1}{r^3}$	$I_0^{(1)}[\psi] \neq 0$ unique obstruction to inverting $T^2$

**In the case of ERN there are additional obstructions to inverting the time operator  $T$  which cause many subtle difficulties in obtaining the precise late-time asymptotics** (see Chaps. 2 and 3).

## 1.9 Physical Importance of Extremal Black Holes

Extremal black holes are of fundamental importance in general relativity. In this section we provide a list of references which underpin the intimate connection of extremal black holes with astronomy/astrophysics, high energy physics and classical general relativity. Results regarding specifically the dynamics of ERN are omitted from this section since they are discussed in detail in the next two chapters.

### Observations of (near) Extremal Black Holes

Astronomical evidence suggests that near-extremal black holes are ubiquitous in the universe. Various techniques have been developed to analyze the mechanisms for the formation and distribution of near-extremal black holes [52, 53]. It has been suggested that 70% of the stellar black holes, which are formed from the collapse of massive stars, are near-extremal [54].

<sup>3</sup>The sharpness of the *decay rate* of the time derivative of  $\psi$  along the event horizon was first established by Luk and Oh [42].

Using techniques from  $X$ -ray reflection spectroscopy, it has been argued that many supermassive black holes (whose mass is at least 1 billion times the mass of the sun) are near-extremal [55, 56]. Such black holes are important for the large scale structure of galaxies and galaxy clusters. Specific near-extremal supermassive black holes are expected to exist in the center of the MCG–06–30–15 galaxy [57] and the NGC 3783 galaxy [58]. Moreover, the stellar black hole Cygnus X-1 (part of a black hole binary system in the Galaxy) has been shown to have an almost extreme value for the spin parameter [59]. Another example is the stellar black hole GRS 1915+105 [60].

### **Observational Signatures of Extremal Black Holes**

Many astronomical conclusions are based on calculations for exactly Kerr spacetimes. However, time variability might introduce additional observational signatures of extremal black holes, that is features in the observations that are characteristic to the dynamics of extremal black holes. The near-horizon geometry provides a great background for probing such signatures. Such signatures can be divided in two main categories: gravitational signatures [61–63] and electromagnetic signatures [64–66]. See also Sect. 2.4.1 for another kind of signature due to scalar perturbations.

### **Uniqueness and Classification of Extremal Black Holes**

Extremal event horizons enjoy various rigidity properties [67–70]. Global uniqueness results for extremal black holes in various settings have been obtained in [71–75]. We also refer to interesting examples of higher dimensional extremal black holes [76].

### **Extremal Black Holes as Mass Minimizers**

Extremal black holes saturate geometric inequalities for the total mass, angular momentum and charge [77–79], even at higher dimensions [80–82]. They also saturate quasi-local versions of these inequalities for the mass, angular momentum and charge contained in the black hole region [83–87].

### **Supersymmetry, Holography and Quantum Gravity**

Extremal black holes are often supersymmetric as a consequence of the BPS bound. They have zero Hawking temperature and hence play an important role in understanding black hole thermodynamics and the Hawking radiation [88]. Quantum considerations of black hole entropy in five-dimensional extremal black holes and applications in string theory can be found in [89, 90]. One can define a near-horizon limit [91–93] which yields new solutions to the Einstein equations with conformally invariant properties. These limiting geometries have been classified in [94–98]. On the other hand, the conformal properties of near-horizon geometries allow for a description of quantum gravity via a holographic duality [99–101] and the study of bodies orbiting near-extremal black holes [102–105]. The near-horizon of a binary system of extremal black holes was found in [106].

### **Quasi-Normal Modes of Extremal Black Holes**

Starobinski [107] first investigated the effects of superradiance and extremality. Extensions for quasi-normal modes of extremal Kerr were obtained in [108] where a

sequence of zero damped modes was computed. Subsequent analysis was presented in [109, 110]. The most precise analysis of quasi-normal modes in extremal Kerr has been presented in [111]. As far as other settings are concerned, rapid modes for near extremal Reissner–Nordström–de Sitter spacetimes were discovered in [112] and slow modes on near-extremal (in fact all sub-extremal) Kerr de Sitter were computed in [113]. Gravitational modes of the near extremal Kerr geometry were studied in [114].

### Extremality and Non-linear Effects

An intriguing aspect of near-extremal black holes is that they exhibit turbulent gravitational behavior [115], that is energy is transferred from high frequencies to low frequencies. Non-linear simulations of formation of binary systems of near-extremal black holes were presented in [116]. Furthermore, numerical simulations of the evolution of the Einstein–Maxwell-scalar field system in a neighborhood of extremal R–N was studied in [117]. A general theory of evolution of extremal black holes was developed here [118]. For other non-linear works pertaining to the dynamics of extremal black holes we refer to [119, 120].

## References

1. S. Hawking, G.F.R. Ellis, *The Large Scale Structure of Spacetime* (Cambridge University Press, Cambridge, 1973)
2. R.M. Wald, *General Relativity* (The University of Chicago Press, Chicago, 1984)
3. M. Dafermos, I. Rodnianski, Lectures on black holes and linear waves, *Evolution Equations*. Clay Mathematics Proceedings, vol. 17 (American Mathematical Society, Providence, 2013), pp. 97–205, [arXiv:0811.0354](https://arxiv.org/abs/0811.0354)
4. Y. Choquet-Bruhat, Théorème d’existence pour certains systèmes d’équations aux dérivées partielles non linéaires. *Acta Math.* **88**, 141–225 (1952)
5. Y. Choquet-Bruhat, R. Geroch, Global aspects of the Cauchy problem in general relativity. *Commun. Math. Phys.* **14**, 329–335 (1969)
6. D. Christodoulou, *Mathematical Problems of General Relativity I* (EMS, 2008)
7. J. Sbierski, On the existence of a maximal Cauchy development for the Einstein equations - a deznornification. *Annales Henri Poincaré* **17**(2), 301–329 (2016)
8. D. Christodoulou, S. Klainerman, *The Global Nonlinear Stability of the Minkowski Space* (Princeton University Press, Princeton, 1994)
9. S. Klainerman, F. Nicolo, *The Evolution Problem in General Relativity*, Progress in Mathematical Physics (Birkhäuser, Basel)
10. D. Christodoulou, On the global initial value problem and the issue of singularities. *Class. Quantum Gravity* **16**, A23–A35 (1999)
11. M. Dafermos, I. Rodnianski, The redshift effect and radiation decay on black hole spacetimes. *Commun. Pure Appl. Math.* **62**, 859–919 (2009), [arXiv:0512.119](https://arxiv.org/abs/0512.119)
12. M. Dafermos, I. Rodnianski, Y. Shlapentokh-Rothman, Decay for solutions of the wave equation on Kerr exterior spacetimes III: the full subextremal case  $|a| < m$ . *Ann. Math.* **183**, 787–913 (2016)
13. M. Dafermos, G. Holzegel, I. Rodnianski, Boundedness and decay for the Teukolsky equation on Kerr spacetimes I: the case  $|a| \ll m$  (2017), [arXiv:1711.07944](https://arxiv.org/abs/1711.07944)
14. M. Dafermos, I. Rodnianski, A proof of Price’s law for the collapse of a self-gravitating scalar field. *Invent. Math.* **162**, 381–457 (2005)

15. P. Blue, A. Soffer, Phase space analysis on some black hole manifolds. *J. Funct. Anal.* **256**, 1–90 (2009)
16. D. Civin, Stability of charged rotating black holes for linear scalar perturbations. Ph.D. thesis, 2014
17. G. Moschidis, The  $r^p$ -weighted energy method of Dafermos and Rodnianski in general asymptotically flat spacetimes and applications. *Ann. PDE* **2**, 6 (2016)
18. V. Schlue, Linear waves on higher dimensional Schwarzschild black holes. *Anal. PDE* **6**(3), 515–600 (2013)
19. D. Tataru, Local decay of waves on asymptotically flat stationary space-times. *Am. J. Math.* **135**, 361–401 (2013)
20. J. Metcalfe, D. Tataru, M. Tohaneanu, Price’s law on nonstationary spacetimes. *Adv. Math.* **230**, 995–1028 (2012)
21. L. Andersson, P. Blue, Hidden symmetries and decay for the wave equation on the Kerr spacetime. *Ann. Math.* **182**, 787–853 (2015)
22. R. Donninger, W. Schlag, A. Soffer, A proof of Price’s law on Schwarzschild black hole manifolds for all angular momenta. *Adv. Math.* **226**, 484–540 (2011)
23. J. Kronthaler, Decay rates for spherical scalar waves in a Schwarzschild geometry (2007), [arXiv:0709.3703](https://arxiv.org/abs/0709.3703)
24. P. Hintz, Global well-posedness of quasilinear wave equations on asymptotically de Sitter spaces. *Annales de l’institut Fourier* **66**(4), 1285–2408 (2016)
25. S. Dyatlov, Quasi-normal modes and exponential energy decay for the Kerr-de Sitter black hole. *Commun. Math. Phys.* **306**, 119–163 (2011)
26. R. Donninger, W. Schlag, A. Soffer, On pointwise decay of linear waves on a Schwarzschild black hole background. *Commun. Math. Phys.* **309**, 51–86 (2012)
27. G. Holzegel, J. Smulevici, Decay properties of Klein–Gordon fields on Kerr–AdS spacetimes. *Commun. Pure Appl. Math.* **66**, 1751–1802 (2013)
28. G. Holzegel, J. Smulevici, Quasimodes and a lower bound on the uniform energy decay rate for Kerr–AdS spacetimes. *Anal. PDE* **7**(5), 1057–1090 (2014)
29. P. Hintz, A. Vasy, The global non-linear stability of the Kerr-de Sitter family of black holes (2016), [arXiv:1606.04014](https://arxiv.org/abs/1606.04014)
30. M. Dafermos, G. Holzegel, I. Rodnianski, The linear stability of the Schwarzschild solution to gravitational perturbations (2016), [arXiv:1601.06467](https://arxiv.org/abs/1601.06467)
31. S. Klainerman, J. Szeftel, Global nonlinear stability of Schwarzschild spacetime under polarized perturbations (2017), [arXiv:1711.07597](https://arxiv.org/abs/1711.07597)
32. G. Moschidis, A proof of the instability of AdS for the Einstein–null dust system with an inner mirror, [arXiv:1704.08681](https://arxiv.org/abs/1704.08681)
33. Y. Angelopoulos, S. Aretakis, D. Gajic, A vector field approach to almost sharp decay for the wave equation on spherically symmetric, stationary spacetimes (2016), [arXiv:1612.01565](https://arxiv.org/abs/1612.01565)
34. Y. Angelopoulos, S. Aretakis, D. Gajic, Late-time asymptotics for the wave equation on spherically symmetric, stationary backgrounds. *Adv. Math.* **323**, 529–621 (2018), [arXiv:1612.01566](https://arxiv.org/abs/1612.01566)
35. Y. Angelopoulos, S. Aretakis, D. Gajic, Asymptotics for scalar perturbations from a neighborhood of the bifurcation sphere (2018), [arXiv:1802.05692](https://arxiv.org/abs/1802.05692)
36. R. Price, Non-spherical perturbations of relativistic gravitational collapse. I. Scalar and gravitational perturbations. *Phys. Rev. D* **3**, 2419–2438 (1972)
37. E.W. Leaver, Spectral decomposition of the perturbation response of the Schwarzschild geometry. *Phys. Rev. D* **34**, 384–408 (1986)
38. C. Gundlach, R. Price, J. Pullin, Late-time behavior of stellar collapse and explosions. I: linearized perturbations. *Phys. Rev. D* **49**, 883–889 (1994)
39. L. Barack, Late time dynamics of scalar perturbations outside black holes. II. Schwarzschild geometry. *Phys. Rev. D* **59** (1999)
40. E.T. Newman, R. Penrose, 10 exact gravitationally conserved quantities. *Phys. Rev. Lett.* **15**, 231 (1965)
41. E.T. Newman, R. Penrose, New conservation laws for zero rest mass fields in asymptotically flat space-time. *Proc. R. Soc. A* **305**, 175204 (1968)

42. J. Luk, S.-J. Oh, Proof of linear instability of the Reissner–Nordström Cauchy horizon under scalar perturbations. *Duke Math. J.* **166**(3), 437–493 (2017)
43. M. Dafermos, Stability and instability of the Cauchy horizon for the spherically symmetric Einstein–Maxwell-scalar field equations. *Ann. Math.* **158**, 875–928 (2003)
44. M. Dafermos, The interior of charged black holes and the problem of uniqueness in general relativity. *Commun. Pure Appl. Math.* **LVIII**, 0445–0504 (2005)
45. M. Dafermos, Black holes without spacelike singularities. *Commun. Math. Phys.* **332**, 729–757 (2014)
46. J. Luk, J. Sbierski, Instability results for the wave equation in the interior of Kerr black holes. *J. Funct. Anal.* **271**(7), 1948–1995 (2016)
47. M. Dafermos, Y. Shlapentokh-Rothman, Time-translation invariance of scattering maps and blue-shift instabilities on Kerr black hole spacetimes. *Commun. Math. Phys.* **350**, 985–1016 (2016)
48. P. Hintz, Boundedness and decay of scalar waves at the Cauchy horizon of the Kerr spacetime (2015), [arXiv:1512.08003](https://arxiv.org/abs/1512.08003)
49. A. Franzen, Boundedness of massless scalar waves on Reissner–Nordström interior backgrounds. *Commun. Math. Phys.* **343**, 601–650 (2014)
50. J. Luk, S.-J. Oh, Strong cosmic censorship in spherical symmetry for two-ended asymptotically flat data I: interior of the black hole region, [arXiv:1702.05715](https://arxiv.org/abs/1702.05715)
51. J. Luk, S.-J. Oh, Strong cosmic censorship in spherical symmetry for two-ended asymptotically flat data II: exterior of the black hole region, [arXiv:1702.05716](https://arxiv.org/abs/1702.05716)
52. G. Compère, R. Oliveri, Self-similar accretion in thin disks around near-extremal black holes. *Mon. Not. R. Astron. Soc.* **468**(4), 4351–4361 (2017)
53. M. Kesden, G. Lockhart, E.S. Phinney, Maximum black-hole spin from quasi-circular binary mergers. *Phys. Rev. D* **82**, 124045 (2010)
54. M. Volonteri, P. Madau, E. Quataert, M. Rees, The distribution and cosmic evolution of massive black hole spins. *Astrophys. J.* **620**, 69–77 (2005)
55. L. Brenneman, *Measuring the Angular Momentum of Supermassive Black Holes*, Springer Briefs in Astronomy (Springer, Berlin, 2013)
56. C.S. Reynolds, The spin of supermassive black holes. *Class. Quantum Gravity* **30**, 244004 (2013)
57. L.W. Brenneman, C.S. Reynolds, Constraining black hole spin via X-ray spectroscopy. *Astrophys. J.* **652**(2) (2006)
58. L. Brenneman et al., The spin of the supermassive black hole in NGC 3783. *Astrophys. J.* **736**, 103 (2011)
59. L. Gou et al., Confirmation via the continuum-fitting method that the spin of the black hole in Cygnus X-1 is extreme. *Astrophys. J.* **790**(1) (2014)
60. J.E. McClintock, R. Shafee, R. Narayan, R.A. Remillard, S.W. Davis, L.-X. Li, The spin of the near-extreme Kerr black hole GRS 1915+105. *Astrophys. J.* **652**, 518–539 (2006)
61. S. Gralla, S. Hughes, N. Warburton, Inspirals into gargantua. *Class. Quantum Gravity* **33**, 155002 (2016)
62. T. Jacobson, Where is the extremal Kerr ISCO? *Class. Quantum Gravity* **28**, 187001 (2011)
63. L. Burko, G. Khanna, Gravitational waves from a plunge into a nearly extremal Kerr black hole. *Phys. Rev. D* **94**(8) (2016)
64. C.T. Cunningham, J.M. Bardeen, The optical appearance of a star orbiting an extreme Kerr black hole. *Astrophys. J.* **183**, 237–264 (1973)
65. C.T. Cunningham, J.M. Bardeen, The optical appearance of a star orbiting an extreme Kerr black hole. *Astrophys. J.* **173**, L137 (1972)
66. S. Gralla, A. Lupasca, A. Strominger, Observational signature of high spin at the event horizon telescope. *Mon. Not. R. Astron. Soc.* **475**(3), 3829–3853 (2018)
67. I. Booth, S. Fairhurst, Extremality conditions for isolated and dynamical horizons. *Phys. Rev. D* **77**, 084005 (2008)
68. J. Lewandowski, T. Pawłowski, Extremal isolated horizons: a local uniqueness theorem. *Class. Quantum Gravity* **20**, 587–606 (2003)

69. P. Hájíček, Three remarks on axisymmetric stationary horizons. *Commun. Math. Phys.* **36**, 305–320 (1974)
70. S. Hollands, A. Ishibashi, On the stationary implies axisymmetric theorem for extremal black holes in higher dimensions. *Commun. Math. Phys.* **291**, 403–441 (2009)
71. P. Figueras, J. Lucietti, On the uniqueness of extremal vacuum black holes. *Class. Quantum Gravity* **27**, 095001 (2010)
72. P. Chruściel, H. Reall, P. Tod, On non-existence of static vacuum black holes with degenerate components of the event horizon. *Class. Quantum Gravity* **23**, 549–554 (2006)
73. P. Chruściel, L. Nguyen, A uniqueness theorem for degenerate Kerr–Newman black holes. *Annales Henri Poincaré* **11**, 585–609 (2010)
74. A.J. Amsel, G.T. Horowitz, D. Marolf, M.M. Roberts, Uniqueness of extremal Kerr and Kerr–Newman black holes. *Phys. Rev. D* **81**, 024033 (2010)
75. R. Meinel, M. Ansorg, A. Kleinwächter, G. Neugebauer, D. Petrof, *Relativistic Figures of Equilibrium* (Cambridge University Press, Cambridge, 2008)
76. H.K. Kunduri, J. Lucietti, Black lenses in string theory. *Phys. Rev. D* **94**, 064007 (2016)
77. S. Dain, Angular-momentum-mass inequality for axisymmetric black holes. *Phys. Rev. Lett.* **96**, 101101 (2006)
78. S. Dain, Proof of the angular momentum-mass inequality for axisymmetric black holes. *J. Diff. Geom.* **79**, 33–67 (2008)
79. P.T. Chruściel, Y. Li, G. Weinstein, Mass and angular-momentum inequalities for axisymmetric initial data sets. II. Angular-momentum. *Ann. Phys.* **323**, 2591–2613 (2008)
80. A. Alaae, M. Khuri, H. Kunduri, Proof of the mass-angular momentum inequality for bi-axisymmetric black holes with spherical topology. *Adv. Theor. Math. Phys.* **20**, 1397–1441 (2016)
81. A. Alaae, M. Khuri, H. Kunduri, Mass-angular momentum inequality for black ring space-times. *Phys. Rev. Lett.* **119**, 071101 (2017)
82. A. Alaae, M. Khuri, H. Kunduri, Bounding horizon area by angular momentum, charge, and cosmological constant in 5-dimensional minimal supergravity (2017), [arXiv:1712.01764](https://arxiv.org/abs/1712.01764)
83. S. Dain, J. Jaramillo, M. Reiris, Area-charge inequality for black holes. *Class. Quantum Gravity* **29**(3) (2012)
84. S. Dain, Extreme throat initial data set and horizon area-angular momentum inequality for axisymmetric black holes. *Phys. Rev. D* **82**, 104010 (2010)
85. S. Dain, M. Reiris, Area-angular-momentum inequality for axisymmetric black holes. *Phys. Rev. Lett.* **107**, 051101 (2011)
86. M.E.G. Clement, J.L. Jaramillo, M. Reiris, Proof of the area-angular momentum-charge inequality for axisymmetric black holes. *Class. Quantum Gravity* **30**(6) (2013)
87. M. Reiris, On extreme Kerr-throats and zero temperature black holes. *Class. Quantum Gravity* **31**(2) (2013)
88. S.W. Hawking, G.T. Horowitz, S.F. Ross, Entropy, area, and black hole pairs. *Phys. Rev. D* **51**, 4302–4314 (1995)
89. A. Strominger, C. Vafa, Microscopic origin of the Bekenstein–Hawking entropy. *Phys. Lett. B* **379**, 99–104 (1996)
90. R. Emparan, G.T. Horowitz, Microstates of a neutral black hole in M theory. *Phys. Rev. Lett.* **97**, 141601 (2006)
91. G. Gibbons, *Aspects of Supergravity Theories. In supersymmetry, Supergravity, and Related topics.* (World Scientific, 1985)
92. P. Claus, M. Derix, R. Kallosh, J. Kumar, P. Townsend, A.V. Proeyen, Black holes and superconformal mechanics. *Phys. Rev. Lett.* **81**, 4553–4556 (1998)
93. A. Saghatelian, Near-horizon dynamics of particle in extreme Reissner–Nordstrom and Clement–Galtsov black hole backgrounds: action-angle variables. *Class. Quantum Gravity* **29**, 245018 (2012)
94. H.K. Kunduri, J. Lucietti, H.S. Reall, Near-horizon symmetries of extremal black holes. *Class. Quantum Gravity* **24**, 4169–4190 (2007)

95. H. Kunduri, J. Lucietti, A classification of near-horizon geometries of extremal vacuum black holes. *J. Math. Phys.* **50**, 082502 (2009)
96. H.K. Kunduri, J. Lucietti, Uniqueness of near-horizon geometries of rotating extremal AdS(4) black holes. *Class. Quantum Gravity* **26**, 055019 (2009)
97. P. Chruściel, K. Tod, The classification of static electro-vacuum space-times containing an asymptotically flat spacelike hypersurface with compact interior. *Commun. Math. Phys.* **271**, 577–589 (2007)
98. S. Hollands, A. Ishibashi, All vacuum near-horizon geometries in D-dimensions with (D-3) commuting rotational symmetries. *Annales Henri Poincaré* **10**(8), 1537–1557 (2010)
99. M. Guica, T. Hartman, W. Song, A. Strominger, The Kerr/CFT correspondence. *Phys. Rev. D* **80**, 124008 (2009)
100. I. Bredberg, T. Hartman, W. Song, A. Strominger, Black hole superradiance from Kerr/CFT. *JHEP* **1004**, 019 (2010)
101. T. Hartman, K. Murata, T. Nishioka, A. Strominger, CFT duals for extreme black holes. *JHEP* **2009**, 04 (2009)
102. A.P. Porfyriadis, A. Strominger, Gravity waves from Kerr/CFT. *Phys. Rev. D* **90**, 044038 (2014)
103. S. Hadar, A.P. Porfyriadis, A. Strominger, Gravity waves from extreme-mass-ratio plunges into Kerr black holes. *Phys. Rev. D* **90**, 064045 (2014)
104. S. Hadar, A. Porfyriadis, A. Strominger, Fast plunges into Kerr black holes. *JHEP* **7**, 78 (2015)
105. A.P. Porfyriadis, Y. Shi, A. Strominger, Photon emission near extreme Kerr black holes. *Phys. Rev. D* **95**, 064009 (2017)
106. J. Ciafre, M.J. Rodriguez, A near horizon extreme binary black hole geometry (2018), [arXiv:1804.06985](https://arxiv.org/abs/1804.06985)
107. A. Starobinski, S. Churilov, Amplification of electromagnetic and gravitational waves scattered by a rotating black hole. *Sov. Phys. JETP* **38**(1), 1–5 (1974)
108. S. Detweiler, Black holes and gravitational waves III. The resonant frequencies of rotating holes. *Astrophys. J.* **239**, 292–295 (1980)
109. N. Andersson, K. Glampedakis, A superradiance resonance cavity outside rapidly rotating black holes. *Phys. Rev. Lett.* **84**, 4537–4540 (2000)
110. K. Glampedakis, N. Andersson, Late-time dynamics of rapidly rotating black holes. *Phys. Rev. D* **64**, 104021 (2001)
111. H. Yang, A. Zimmerman, A. Zenginoglu, F. Zhang, E. Berti, Y. Chen, Quasinormal modes of nearly extremal Kerr spacetimes: spectrum bifurcation and power-law ringdown. *Phys. Rev. D* **88**, 044047 (2013)
112. V. Cardoso, J.L. Costa, K. Destounis, P. Hintz, A. Jansen, Quasinormal modes and strong cosmic censorship. *Phys. Rev. Lett.* **120**, 031103 (2018)
113. O.J. Dias, F.C. Eperon, H.S. Reall, J.E. Santos, Strong cosmic censorship in de Sitter space (2018), [arXiv:1801.09694](https://arxiv.org/abs/1801.09694)
114. O.J. Dias, H.S. Reall, J.E. Santos, Kerr-CFT and gravitational perturbations. *JHEP* **101** (2009)
115. H. Yang, A. Zimmerman, L. Lehner, Turbulent black holes. *Phys. Rev. Lett.* **114**, 081101 (2015)
116. G. Lovelace, R. Owen, H.P. Pfeiffer, T. Chu, Binary-black-hole initial data with nearly-extremal spins. *Phys. Rev. D* **78**, 084017 (2008)
117. K. Murata, H.S. Reall, N. Tanahashi, What happens at the horizon(s) of an extreme black hole? *Class. Quantum Gravity* **30**, 235007 (2013)
118. I. Booth, Evolutions from extremality. *Phys. Rev. D* **93**, 084005 (2016)
119. Y. Angelopoulos, S. Aretakis, D. Gajic, Asymptotic blow-up for a class of semi-linear wave equations on extremal Reissner–Nordström spacetimes (2016), [arXiv:1612.01562](https://arxiv.org/abs/1612.01562)
120. P. Bizon, M. Kahl, A Yang–Mills field on the extremal Reissner–Nordström black hole. *Class. Quantum Gravity* **33**, 175013 (2016)

# Chapter 2

## Extremal Reissner–Nordström Black Holes



In this Chapter we thoroughly review the geometry of extremal Reissner–Nordström black holes. We also present the main results on the asymptotics of linear perturbations on such backgrounds.

### 2.1 The Geometry of ERN

#### 2.1.1 The ERN Metric

The *Reissner–Nordström* family  $(\mathcal{M}_{M,e}, g_{M,e})$  forms the unique family of spherically symmetric asymptotically flat four-dimensional solutions to the Einstein–Maxwell equations. These spacetimes, discovered in 1916 [1] and 1918 [2], have two parameters the mass  $M$  and the (electromagnetic) charge  $e$ . Extremal Reissner–Nordström (ERN) corresponds to  $M = |e|$ .

We will first present the ERN metric in local Boyer–Lindquist coordinates  $(t, r, \theta, \phi)$ . In these coordinates, one metric component blows up for various values of  $r$  and it is not a priori obvious what is the appropriate underlying manifold to study the geometry of this solution. As we shall see, the maximally extended solutions will be patched by various coordinate charts. The ERN metric  $g = g_M$  in the coordinates  $(t, r, \theta, \varphi)$  is given by

$$g = -Ddt^2 + \frac{1}{D}dr^2 + r^2d\Omega, \quad (2.1.1)$$

where

$$D = D(r) = \left(1 - \frac{M}{r}\right)^2 \quad (2.1.2)$$

and  $d\Omega = \sin\theta d\theta d\varphi$  is the standard metric on  $\mathbb{S}^2$ . Note that the Maxwell potential  $A$  in these coordinates is given by

$$A = -\frac{Q}{r}dt - B \cos \theta d\phi$$

where  $M = |e| = \sqrt{Q^2 + B^2}$ ,  $(\theta, \phi) \in \mathbb{S}^2$  and  $Q, B$  are the electric and magnetic charge, respectively.

Clearly,  $SO(3)$  acts by isometry on these spacetimes. We will refer to the  $SO(3)$ -orbits as (symmetry) spheres. The coordinate  $r$  is defined intrinsically such that the area of the spheres of symmetry is  $4\pi r^2$  (and thus should be thought of as a purely geometric function of the spacetime). From now on, we will omit writing the coordinates  $(\theta, \varphi)$  unless otherwise stated.

One could now pose the following question: On what manifold is the metric (2.1.1) most naturally defined? In the above coordinates, it is clear that the metric component  $g_{rr}$  is singular at  $r = 0$  and  $r = M$  (the latter is double root of  $D$ ). The computation of the curvature shows that as  $r \rightarrow 0$  the curvature blows up and so the singularity of  $r = 0$  in (2.1.1) is essential (for a very detailed description of these phenomena in Schwarzschild case see [3]). However, the points where  $r = M$  form coordinate singularities<sup>1</sup> which can be eliminated by introducing the so-called *tortoise* coordinate  $r^*$

$$\frac{\partial r^*(r)}{\partial r} = \frac{1}{D}.$$

We can easily see that

$$r^*(r) = r + 2M \ln|r - M| - \frac{M^2}{r - M} - 2M \ln M - M. \quad (2.1.3)$$

The fact that in extreme case  $r^*$  is inverse linear (instead of logarithmic in the non-extreme case) is crucial. Note that  $r^*$  is normalized such that  $r^*(r = 2M) = 0$  and that

$$\text{for } r < M : \quad r^*(r = 0) = 0, \quad \lim_{r \rightarrow M^-} r^* = +\infty, \quad (2.1.4)$$

$$\text{for } r > M : \quad \lim_{r \rightarrow M^+} r^* = -\infty, \quad r^*(r = \infty) = \infty. \quad (2.1.5)$$

By introducing the coordinate system  $(t, r^*)$  the metric becomes

$$g = -Ddt^2 + D(dr^*)^2 + r^2 d\Omega. \quad (2.1.6)$$

This metric breaks down at  $r = M$ . A coordinate system that allows us to extend the metric beyond  $r = M$  is the *ingoing Eddington–Finkelstein coordinates*  $(v, r)$  where

$$v = t + r^*. \quad (2.1.7)$$

In these coordinates the metric is given by

$$g = -Ddv^2 + 2dvdr + r^2 d\Omega. \quad (2.1.8)$$

---

<sup>1</sup>It is the function  $t$  that is singular at these points.

The coordinate vector field  $\partial_v$  is Killing and is everywhere timelike except on the hypersurface  $\{r = M\}$  where it is null. In view of (2.1.8) and the fact that  $\partial_v$  is tangent and null on  $\mathcal{H}^+$  we have that the vector  $\partial_v$  is normal to  $\mathcal{H}^+$ . Recall that if the normal of a null hypersurface is Killing then the hypersurface is called a *Killing horizon*. We will use the notation

$$T = \partial_v \quad (2.1.9)$$

and call  $T$  the stationary vector field. Note that  $T$  is normalized at infinity such that  $g(T, T) \rightarrow -1$  as  $r \rightarrow \infty$ . We define the time-orientability of ERN to be so that the causal vector field  $T$  is future-directed. A future-directed timelike vector field is  $T - \partial_r$ .

The level sets  $\{v = c\}$  are null hypersurfaces and hence  $v$  is an optical function. This means that the coordinate vector field  $-\partial_r$  is future-directed null, normal on  $\{v = c\}$  and differentiates with respect to  $r$  on these null hypersurfaces. In fact it is geodesic. Indeed, a computation gives the following Christoffel symbols

$$\nabla_v \partial_v = \left(\frac{D'}{2}\right) \partial_v + \left(\frac{D \cdot D'}{2}\right) \partial_r, \quad \nabla_v \partial_r = \left(-\frac{D'}{2}\right) \partial_r, \quad \nabla_r \partial_r = 0. \quad (2.1.10)$$

We see that the coordinates  $(v, r)$  extend the domain that the coordinates  $(t, r)$  cover. Therefore, using the coordinates  $(v, r)$ , let us define

$$\mathcal{M} = \{(v, r, \Omega) \in (-\infty, +\infty) \times (0, +\infty) \times \mathbb{S}^2\}. \quad (2.1.11)$$

We introduce yet one more optical function given by

$$u = t - r^* \quad (2.1.12)$$

and define the *outgoing Eddington–Finkelstein coordinates*  $(u, r)$ . The metric in these coordinates takes the form

$$g = -Ddu^2 - 2dudr + r^2 d\Omega. \quad (2.1.13)$$

In these coordinates,  $\partial_u = T$  and  $\partial_r$  is future-directed null. Another coordinate system that covers  $\mathcal{M} \cap \{r > M\}$  is the *double null coordinate system*  $(u, v)$ , where  $v$  and  $u$  are given by (2.1.7) and (2.1.12), respectively, which satisfies

$$\boxed{u - v = -2r^*} \quad (2.1.14)$$

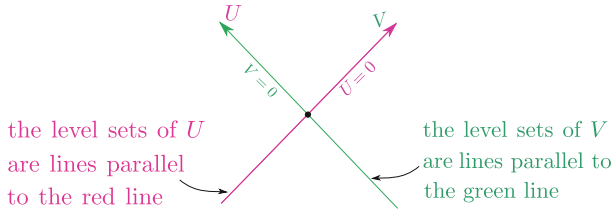
and with respect to which the ERN metric is

$$g = -Ddudv + r^2 d\Omega. \quad (2.1.15)$$

In this system,  $\partial_v$  and  $\partial_u$  are both future-directed null vector fields.

### 2.1.2 Penrose Diagrams

The Penrose diagram is a planar depiction of the domain of two optical functions forming a double null coordinate system. Let’s consider the system  $(u, v)$  with respect to which the ERN metric takes the form (2.1.15). We will crucially use (2.1.14) throughout this section since it relates the range of  $u, v$  with the values of  $r$ . The Penrose diagram will be represented in terms of the domain a coordinate system  $(U, V)$  of  $\mathbb{R}^2$  as in the figure below



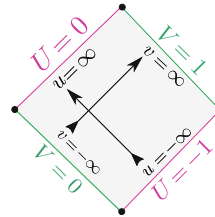
Let’s first consider the case where  $r > M$ . Then, in view of (2.1.5),  $r^* \in \mathbb{R}$  and hence  $u \in \mathbb{R}$  and  $v \in \mathbb{R}$ . In this case, the coordinates  $U, V$  will be taken to be smooth strictly increasing functions  $U = U(u)$  and  $V = V(v)$  such that

$$\begin{aligned}
 U(u) &= -1 - \frac{1}{u} \text{ for } u \leq -4, & U(u) &= -\frac{1}{u} \text{ for } u \geq 4, \\
 V(v) &= -\frac{1}{v} \text{ for } v \leq -4, & V(v) &= 1 - \frac{1}{v} \text{ for } v \geq 4,
 \end{aligned}
 \tag{2.1.16}$$

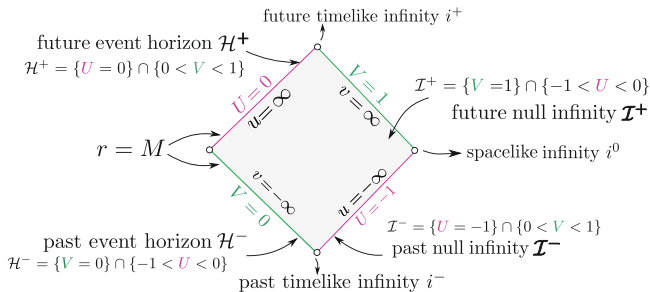
as shown below

$$\begin{aligned}
 \lim_{u \rightarrow +\infty} U &= 0 \\
 \lim_{u \rightarrow -\infty} U &= -1
 \end{aligned}$$

$$\begin{aligned}
 \lim_{v \rightarrow +\infty} V &= 1 \\
 \lim_{v \rightarrow -\infty} V &= 0
 \end{aligned}$$



The interior of the square above represents the domain  $\mathbb{R} \times \mathbb{R} \times \mathbb{S}^2$  in terms of the double null coordinates  $(u, v, \Omega)$ . For reasons that will be apparent below, this region is called the *domain of outer communications*. Recall again that this region corresponds to  $r > M$ . The event horizon and null infinity are defined by the boundary of this square, as follows:



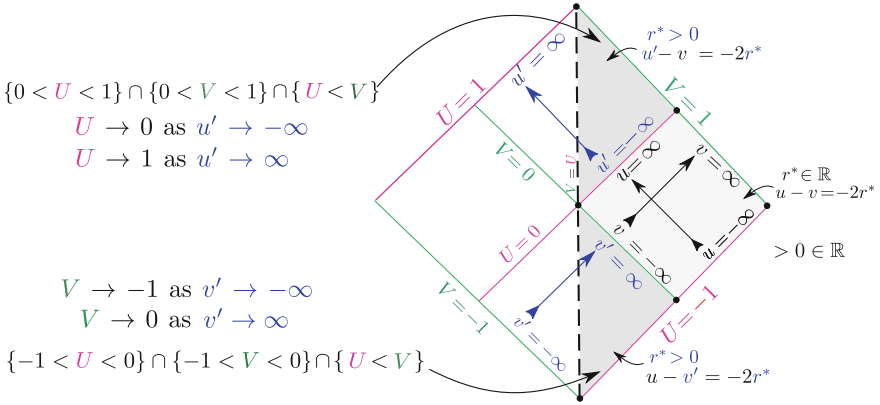
It can be easily shown that the limit points of future-directed null geodesics along which  $r \rightarrow \infty$  lie on  $\mathcal{I}^+$  as defined above. Hence, our definition of future null infinity for ERN agrees with that in Sect. 1.4. Furthermore, it can be checked that  $\mathcal{I}^+$  is past and future complete, in the sense of Sect. 1.4. On the other hand, the future event horizon  $\mathcal{H}^+$  and the past event horizon  $\mathcal{H}^-$  as defined above, are actual null hypersurfaces of the ERN spacetime where, in view of (2.1.16), the metric (2.1.15) extends smoothly. Indeed, in view of (2.1.14), that the future and past event horizon both have  $r = M$ . Hence, the future event horizon  $\mathcal{H}^+$  is covered by the ingoing EF system  $(v, r)$  and the past event horizon  $\mathcal{H}^-$  is covered by the outgoing EF system  $(u, r)$ . The optical function  $v$  “parametrizes”  $\mathcal{H}^+$  and  $\mathcal{I}^-$  and for this reason it is known as the *advanced time*. The optical function  $u$  “parametrizes”  $\mathcal{H}^-$  and  $\mathcal{I}^+$  and for this reason it is known as the *retarded time*. Summarizing,

$$\mathcal{H}^+ = \{r = M\} \cap \{v \in \mathbb{R}\}, \quad \mathcal{H}^- = \{r = M\} \cap \{u \in \mathbb{R}\}.$$

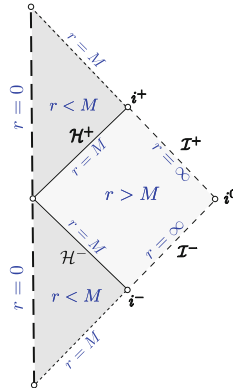
Having obtained a complete picture of the  $r \geq M$  region, let’s move to the  $r < M$ . The extension of ERN covering  $r < M$  can be represented by the domain of the extended (smooth and increasing) functions  $U = U(u')$  and  $V = V(v')$  such that

$$\begin{aligned} U(u') &= -\frac{1}{u'} \text{ for } u' \leq -4, & U(u') &= 1 - \frac{1}{u} \text{ for } u' \geq 4, \\ V(v') &= -1 - \frac{1}{v'} \text{ for } v' \leq -4, & V(v') &= -\frac{1}{v} \text{ for } v' \geq 4, \end{aligned} \tag{2.1.17}$$

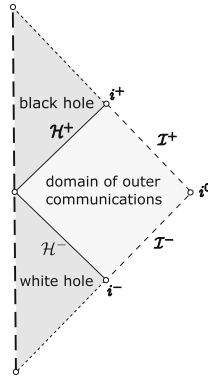
as is shown below



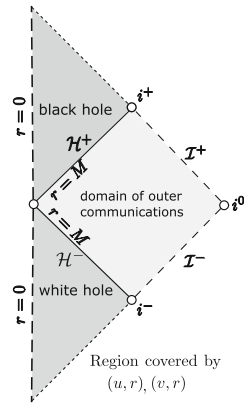
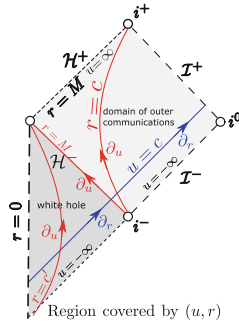
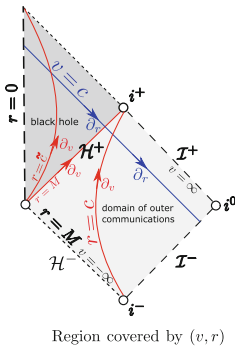
The two shaded regions in the  $U - -V$  plane are covered by two new sets of double null coordinates, namely  $(u', v)$  and  $(v', u)$  as is shown above. The reason we need the new optical functions  $u', v'$  in each of the two regions is because in  $r < M$  the function  $r^*$  behaves differently compared to the region  $r > M$  (see (2.1.4)). Let's use the (blue) notation  $r^*$  for the function  $r^*$  defined for  $r < M$  given by (2.1.3) and (2.1.4). For any given value of the advanced time  $v$  we can pass to  $r < M$  by considering the optical function  $u'$  which, in view of (2.1.14), solves  $u' - v = -2r^*$ . Similarly, for any given value of the retarded time  $u$  we can pass to  $r < M$  by considering the optical function  $v'$  which, in view of (2.1.14), solves  $u - v' = -2r^*$ . The metric with respect to the systems  $(u', v)$  and  $(v', u)$  is given by (2.1.15). The restriction  $U < V$  accounts for the conditions  $u < v'$  and  $u' < v$  which are due to the fact that  $r^* > 0$ . Summarizing, we obtained a representation of ERN in the domain  $\{-1 < U < 1\} \cap \{-1 < V < 1\} \cap \{U < V\}$  of the  $U - V$  plane. Suppressing  $U, V$  the relevant diagram is as follows



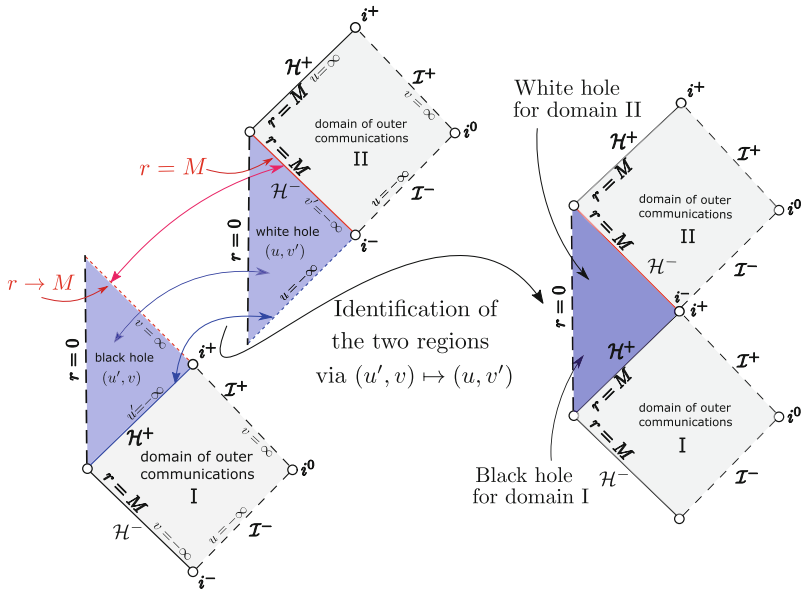
The above representation of ERN allows us to immediately single out the *black hole region* and the *white hole region* as the complement of the past (resp. future) of future (resp. past) null infinity:



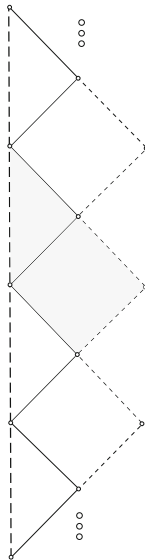
The black hole region and the domain of outer communications are covered by the ingoing EF system  $(v, r)$ . The white hole region and the domain of outer communications are covered by the outgoing EF system  $(u, r)$ . The extended ERN spacetime remains time-oriented by defining the causal vector fields  $\partial_v$  (with respect to  $(v, r)$ ) and  $\partial_u$  (with respect to  $(u, r)$ )—the red vector fields in the figure below—to be future-directed in their respective coordinate charts.



The metric remains analytic in the black hole interior region away from  $r = 0$  and it can be smoothly (non-uniquely) extended. The unique analytic extension is illustrated in the diagram below. Note that the systems  $(u', v)$  and  $(v, u')$  are defined on the same open set of  $\mathbb{R}^2$ .



The hypersurface  $\{r = M\}$  in the black hole interior is the *Cauchy horizon*  $\mathcal{CH}^+$  for the domain of outer communications I. In view of (2.1.17), the metric extends smooth on  $\mathcal{CH}^+$ . By repeating the above process indefinitely we arrive at the Penrose diagram of the maximally extended (analytic) ERN spacetime in the  $U - V$  plane as shown below. A fundamental domain is shaded.

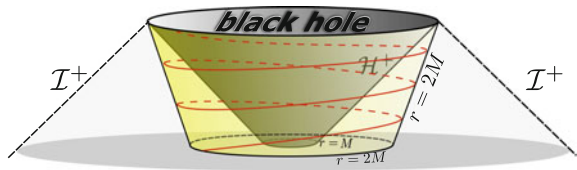


### 2.1.3 Global Properties of ERN

The stationary Killing field  $T$  is normal to the event horizon and, by virtue of (2.1.10), satisfies  $\nabla_T T = 0$ . Hence, *the event horizon in ERN has vanishing surface gravity*. See also Sect. 1.5.2.

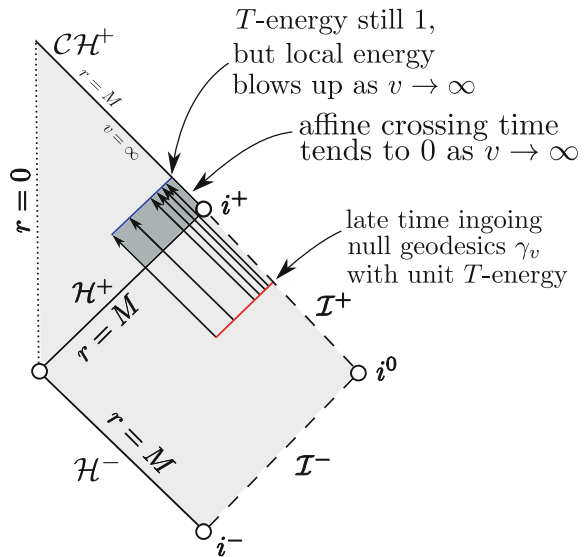
Another important property of ERN is that the timelike hypersurface  $\{r = 2M\}$  is spanned by null geodesics. These null geodesics orbit the black hole region (that is, neither cross the event horizon nor escape at null infinity) and for this reason they are called trapped null geodesics. One of them is depicted by the red curve (Fig. 2.1)

Fig. 2.1 The photon sphere



We conclude with yet another aspect of ERN: Late time ( $v \rightarrow \infty$ ) ingoing null geodesics, emanating from an outgoing null curve (see Fig. 2.2) and normalized such that their  $T$ -energy is one, experience larger and larger local energies after crossing the event horizon. Their  $T$ -energy remains one. However, the vector field  $T$  tends to the null normal on the Cauchy horizon so the  $T$ -energy does not accurately represent the local energy of the geodesics in the region near the Cauchy horizon. Furthermore, the affine time it takes the geodesics to cross the shaded regions below tends to zero as the advanced time  $v \rightarrow \infty$ .

Fig. 2.2 Null geodesics experience large gradients after crossing  $\mathcal{H}^+$



For more details and applications of this property of ERN see [4–6].

### 2.1.4 The Couch–Torrence Conformal Inversion

ERN has a discrete conformal symmetry  $\Phi$  discovered by Couch and Torrence [7]. It is easiest to understand its action in terms of the  $(t, r^*)$  coordinates:

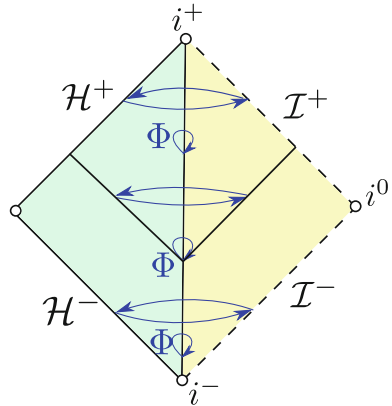
$$\Phi(t, r^*, \theta, \varphi) = (t, -r^*, \theta, \varphi).$$

Recall that  $r^* = 0$  precisely on the photon sphere. Note also that

$$\Phi^{-1} = \Phi.$$

This conformal symmetry “inverses” the domain of outer communications while fixing the photon sphere  $r = 2M$ . It sends the future (resp. past) event horizon to future (resp. past) null infinity and vice versa. It maps the green region below to the yellow region by reversing the spherically symmetric null hypersurfaces emanating from the photon sphere (Fig. 2.3):

**Fig. 2.3** The Couch–Torrence conformal symmetry



It is easy to see that for any point  $p$  in the domain of outer communications we have

$$\Phi^*(g_p) = \Omega^2 \cdot g_{\Phi(p)} \quad \text{with conformal factor} \quad \Omega = \frac{r}{r - M}.$$

In Boyer–Lindquist coordinates  $(t, r)$  the Couch–Torrence inversion takes the form (suppressing the angular coordinates)

$$\Phi(t, r) = (t, r')$$

where

$$r'(r) = M + \frac{M^2}{r - M}. \tag{2.1.18}$$

In double null coordinates we have

$$\Phi(u, v) = (v, u).$$

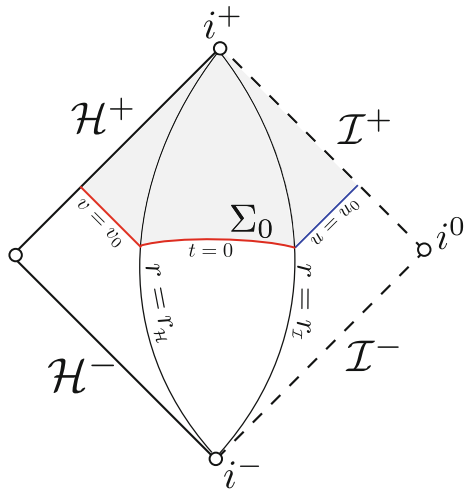
Finally, if  $(u, v)_{in}$  and  $(u, v)_{out}$  denote the ingoing and outgoing EF coordinates, respectively, then

$$\Phi(u = c, r)_{out} = (v = c, r')_{in}.$$

The Couch–Torrence inversion demonstrates that null infinity is in fact a rescaled version of extremal horizons; in fact the near-infinity region is a rescaled version of the near-horizon region. We will call this relation “*the extremal horizon–null infinity correspondence*”. For applications of this correspondence see [8].

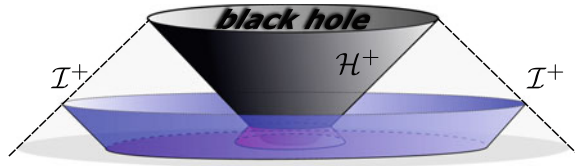
It is convenient to work with hypesurfaces which are **invariant** under the action of the Couch–Torrence inversion. An example of such a hypersurface is  $\{t = 0\}$ . This hypersurface, however, does not cross the event horizon and does not terminate at null infinity. Instead, we consider another spacelike-null hypersurface, which we call  $\Sigma_0$ . The null pieces are given by  $v = v_0 = r^*(r_{\mathcal{H}})$  for  $r \leq r_{\mathcal{H}}$  with  $r_{\mathcal{H}}$  close to  $M$  and by  $u = u_0 = -r^*(r_{\mathcal{I}})$  for  $r_{\mathcal{I}} \leq r$  with  $r_{\mathcal{I}}$  sufficiently large. We assume also that  $r^*(r_{\mathcal{H}}) = -r^*(r_{\mathcal{I}})$ . The spacelike part  $r_{\mathcal{H}} \leq r \leq r_{\mathcal{I}}$  is given by  $t = 0$  (Fig. 2.4).

**Fig. 2.4** The spacelike-null hypersurface  $\Sigma_0$



A heuristic representation of  $\Sigma_0$  is as follows (Fig. 2.5)

**Fig. 2.5** The spacelike-null hypersurface  $\Sigma_0$  with the blue and red pieces



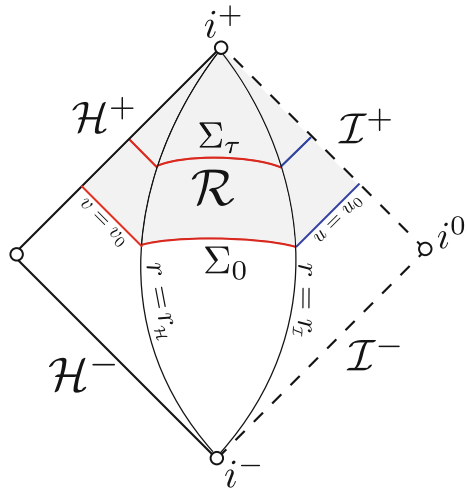
## 2.2 The Horizon Instability of ERN

Our goal is to investigate the late-time behavior of solutions to the wave equation

$$\square_g \psi = 0$$

on ERN. We consider initial data on the Cauchy hypersurface  $\Sigma_0$  (as in the previous section) and we study the behavior of  $\psi|_{\Sigma_\tau}$  and derivatives  $\partial^k \psi|_{\Sigma_\tau}$ ,  $k \geq 1$ , for  $\tau > 0$ , where  $\Sigma_\tau = F_\tau^T(\Sigma_0)$  and where  $F_\tau^T$  denotes the flow of the stationary Killing vector field  $T$  (Fig. 2.6).

**Fig. 2.6** The spacelike-null foliation  $\Sigma_\tau$



The wave equation on ERN in ingoing Eddington–Finkelstein  $(v, r, \theta, \varphi)$  coordinates takes the form

$$\square_g \psi = D \partial_r \partial_r \psi + 2 \partial_v \partial_r \psi + \frac{2}{r} \partial_v \psi + R \partial_r \psi + \Delta \psi = 0 \quad (2.2.1)$$

where  $D(r) = (1 - \frac{M}{r})^2$  and  $R(r) = \frac{dD}{dr} + \frac{2D}{r}$ . Here we denote

$$\Delta = \frac{1}{r^2} \Delta_{\mathbb{S}^2},$$

where  $\Delta_{\mathbb{S}^2}$  is the standard Laplacian on the unit round sphere  $\mathbb{S}^2$ .

We next review the “horizon instability of extremal black holes” established in [9–12].

### 2.2.1 Conservation Laws Along the Event Horizon

Define the spherical sections  $S_\tau = \Sigma_\tau \cap \mathcal{H}^+$  of the event horizon. Considering the spherical mean of the wave equation (2.2.1) on the event horizon and using that  $D(M) = \frac{dD}{dr}(M) = 0$  yields

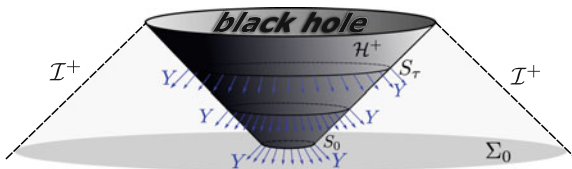
$$\partial_v \left( \int_{S_\tau} (2\partial_r \psi + 2M^{-1}\psi) M^2 d\Omega \right) = 0.$$

Since  $\partial_v$  is null and normal to the event horizon  $\mathcal{H}^+$ , it immediately follows that the surface integrals

$$H_0[\psi] := -\frac{1}{4\pi} \int_{S_\tau} \partial_r(r\psi) M^2 d\Omega \tag{2.2.2}$$

are independent of  $\tau$ . Here  $\Omega = (\theta, \varphi) \in \mathbb{S}^2$  and  $d\Omega = \sin \theta d\theta d\varphi$ . Recall that the vector field  $\partial_r$  is transversal to the event horizon (Fig. 2.7):

**Fig. 2.7** The sections  $S_\tau$  of  $\mathcal{H}^+$  and the transversal  $\partial_r$  vector field  $\partial_r$



This gives rise to a conservation law along the event horizon. Note that the relation  $\frac{dD}{dr}(M) = 0$  follows from the fact that the surface gravity of the event horizon of ERN vanishes. An analogous conservation law holds for each projection on the eigenspace of the angular Laplacian. Indeed, it can be similarly shown that if  $\psi_\ell$  denotes the projection of  $\psi$  on the eigenspace  $E_\ell$  of  $\Delta$  with eigenvalue  $-\frac{\ell(\ell+1)}{r^2}$ , then the following higher order derivative transversal to  $\mathcal{H}^+$

$$\partial_r^\ell \left( r \partial_r (r \psi_\ell) \right),$$

is constant along the null generators of the event horizon. Concluding, we have

- **Hierarchy of conservation laws on ERN:** *for every fixed angular frequency  $\ell$  we have a conservation law along the event horizon involving exactly the first  $\ell + 1$  translation-invariant, transversal derivatives of the scalar field on the event horizon.*

### 2.2.2 Non-decay and Blow-up for Transversal Derivatives

The previous conservation laws on the event horizon provide non-trivial *obstructions to decay*, since the derivative  $\partial_r$  is translation-invariant (since  $[\partial_r, \partial_v] = 0$ ) and hence carries not growing  $v$  weights. Recall that the surface integrals  $-\frac{1}{4\pi} \int_{S_\tau} (\partial_r \psi + M^{-1} \psi) d\Omega$  are conserved. Furthermore, for generic initial data on  $\Sigma_0$  we have  $-\frac{1}{4\pi} \int_{S_0} (\partial_r \psi + M^{-1} \psi) d\Omega = \frac{1}{M^3} H_0[\psi] \neq 0$ . Assuming for now that  $|\psi| \rightarrow 0$  as  $\tau \rightarrow 0$  (this is true; we will in fact present the precise asymptotics in the next section), we conclude the following

- **Non-decay:** *the spherical mean of the transversal derivative generically does not decay along the event horizon of ERN. In fact,*

$$-\frac{1}{4\pi} \int_{S_\tau} \partial_r \psi d\Omega \rightarrow \frac{1}{M^3} H_0[\psi], \text{ as } \tau \rightarrow \infty.$$

It was observed in [13] that the above non-decay result implies that *the component  $\mathbf{T}_{rr}[\psi]$  of the energy-momentum tensor of the scalar field  $\psi$  does not decay along  $\mathcal{H}^+$* . In fact, we have

$$\frac{1}{4\pi} \int_{S_\tau} \mathbf{T}_{rr}[\psi] d\Omega \rightarrow \frac{1}{M^6} (H_0[\psi])^2.$$

Since,  $\mathbf{T}_{rr}[\psi]$  is related to the energy density measured by an observer crossing  $\mathcal{H}^+$ , the authors of [13] concluded that the conserved charge  $H_0[\psi]$  might be thought of as “hair” of the extremal event horizon since it does not disappear in the evolution along the horizon.

On the other hand, as we shall see in Chap. 4,  $\psi$  and all higher order derivatives  $\partial_r^k \psi, k \geq 1$  decay along the hypersurfaces  $\{r = r_0 > M\}$  away from the event horizon  $\mathcal{H}^+$ . The non-decaying transversal derivative along the event horizon suggests that *the decay rate of  $\psi$  along the event horizon is slower than the decay rate of  $\psi$  away from the horizon*. We will see in the next section that this is indeed correct. In view of the decay of  $\psi$  and all its derivatives away from the horizon, it makes sense to refer to  $H_0$  as the “horizon hair” of  $\psi$ . It is important to remark that *the results outlined in this brief yield a way in potentially measuring this hair from observations along null infinity*. See Sect. 2.4.1.

By commuting the wave equation (2.2.1) with  $\partial_r$ , restricting on the event horizon and using the previous results we conclude the following

- **Blow-up:** *the spherical mean of higher-order transversal derivatives generically blows up along the event horizon of ERN. In fact,*

$$\frac{1}{4\pi} \int_{S_\tau} |\partial_r^k \psi| d\Omega \geq c_k \cdot H_0[\psi] \cdot \tau^{k-1}, \text{ as } \tau \rightarrow \infty.$$

Furthermore, for any  $\epsilon > 0$ , the following *higher-order energy blow-up* result generically holds:

$$\int_{\Sigma_\tau \cap \{r \leq M + \epsilon\}} (\partial_r^k \psi)^2 d\mu_{\Sigma_\tau} \rightarrow \infty$$

for all  $k \geq 2$  as  $\tau \rightarrow \infty$ .

The growth along the horizon and decay away from it for higher derivatives is illustrated in the figure below where the blue color represents the magnitude of the second order radial derivatives of  $\psi$ .



As we shall see, the horizon instability holds even for initial data which are supported away from the horizon (and hence satisfy  $H_0 = 0$ ). An extension of the above instabilities to linearized electromagnetic and gravitational perturbations of ERN was presented by Lucietti, Murata, Reall and Tanahashi [13] and by Sela [14]. Nonlinear extensions have been presented in [5, 15–19]. For higher-dimensional extensions we refer to [20, 21]. For a more detailed discussion of works in the physics literature see the next section.

### 2.3 The Precise Late-Time Asymptotics

The above results do *not* provide an insight into the precise asymptotic behavior for  $\psi$ . There is extensive work in the physics literature regarding late-time asymptotics for scalar fields on extremal Reissner–Nordström via heuristic or numerical methods, see [13, 14, 22–27] and the subsequent sections for more details. A derivation and rigorous proof of the late-time asymptotics was obtained in [28]. In this section we will review the main results of [28]. As we shall see, the *exact coefficients of the leading-order terms in the asymptotic estimates are obtained in terms of explicit expressions of the initial data*. An overview of the proofs is given in Chap. 4.

### 2.3.1 Scalar Perturbations of Type A, B, C, and D

We introduce four types of perturbations. As we shall see, each of these types requires a separate treatment and exhibits different asymptotic behavior. Recall that ERN admits two independent conserved charges: (1) the horizon charge  $H_0[\psi]$  given by (2.2.2), and (2) the Newman–Penrose constant  $I_0[\psi]$  at null infinity given by (1.8.4). It is important to emphasize that the values of  $H_0[\psi]$  and  $I_0[\psi]$  depend **only** on the initial data of  $\psi$ . Compactly supported initial data satisfy  $I_0[\psi] = 0$  and data supported away from the horizon satisfy  $H_0[\psi] = 0$ .

- Initial data on a Cauchy hypersurface  $\Sigma_0$  are called **horizon-penetrating** if the horizon charge  $H_0[\psi] \neq 0$ .
- Initial data on a Cauchy hypersurface  $\Sigma_0$  are called **null-infinity-extending** if the Newman–Penrose constant  $I_0[\psi] \neq 0$ .

In the physics literature, the latter data are said to have an “initial static moment”. We will consider the following four types of initial data.

**Type A:** *Compactly supported data but horizon-penetrating.*

These data should be thought of as local data in the sense that they reflect perturbations in a neighborhood of the event horizon.



**Type B:** *Compactly supported data and supported away from the event horizon.*

These data correspond to compact perturbations from afar, that is away from the event horizon.



**Type C:** *Null-infinity-extending and horizon-penetrating data.*

These data correspond to global perturbations with non-trivial support across the whole initial hypersurface  $\Sigma_0$ .



**Type D:** *Null-infinity-extending but supported away from the horizon data.*

These data correspond to perturbations from afar extending all the way to null infinity.



### 2.3.2 Review of Physics Literature

#### The Blaksley–Burko Asymptotic Analysis

The first work on asymptotics of scalar fields on ERN goes back to 1972 when Bičák suggested in [29] that scalar fields  $\psi_\ell$  on ERN with non-vanishing Newman–Penrose constant and with angular frequency  $\ell$  decay with the rate  $\frac{1}{t^{\ell+2}}$ . However, this result was shown to be false in 2007 when Blaksley and Burko [24] performed a more accurate heuristic and numerical analysis. Their work considered data of Type **B** and **C**. Define  $\mu \in \{0, 1\}$  such that  $\mu = 0$  for data of Type **B** and  $\mu = 1$  for data of Type **C**. The authors argued that the *sharp* decay rates for the scalar field are the following:

- Away  $\mathcal{H}^+$  and  $\mathcal{I}^+$ :  $|\psi_\ell|_{r=r_0 > M}$  decays like  $\frac{1}{\tau^{2\ell+2+\mu}}$ ,
- On  $\mathcal{H}^+$ :  $|\psi_\ell|_{\mathcal{H}^+}$  decays like  $\frac{1}{\tau^{\ell+1+\mu}}$ ,
- On  $\mathcal{I}^+$ :  $|r\psi_\ell|_{\mathcal{I}^+}$  decays like  $\frac{1}{\tau^{\ell+1+\mu}}$ .

Reference [24] did not obtain the precise late-time asymptotics in the above two cases. Moreover, [24] did not study other types of initial data, and in particular, did not study horizon penetrating compactly supported initial data.

#### The Lucietti–Murata–Reall–Tanahashi Numerical Analysis

The asymptotic analysis of Lucietti–Murata–Reall–Tanahashi [13] was the first work to numerically investigate the precise late-time asymptotics for scalar fields on ERN. Their first major result is the following precise late-time asymptotics for Type **A** perturbations

$$M \cdot \psi|_{\mathcal{H}^+} \sim 2H_0[\psi] \cdot \frac{1}{\tau} + 4MH_0[\psi] \cdot \frac{\log \tau}{\tau^2}, \quad \text{as } \tau \rightarrow \infty. \quad (2.3.1)$$

Furthermore, the authors suggested, using a near-horizon calculation, that the following precise late-time asymptotic behavior off the horizon along  $r = r_0 > M$  holds:

$$\psi|_{\{r=r_0\}} \sim \frac{4M}{r_0 - M} H_0[\psi] \cdot \frac{1}{\tau^2}, \quad \text{as } \tau \rightarrow \infty. \quad (2.3.2)$$

Moreover, the authors, extrapolating from numerical simulations for the  $\ell = 1, 2$  angular frequencies, found the following sharp rate off the horizon along  $r = r_0 > M$

$$|\psi_\ell|_{\{r=r_0\}} \text{ decays like } \frac{1}{\tau^{2\ell+2}}. \quad (2.3.3)$$

For Type **B** perturbations, the authors obtained the following asymptotic statement

$$\psi|_{\mathcal{H}^+} \sim \frac{C_0}{\tau^2}, \text{ as } \tau \rightarrow \infty. \quad (2.3.4)$$

However, the constant  $C_0$  was not explicitly computed in terms of the initial data. Another important question that was first raised and investigated in [13] is whether one can trigger the horizon instability using ingoing radiation; that is, using perturbations which are initially supported away from the event horizon and hence necessarily satisfy  $H_0[\psi] = 0$ . The authors found the following stability results

$$|\psi|_{\mathcal{H}^+} \rightarrow 0, \quad |\partial_r \psi|_{\mathcal{H}^+} \rightarrow 0 : \text{ along } \mathcal{H}^+,$$

and uncovered the following (generic) instability behavior

$$|\partial_r^2 \psi|_{\mathcal{H}^+} \rightarrow 0 \quad |\partial_r^3 \psi|_{\mathcal{H}^+} \rightarrow \infty : \text{ along } \mathcal{H}^+.$$

This instability behavior, which has also been discussed in [30], was subsequently rigorously proved in [31].

Reference [13] also investigated the late-time behavior of massive scalar fields which solve  $\square_g \psi = m^2 \psi$ . For such massive fields it is widely believed that the late-time behavior is dominated by the  $\omega = m$  frequency (instead of the  $\omega = 0$  frequency for massless fields on sub-extremal black holes) which leads to damped oscillations. In particular, massive fields and all their derivatives are expected to decay like  $\tau^{-\frac{5}{6}}$  in the domain of outer communications (up to and including the event horizon) of a sub-extremal black hole. Reference [13] found that this remains true on ERN backgrounds off the horizon (a result that had also been seen in [32]). On the other hand, [13] found that the horizon instability persists for a *discrete* set of masses  $m^2$ . Specifically, if  $(mM)^2 = n(n+1)$  then the authors argued that

$$|\partial_r^{n+1} \psi|_{\mathcal{H}^+} \rightarrow 0 \quad |\partial_r^{n+2} \psi|_{\mathcal{H}^+} \rightarrow \infty : \text{ along } \mathcal{H}^+.$$

More generally, the numerical analysis of [5] suggests the following asymptotic behavior for *general* masses  $m^2$ :

$$\partial_r^k \psi \text{ behaves like } \tau^{k-\frac{1}{2}-\sqrt{(mM)^2+\frac{1}{4}}},$$

for all  $k \geq 0$ . A rigorous proof of the above statements for massive fields is an open problem.

### The Ori–Sela Asymptotic Analysis

Ori [25] and Sela [26] used the conservation laws that hold for each fixed angular frequency  $\ell$  (see Sect. 2.2.1) to heuristically obtain the precise late-time asymptotics of  $\psi_\ell$  for Type **A** perturbations. Specifically, Ori and Sela found the following asymptotics along  $r = r_0 > M$  off the horizon:

$$\psi_\ell|_{\{r=r_0\}} \sim (-4)^{\ell+1} e M^{3\ell+2} \frac{r}{(r-M)^{\ell+1}} \cdot \frac{1}{\tau^{2\ell+2}}, \quad \text{as } \tau \rightarrow \infty,$$

where  $e$  is an explicit expression of the conserved charge  $H_\ell[\psi_\ell]$  for  $\psi_\ell$ . Hence, the above result improves the statement (2.3.3) of [13].

Furthermore, Ori and Sela derived the precise late-time asymptotics of  $\psi_\ell$  along the horizon

$$\psi_\ell|_{\mathcal{H}^+} \sim e(-M)^{\ell+1} \cdot \frac{1}{\tau^{\ell+1}}, \quad \text{as } \tau \rightarrow \infty,$$

where  $e$  is as above. Sela [14] subsequently used the decay rates obtained in [25, 26] in order to obtain decay rates for the coupled electromagnetic and gravitational system for ERN. Recently, [33] supported the validity of the above rates using Fourier based arguments.

### 2.3.3 The New Horizon Charge $H_0^{(1)}[\psi]$

We introduce the *dual* scalar field  $\tilde{\psi}$  of  $\psi$  given by

$$\tilde{\psi} = \frac{M}{r-M} \psi \circ \Phi, \quad (2.3.5)$$

where  $\Phi$  denotes the Couch–Torrence conformal inversion (see Sect. 2.1.4). Observe that  $\tilde{\tilde{\psi}} = \psi$  and that  $\psi$  satisfies the wave equation on ERN if and only if its dual  $\tilde{\psi}$  satisfies the wave equation on ERN. References [30, 34] showed that this duality can be used to relate the horizon charge with the Newman–Penrose constant as follows:

$$H_0[\psi] = I_0[\tilde{\psi}].$$

Recall that if the Newman–Penrose constant vanishes  $I_0[\psi] = 0$  then one can define the time-inverted Newman–Penrose constant  $I_0^{(1)}[\psi]$ , given by (1.8.7), which is finite and conserved (see Sect. 1.8.2). Note that  $I_0^{(1)}[\psi]$  is only defined for initial data of Type **A** and **B**.

Note next that the dual of perturbations of Type **B** and **D** is of Type **B** and **A**, respectively. Hence, if  $H_0[\psi] = 0$  (which holds for Type **B** and **D** perturbations) then we can introduce the following

$$H_0^{(1)}[\psi] := I_0^{(1)}[\tilde{\psi}]. \quad (2.3.6)$$

We will refer to  $H_0^{(1)}[\psi]$  as the *time-inverted horizon charge*. Clearly,  $H_0^{(1)}[\psi]$  is only defined for initial data of type **B** and **D**.

As we shall see,  $H_0^{(1)}[\psi]$  plays a fundamental role in understanding the asymptotics for Type **B** and **D** perturbations.

We will next outline the asymptotics derived in [28].

### 2.3.4 Asymptotics for Type C Perturbations

We first consider **global** perturbations of Type C. These perturbations satisfy  $H_0 \neq 0$  and  $I_0 \neq 0$ . The non-vanishing of the conserved constants  $H_0$  and  $I_0$  allows for the possibility that they appear in a potentially complicated way in the asymptotics for  $\psi$ . In fact, [13] conjectured that both  $H_0$  and  $I_0$  appear in the asymptotics of  $\psi$  along the event horizon  $\mathcal{H}^+$ . This conjecture was falsified in [28] where it was shown that *the asymptotics along the event horizon are independent of the Newman–Penrose constant  $I_0$* :

$$r\psi|_{\mathcal{H}^+} \sim 2H_0[\psi] \cdot \frac{1}{\tau} + 4MH_0[\psi] \cdot \frac{\log \tau}{\tau^2} \quad \text{as } \tau \rightarrow \infty. \quad (2.3.7)$$

On the other hand, it was shown that *both constants  $H_0$  and  $I_0$  appear in the leading-order terms for the late-time asymptotics of  $\psi|_{\{r=r_0\}}$  along  $r = r_0$  hypersurfaces away from the event horizon ( $r_0 > M$ )*:

$$\psi|_{\{r=r_0\}} \sim \left( 4I_0[\psi] + \frac{4M}{r-M} H_0[\psi] \right) \cdot \frac{1}{\tau^2} \quad \text{as } \tau \rightarrow \infty. \quad (2.3.8)$$

The proof of (2.3.8) is particularly subtle since both the horizon region and the null infinity region contribute to the asymptotics of  $\psi|_{\{r=r_0\}}$  via the constants  $H_0$  and  $I_0$ , respectively. This is in stark contrast with the sub-extremal case (see Sect. 1.8.3) where the dominant terms originate only from the null infinity region. Note that *the coefficient  $\frac{4M}{r-M}$  of  $H_0$  is itself a static solution on ERN*. We remark that to show the asymptotics (2.3.8), we need to derive first the asymptotics for the radial derivative<sup>2</sup>  $\partial_\rho \psi$  of  $\psi$  along  $\Sigma_0$ :

$$\partial_\rho \psi|_{\{r=r_0\}} \sim -\frac{4M}{(r-M)^2} H_0[\psi] \cdot \frac{1}{\tau^2} \quad \text{as } \tau \rightarrow \infty. \quad (2.3.9)$$

The crucial insight of (2.3.9) is that *the leading-order asymptotics of  $\partial_\rho \psi|_{\{r=r_0\}}$  are independent of  $I_0$  for all values of  $r_0 > M$* ! This is somewhat surprising; it shows that only the near-horizon region contributes to the asymptotics of  $\partial_\rho \psi$  and not, in particular, the near-infinity region. Furthermore, note that the decay rate of  $\partial_\rho \psi|_{\{r=r_0\}}$  is only  $\tau^{-2}$  which is equal to the decay rate of  $\psi$ . This is again in stark contrast with the sub-extremal case where  $\partial_\rho \psi|_{\{r=r_0\}}$  decays like  $\tau^{-3}$ .

The following asymptotics have been derived along null infinity  $\mathcal{I}^+$ :

---

<sup>2</sup>With respect to the coordinate system  $(\rho = r, \theta, \varphi)$  on  $\Sigma_0$ .

$$r\psi|_{\mathcal{I}^+} \sim 2I_0[\psi] \cdot \frac{1}{\tau} + 4MI_0[\psi] \cdot \frac{\log \tau}{\tau^2} \quad \text{as } \tau \rightarrow \infty. \quad (2.3.10)$$

Note that these asymptotics are independent of the horizon charge  $H_0$ .

### 2.3.5 Asymptotics for Type A Perturbations

We next consider horizon-penetrating perturbations of Type **A**. These perturbations, which satisfy  $H_0 \neq 0$  and  $I_0 = 0$ , are the most physically relevant since they represent **local** perturbations of ERN. In the physics literature, they represent *outgoing radiation*.

The asymptotics (2.3.7) along  $\mathcal{H}^+$ , and (2.3.8) and (2.3.9) along  $\{r = r_0\}$  hold in this case as well, where in (2.3.8) we have to use that  $I_0 = 0$ . On the other hand, the asymptotics along null infinity for the radiation field  $r\psi|_{\mathcal{I}^+}$  cannot be read off from (2.3.10). Instead, the following asymptotics were derived in [28]

$$r\psi|_{\mathcal{I}^+} \sim \left(4MH_0[\psi] - 2I_0^{(1)}[\psi]\right) \cdot \frac{1}{\tau^2} \quad \text{as } \tau \rightarrow \infty. \quad (2.3.11)$$

Here  $I_0^{(1)}$  is the time-inverted Newman–Penrose constant given by (1.8.7). We observe that for Type **A** perturbations the dominant term in the asymptotics of the radiation field  $r\psi|_{\mathcal{I}^+}$  contains the horizon charge  $H_0$ . Therefore, the precise asymptotics (2.3.11) yield a way to potentially measure the horizon charge  $H_0$  and hence detect the horizon instability of extremal black holes from observations in the far away radiation region. For more on this see Sect. 2.4.1.

### 2.3.6 Asymptotics for Type B Perturbations

Perturbations of Type **B** satisfy  $H_0 = 0$  and  $I_0 = 0$  and hence represent **local** perturbations **from afar**. In the physics literature, such perturbations represent *ingoing radiation*.

Recall that Lucietti–Murata–Reall–Tanahashi [13] numerically demonstrated that such perturbations exhibit a *weaker* version of the horizon instability (see Sect. 2.3.2), namely

$$|\psi|_{\mathcal{H}^+} \rightarrow 0, \quad |\partial_r \psi|_{\mathcal{H}^+} \rightarrow 0, \quad |\partial_r^2 \psi|_{\mathcal{H}^+} \rightarrow 0, \quad |\partial_r^3 \psi|_{\mathcal{H}^+} \rightarrow \infty : \quad \text{along } \mathcal{H}^+. \quad (2.3.12)$$

Perturbations of Type **B** which exhibit the above behavior were rigorously constructed in [31]. However, [31] did not provide a necessary and sufficient condition for perturbations of Type **B** so that (2.3.12) holds. Such a condition and moreover

the precise late-time asymptotics for all perturbations of Type **B** were obtained in [28].

Recall that the horizon charge  $H_0^{(1)}[\psi]$  given by (2.3.6) is well-defined for all Type **B** perturbations. It turns out that *the weak horizon instability (2.3.12) holds if and only if  $H_0^{(1)}[\psi] \neq 0$* . Specifically,

$$\partial_r^2 \psi \sim \frac{1}{M^5} H_0^{(1)}[\psi], \quad \partial_r^3 \psi \sim -\frac{3}{M^7} H_0^{(1)}[\psi] \cdot \tau \quad \text{as } \tau \rightarrow \infty. \quad (2.3.13)$$

In fact,  $H_0^{(1)}[\psi]$  determines the leading-order asymptotics along the event horizon

$$r\psi|_{\mathcal{H}^+} \sim -2H_0^{(1)}[\psi] \cdot \frac{1}{\tau^2} \quad \text{as } \tau \rightarrow \infty. \quad (2.3.14)$$

On the other hand, the asymptotics of the radiation field depend **only** on the value of the time-inverted Newman–Penrose constant  $I_0^{(1)}$ :

$$r\psi|_{\mathcal{I}^+} \sim -2I_0^{(1)}[\psi] \cdot \frac{1}{\tau^2} \quad \text{as } \tau \rightarrow \infty. \quad (2.3.15)$$

Finally, the asymptotics along  $\{r = r_0\}$  depend on the value of both constants  $H_0^{(1)}[\psi]$  and  $I_0^{(1)}[\psi]$ :

$$\psi|_{\{r=r_0\}} \sim -8 \left( I_0^{(1)}[\psi] + \frac{M}{r-M} H_0^{(1)}[\psi] \right) \cdot \frac{1}{\tau^3} \quad \text{as } \tau \rightarrow \infty. \quad (2.3.16)$$

Note the decay rate of (2.3.16) agrees with the decay rate of (1.8.9) for Schwarzschild spacetimes. However, in contrast to Schwarzschild, the coefficient of the asymptotic term in (2.3.16) depends additionally on the new horizon charge  $H_0^{(1)}[\psi]$ .

### 2.3.7 Asymptotics for Type **D** Perturbations

Type **D** perturbations satisfy  $H_0 = 0$  and  $I_0 \neq 0$  and admit a well-defined  $H_0^{(1)}$ . The first result for this case shows that the radiation field  $r\psi|_{\mathcal{I}^+}$  and the scalar field  $\psi|_{\{r=r_0\}}$  “see” to leading order **only**  $I_0$ :

$$r\psi|_{\mathcal{I}^+} \sim 2I_0[\psi] \cdot \frac{1}{\tau}, \quad \psi|_{\{r=r_0\}} \sim 4I_0[\psi] \cdot \frac{1}{\tau^2} \quad \text{as } \tau \rightarrow \infty.$$

On the other hand, the asymptotics along  $\mathcal{H}^+$  to leading order to depend on **both**  $I_0$  and the horizon charge  $H_0^{(1)}$ :

$$r\psi|_{\mathcal{H}^+} \sim \left(4MI_0 - 2H_0^{(1)}[\psi]\right) \cdot \frac{1}{\tau^2} \quad \text{as } \tau \rightarrow \infty.$$

Type **D** perturbations exhibit the weak version of the horizon instability. Indeed, the exact non-decay and blow-up along the event horizon results given by (2.3.13) hold for Type **D** perturbations as well. In contrast to Type **A** perturbations, the derivative  $\partial_r \psi$  decays faster than  $\psi$  away from the horizon:

$$\partial_r \psi|_{\{r=r_0\}} \sim \left( \frac{8M}{(r-M)^2} \cdot H_0^{(1)} + \frac{8(r^2 - M^2)}{(r-M)^2} \cdot I_0 \right) \cdot \tau^{-3}.$$

### 2.3.8 Asymptotics for Higher Order Derivatives

In this section we will present the asymptotics for the higher order derivatives  $\partial_r^k T^m \psi$ . We will consider Type **A** data and hence that  $H_0[\psi] \neq 0$ . For simplicity, we will present the asymptotics only along the event horizon. Define

$$a_{k+1} = -\frac{k(k+1)}{2M^2}, \quad \text{for } k \geq 1 \text{ and } a_1 = \frac{1}{M^2}, \quad (2.3.17)$$

and

$$c_k = (-1)^{k-1} \frac{k!}{(2M^2)^{k-1}} \cdot c_1 = (-1)^k \frac{1}{M^3} \frac{k!}{(2M^2)^{k-1}}, \quad \text{for } k \geq 1. \quad (2.3.18)$$

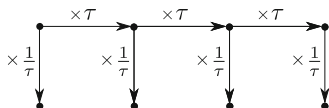
The asymptotics of the higher-order derivatives along  $\mathcal{H}$  are as follows

$$\begin{aligned} \partial_r^k \psi &\sim c_k \cdot H_0 \cdot \tau^{k-1}, \quad k \geq 1, \\ \partial_r^{m+j} T^m \psi &\sim \prod_{i=1}^{j+m} a_i \cdot c_m \cdot H_0 \cdot \tau^{m-1}, \quad j \geq 1, \\ T^m \psi &\sim (-1)^m \cdot \frac{2}{M} \cdot m! \cdot H_0 \cdot \frac{1}{\tau^{m+1}}, \quad m \geq 0, \\ \partial_r^m T^{m+j} \psi &\sim (-1)^j \prod_{i=1}^m a_i \cdot (j+1)! \cdot H_0 \cdot \frac{1}{\tau^{2+j}}, \quad m \geq 1, \quad j \geq 0. \end{aligned} \quad (2.3.19)$$

The black terms decay in time, the blue terms converge to non-zero constants and the red terms grow unboundedly. It might be easier to illustrate this using the table below

$\psi$	$\partial_r \psi$	$\partial_r^2 \psi$	$\partial_r^3 \psi$	$\partial_r^4 \psi$	$\partial_r^5 \psi$	•
$T\psi$	$\partial_r T\psi$	$\partial_r^2 T\psi$	$\partial_r^3 T\psi$	$\partial_r^4 T\psi$	$\partial_r^5 T\psi$	•
$T^2\psi$	$\partial_r T^2\psi$	$\partial_r^2 T^2\psi$	$\partial_r^3 T^2\psi$	$\partial_r^4 T^2\psi$	$\partial_r^5 T^2\psi$	•
$T^3\psi$	$\partial_r T^3\psi$	$\partial_r^2 T^3\psi$	$\partial_r^3 T^3\psi$	$\partial_r^4 T^3\psi$	$\partial_r^5 T^3\psi$	•
$T^4\psi$	$\partial_r T^4\psi$	$\partial_r^2 T^4\psi$	$\partial_r^3 T^4\psi$	$\partial_r^4 T^4\psi$	$\partial_r^5 T^4\psi$	•
•	•	•	•	•	•	•

A horizontal, resp. vertical, step in the above table results in a multiplication by  $\tau$ , resp.  $\frac{1}{\tau}$  of the respective sharp rates as is shown below



The bold black terms decay one power faster than what results from the above rule and hence form a *skip*. This skip was also previously observed in [27]. The decay rates can be summarized as follows

$$\partial_r^k T^m \psi \sim \tau^{k-m-1-\epsilon(k,m)}, \quad \epsilon(k,m) = \begin{cases} 0, & \text{if } k = 0 \text{ or } k \geq m + 1, \\ 1, & \text{if } 1 \leq k \leq m. \end{cases} \quad (2.3.20)$$

For overview of the proof of this skip, see Sect. 4.8.7. Hadar and Reall [19] showed that (2.3.20) implies that *the scalar invariants*  $|\nabla^k \psi|^2$  *decay in time*. Similar decay results were presented in [35, 36]. Let's briefly recall the argument of [19]. First of all note that the Christoffel symbols vanish on the event horizon  $\Gamma_{bc}^a = 0$ , with  $a, b, c \in \{v, r\}$ , and hence, if  $\partial_{i_1}, \dots, \partial_{i_k} \in \{v, r\}$  then  $\nabla^k \psi_{i_1 \dots i_k} = \partial_{i_1} \dots \partial_{i_k} \psi$  on the event horizon. Then,

$$\begin{aligned} |\nabla^k \psi|^2 &\sim \sum_{k_1+k_2=k} \partial_r^{k_1} T^{k_2} \psi \cdot \partial_r^{k_2} T^{k_1} \psi \sim \sum_{k_1+k_2=k} \tau^{k_1-k_2-1-\epsilon(k_1,k_2)} \cdot \tau^{k_2-k_1-1-\epsilon(k_2,k_1)} \\ &\sim \sum_{k_1+k_2=k} \tau^{-2-\epsilon(k_1,k_2)-\epsilon(k_2,k_1)} \sim \tau^{-2} \end{aligned}$$

for all  $k \geq 1$ , since  $\epsilon(k_1, k_2), \epsilon(k_2, k_1) \geq 0$  and  $\epsilon(k, 0) = \epsilon(0, k) = 0$ . Note that the decay rate for  $|\nabla^k \psi|^2$  is independent of  $k$ .

### 2.3.9 Summary of the Precise Asymptotics

In this section we summarize the asymptotics for scalar perturbations  $\psi$  on ERN. The global asymptotics are given in the table below

Data	Asymptotics of $\psi$
Type A	$4I_0^{(1)}[\psi] \cdot T\left(\frac{1}{u-v}\right) + \frac{4M}{r-M} H_0[\psi] \cdot T\left(\frac{1}{u(v+4M-2r)}\right)$
Type B	$4\left(I_0^{(1)}[\psi] + \frac{M}{r-M} H_0^{(1)}[\psi]\right) \cdot T\left(\frac{1}{v-u}\right)$
Type C	$\left(4I_0[\psi] + \frac{4M}{r-M} H_0[\psi]\right) \cdot \frac{1}{u-v}$
Type D	$\frac{4r}{r-M} H_0^{(1)}[\psi] \cdot T\left(\frac{1}{u-v}\right) + 4I_0[\psi] \cdot \frac{1}{v(u+2M-2M^2(r-M)^{-1})}$

The asymptotics on  $\mathcal{H}^+$ ,  $r = r_0$  and  $\mathcal{I}^+$ , as special cases of the above table, are given in Table 2.1.

**Table 2.1** Asymptotics for  $\psi$

Data	Asymptotics		
	$r\psi _{\mathcal{H}^+}$	$\psi _{\{r=r_0\}}$	$r\psi _{\mathcal{I}^+}$
Type A	$2H_0 \cdot \tau^{-1}$	$\frac{4M}{r-M} H_0 \cdot \tau^{-2}$	$\left(4MH_0 - 2I_0^{(1)}\right) \cdot \tau^{-2}$
Type B	$-2H_0^{(1)} \cdot \tau^{-2}$	$-8\left(I_0^{(1)} + \frac{M}{r-M} H_0^{(1)}\right) \cdot \tau^{-3}$	$-2I_0^{(1)} \cdot \tau^{-2}$
Type C	$2H_0 \cdot \tau^{-1}$	$4\left(I_0 + \frac{M}{r-M} H_0\right) \cdot \tau^{-2}$	$2I_0 \cdot \tau^{-1}$
Type D	$\left(4MI_0 - 2H_0^{(1)}\right) \cdot \tau^{-2}$	$4I_0 \cdot \tau^{-2}$	$2I_0 \cdot \tau^{-1}$

The asymptotic expressions for  $T^k\psi$  for all  $k \geq 0$  can be (informally) computed by taking the  $\frac{\partial^k}{\partial \tau^k}$  derivative of the expressions in Table 2.1. At the horizon, we have the following asymptotics for the higher order transversal derivatives  $\partial_r^k\psi$  revealing the strong horizon instability for Type A and C and the weak horizon instability for Type B and D (Table 2.2).

**Table 2.2** Strong (blue) and weak (red) horizon instability

Data	Asymptotics			
	$\partial_r\psi _{\mathcal{H}^+}$	$\partial_r^2\psi _{\mathcal{H}^+}$	$\partial_r^3\psi _{\mathcal{H}^+}$	$\partial_r^k\psi _{\mathcal{H}^+}, k \geq 2$
Type A	$-\frac{1}{M^3} \cdot H_0$	$\frac{1}{M^5} \cdot H_0 \cdot \tau$	$-\frac{3}{2M^7} \cdot H_0 \cdot \tau^2$	$c_k \cdot H_0 \cdot \tau^{k-1}$
Type B	$\frac{2}{M^2} \cdot H_0^{(1)} \cdot \tau^{-2}$	$\frac{1}{M^5} \cdot H_0^{(1)}$	$-\frac{3}{M^7} \cdot H_0^{(1)} \cdot \tau$	$a_k \cdot c_{k-1} \cdot H_0^{(1)} \cdot \tau^{k-2}$
Type C	$-\frac{1}{M^3} \cdot H_0$	$\frac{1}{M^5} \cdot H_0 \cdot \tau$	$-\frac{3}{2M^7} \cdot H_0 \cdot \tau^2$	$c_k \cdot H_0 \cdot \tau^{k-1}$
Type D	$\frac{2}{M^2} \cdot H_0^{(1)} \cdot \tau^{-2}$	$\frac{1}{M^5} \cdot H_0^{(1)}$	$-\frac{3}{M^7} \cdot H_0^{(1)} \cdot \tau$	$a_k \cdot c_{k-1} \cdot H_0^{(1)} \cdot \tau^{k-2}$

Where  $a_k$  and  $c_k$  are defined by (2.3.17) and (2.3.18), respectively. The following asymptotics for the transversal derivative  $\partial_r\psi$  on and away from  $\mathcal{H}^+$  reveal that  $\partial_r\psi$  always decays away from  $\mathcal{H}^+$  (Table 2.3):

**Table 2.3** Asymptotics for  $\partial_r \psi$ 

Data	Asymptotics	
	$\partial_r \psi _{\mathcal{H}^+}$	$\partial_r \psi _{\{r=r_0\}}$
Type A	$-\frac{1}{M^3} \cdot H_0$	$-\frac{4M}{(r-M)^2} \cdot H_0[\psi] \cdot \tau^{-2}$
Type B	$\frac{2}{M^2} \cdot H_0^{(1)} \cdot \tau^{-2}$	$\frac{8M}{(r-M)^2} \cdot H_0^{(1)}[\psi] \cdot \tau^{-3}$
Type C	$-\frac{1}{M^3} \cdot H_0$	$-\frac{4M}{(r-M)^2} \cdot H_0[\psi] \cdot \tau^{-2}$
Type D	$\frac{2}{M^2} \cdot H_0^{(1)} \cdot \tau^{-2}$	$\left( \frac{8M}{(r-M)^2} \cdot H_0^{(1)} + \frac{8(r^2-M^2)}{(r-M)^2} \cdot I_0 \right) \cdot \tau^{-3}$

## 2.4 Applications and Additional Remarks

In this section we present a few applications and remarks about late-time asymptotics on ERN.

### 2.4.1 Measuring the Horizon Hair from Null Infinity

It is not yet clear how to put the horizon instability for extremal black holes in the context of the (X-ray based) astronomical observations which suggest that many stellar and supermassive black holes are near extremal. One idea would be that the horizon instability does not mean that extremal (or near extremal) black holes are unlikely to occur in nature but rather that these black holes have characteristic signatures which can potentially be used to detect them. This leads us to the following:

- *Is the horizon instability observable far away from the event horizon?*

As a toy model, let's consider outgoing radiation represented by Type A (scalar) perturbations. Recall that for this type of perturbations the strong horizon instability holds

$$\partial_r \psi|_{\mathcal{H}^+} \sim -\frac{1}{M^3} H_0[\psi], \quad \partial_r^2 \psi|_{\mathcal{H}^+} \sim \frac{1}{M^5} H_0[\psi] \cdot \tau : \text{ along } \mathcal{H}^+. \quad (2.4.1)$$

The source of this instability is the conserved charge  $H_0[\psi]$ . The effects of this instability can be observed by incoming observers in view of the non-decay of the component  $\mathbf{T}_{rr}[\psi]$  of the energy-momentum tensor. This means that  $H_0$  is a horizon “hair”. It is a *horizon* hair, because away from the horizon all the geometric quantities do decay. A crucial question arises: *Could we, in principle, measure the horizon hair  $H_0$  from observations away from the event horizon, that is, from observations on the hypersurfaces  $\{r = r_0\}$  or, ideally, on null infinity?*

The answer for both cases is yes [37]! The leading late-time behavior for  $\psi$  along  $\{r = r_0\}$  is given by  $\frac{4M}{r_0-M} H_0 \tau^{-2}$  which means that, for fixed  $M$ , late-time observations along  $\{r = r_0\}$  can be used to determine the value of  $H_0$ . Similarly, we saw that

the leading late-time behavior for the radiation field along null infinity is given by  $(4MH_0 - 2I_0^{(1)})\tau^{-2}$ . We see that in this case the asymptotics do not depend purely on  $H_0$ . However, one can show that for Type **A** perturbations on ERN we have

$$I_0^{(1)}[\psi] = \frac{M}{4\pi} \int_{\mathcal{I}^+ \cap \{\tau \geq 0\}} r\psi \, d\Omega \, d\tau.$$

The above identity implies that  $I_0^{(1)}$  can, in principle, be read from observations along null infinity only! Moreover, from late-time observations we can independently measure  $(4MH_0 - 2I_0^{(1)})$  which finally yields the value for  $H_0$ . The fact that one can read the value of the horizon hair from null infinity might also be thought of as a “leakage” of horizon information to null infinity.

### 2.4.2 Singular Time Inversion and the New Horizon Charge

Recall from Sect. 1.8.2 that the constants  $I_0$  and  $I_0^{(1)}$  are obstructions to inverting the time operators  $T$  and  $T^2$ , respectively. Specifically,  $I_0$  and  $I_0^{(1)}$  are obstructions to defining the operators  $T^{-1}$  and  $T^{-2}$ , respectively, on solutions the wave equation (1.7.1) such that their target functional space consists of solutions the wave equation which decay appropriately in  $r$  towards null or spacelike infinity. In sub-extremal black holes,  $I_0$  and  $I_0^{(1)}$  are the only such obstructions. However, for ERN we have an additional obstruction that originates from the geometry of the horizon, namely the conserved charge  $H_0$ . Indeed, for any smooth solution  $\psi$  to the wave equation (1.7.1) on ERN we have

$$H_0[T\psi] = 0. \tag{2.4.2}$$

Hence,  $H_0$  is an obstruction to defining the inverse operator  $T^{-1}$  from smooth solutions of (1.7.1) to smooth solutions of (1.7.1). On the other hand, if  $\psi$  is a smooth solution of (1.7.1) with  $H_0 = 0$  then the horizon charge  $H_0^{(1)}$  is well-defined and satisfies

$$H_0^{(1)}[T^2\psi] = 0.$$

Hence,  $H_0^{(1)}$  is an obstruction to defining the inverse operator  $T^{-2}$  from smooth solutions of (1.7.1) with  $H_0 = 0$  to smooth solutions of (1.7.1). The above imply that the horizon charges  $H_0$  and  $H_0^{(1)}$  are related to singularities at time frequencies  $\omega \sim 0$ . We thus conclude that *the leading order terms in the late-time asymptotic expansion are dominated by the  $\omega \sim 0$  frequencies.*

An important aspect of the proofs of the asymptotics is that we invert the operators  $T$  and  $T^2$  even if the images of  $T^{-1}$  and  $T^{-2}$  do not contain smooth function. This is accomplished by developing a **singular time inversion theory**. This theory is needed for Type **A** and Type **D** perturbations. Let’s first consider Type **A** perturbations. Since such perturbations satisfy  $H_0 \neq 0$  and  $I_0 = 0$ ,  $I_0^{(1)}$  is well-defined whereas

$H_0^{(1)}$  is undefined. Clearly, there is no smooth solution  $T^{-1}\psi$  to (1.7.1). Indeed, if a smooth solution  $T^{-1}\psi$  to (1.7.1) existed then by replacing  $\psi$  with  $T^{-1}\psi$  in (2.4.2) we would obtain  $H_0[\psi] = H_0[T(T^{-1}\psi)] = 0$ , contradiction. It turns out that we can still *canonically* define a *singular* time inversion  $T^{-1}\psi$  such that

- $T^{-1}\psi \rightarrow 0$  as  $r \rightarrow \infty$ ,
- $I_0[T^{-1}\psi] < \infty$ ,
- $\partial_r(T^{-1}\psi) \sim -2H_0[\psi] \cdot \frac{1}{r-M}$  in the region  $r \sim M$ .

Similar results hold for Type **D** perturbations. In fact, for perturbations of Type **A** and **D**, a *low regularity theory* allows us to obtain the *precise late-time asymptotics* for the singular scalar fields  $T^{-1}\psi$ . We remark that for Type **B** perturbations we need a **regular** time inversion theory, whereas no time inversion is needed for Type **C** perturbations. Summarizing, we obtain the (Table 2.4) below:

**Table 2.4** The time inversion and its singular support

Data	Time inversion theory				
	$H_0[\psi]$	$H_0^{(1)}[\psi]$	$I_0[\psi]$	$I_0^{(1)}[\psi]$	$T^{-1}\psi$
Type <b>A</b>	$\neq 0$	$= \infty$	$= 0$	$< \infty$	Singular at $\mathcal{H}^+$
Type <b>D</b>	$= 0$	$< \infty$	$\neq 0$	$= \infty$	Singular at $\mathcal{I}^+$
Type <b>B</b>	$= 0$	$< \infty$	$= 0$	$< \infty$	Regular

## 2.5 The Murata–Reall–Tanahashi Spacetimes

In a very beautiful work [5], *Murata, Reall and Tanahashi studied numerically the fully non-linear evolution of the horizon instability of ERN*. Specifically, the authors of [5] investigated perturbations of ERN in the context of the Cauchy problem for the *spherically symmetric Einstein–Maxwell-(massless) scalar field system*. The authors studied various types of perturbations and obtained a great number of results, all of which are consistent with the linear theory described in the previous sections. We will next provide a more detailed summary of their results. It is important to remark that a rigorous treatment of this system remains a (very interesting) open problem.

The initial data on a Cauchy hypersurface  $\Sigma_0$  for the spherically symmetric Einstein–Maxwell-scalar field system are completely determined (modulo gauge fixing) by the value of the initial Bondi mass  $M$ , the conserved charge  $e > 0$  and the profile of the scalar field  $\psi$  on  $\Sigma_0$ . Note that ERN corresponds to data for which  $M = e$  and  $\psi$  is trivial on  $\Sigma_0$ . The authors of [5] considered compactly supported scalar fields  $\psi$  of size  $\epsilon > 0$

$$\max_{\Sigma_0} |\psi| = \epsilon.$$

The authors considered the following three types of perturbations of ERN:

**Type I:** *First-order mass perturbation*  $M = e + O(\epsilon)$ .

This is the “largest” of three types of perturbations. An open neighborhood  $\mathcal{O}_{\text{trap}}$  of the initial hypersurface  $\Sigma_0$  contains trapped surfaces. The Cauchy development contains a complete null infinity and a well-defined black hole region bounded by a smooth event horizon  $\mathcal{H}^+$ . In fact, the spacetime converges asymptotically in time to a sub-extremal RN background with surface gravity  $\kappa = O(\sqrt{\epsilon})$ , which, in particular, implies that  $\psi$  and all higher-order transversal derivatives  $\partial_r^k \psi$  decay along  $\mathcal{H}^+$ . On the other hand, the proximity to ERN on the initial hypersurface creates non-trivial effects at initial times, and more specifically at the time scale  $\tau \in \left[0, \frac{1}{\sqrt{\epsilon}}\right]$ . During this time scale, the third-order transversal derivative  $\partial_r^3 \psi$  **grows** along the event horizon  $\mathcal{H}^+$ , reaches a maximum value and then starts decaying. The crucial observation of Murata, Reall and Tanahashi is that

$$\max_{\mathcal{H}^+} \partial_r^3 \psi \sim \frac{H_0[\psi_0]}{\kappa_1},$$

where  $\psi_0$  is the linearization (in  $\epsilon$ ) of the scalar field  $\psi$ ,  $H_0$  is the conserved charged on exactly ERN and  $\kappa_1$  is the linearization (in  $\epsilon$ ) of the square of the surface gravity  $\kappa^2$ . The above clearly implies that for this kind of perturbations

$$\max_{\mathcal{H}^+} \partial_r^3 \psi \rightarrow 0 \text{ as } \epsilon \rightarrow 0.$$

In other words, *even though the size of the perturbation goes to zero (as  $\epsilon \rightarrow 0$ ) initially, the maximum size of higher-order derivatives of the scalar fields does not go to zero*. This implies that the horizon instability persists in the non-linear theory as well. We will see below that the situation gets more dramatic when we consider “smaller” perturbations of ERN.

**Type II:** *Second-order mass perturbation*  $M = e + O(\epsilon^2)$ .

In view of the fact that ERN does not contain trapped surfaces, one would like to consider perturbations which do not contain trapped surfaces on the initial hypersurface. In order to achieve this, one needs to reduce the size of the initial Bondi mass  $M$  so that the region  $\mathcal{O}_{\text{trap}}$  of trapped surfaces on  $\Sigma_0$  reduces to a single surface, namely a marginally trapped surfaces. This leads to a second-order mass perturbation for which  $M = e + O(\epsilon^2)$ . According to [5], the Cauchy development converges asymptotically in time to a sub-extremal RN background with surface gravity  $\kappa = O(\epsilon)$ , which again implies that  $\psi$  and all higher-order transversal derivatives  $\partial_r^k \psi$  decay along  $\mathcal{H}^+$ . In this case, the proximity to ERN on the initial hypersurface creates non-trivial effects at the time scale  $\tau \in \left[0, \frac{1}{\epsilon}\right]$  during which the second-order transversal derivative  $\partial_r^2 \psi$  **grows** along the event horizon  $\mathcal{H}^+$  reaching a maximum value and then decaying to zero. In fact, the authors calculated

$$\max_{\mathcal{H}^+} \partial_r^2 \psi \sim \frac{H_0[\psi_0]}{\kappa_0},$$

where  $\psi_0$  is the linearization (in  $\epsilon$ ) of the scalar field  $\psi$ ,  $H_0$  is the conserved charged on exactly ERN and  $\kappa_0$  is the linearization (in  $\epsilon$ ) of the surface gravity  $\kappa$ . The above clearly implies that for this kind of perturbations

$$\max_{\mathcal{H}^+} \partial_r^2 \psi \rightarrow 0 \text{ as } \epsilon \rightarrow 0.$$

Once again, we see that the horizon instability is present in the non-linear theory.

**Type III:** *Fine-tuned perturbations*  $M = M^*(e, \epsilon)$ .

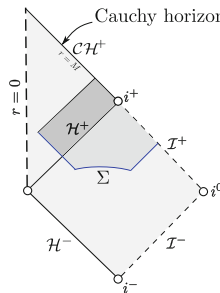
In the above two cases, the evolved spacetimes converged to sub-extremal RN. In particular, they contained trapped surfaces. The third type of perturbations that were studied by Murata, Reall and Tanahashi treats the case where the evolved spacetime has a regular black hole region but does not have any trapped surfaces and hence has properties which are reminiscent of ERN. For this reason, in fact, the authors called these spacetimes *dynamically extremal*.<sup>3</sup> In order to numerically construct such spacetimes, the authors considered even smaller fine-tuned values  $M^*(e, \epsilon)$  of  $M$  compared to the case above. We remark that it is conjectured that for initial masses which are less than  $M^*(e, \epsilon)$  the evolved spacetimes contain naked singularities. Returning the case where the initial mass is exactly equal to  $M^*(e, \epsilon)$ , the evolved spacetime converges has a black hole region and converges to ERN **outside** the event horizon. However, on the event horizon, the instability kicks in:

$$|\partial_r \psi| \rightarrow 0 \quad |\partial_r \partial_r \psi| \rightarrow \infty : \text{ along } \mathcal{H}^+$$

for each of these critical perturbations of ERN. This suggests that *dynamically extremal black holes exhibit a non-linear version of the horizon instability*.

## 2.6 The Interior of ERN and Strong Cosmic Censorship

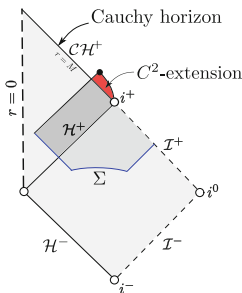
An important problem is the study of the dynamics of the interior of black holes. One can consider initial data on a hypersurface  $\Sigma$  that extends into the black hole and study the solution to the wave equation in the domain of dependence as in the figure below



<sup>3</sup>See also Sect. 2.6 for a discussion on the interior of dynamical extremal black holes.

An analysis of the behavior of solutions to (1.7.1) in the black hole *interior* of extremal Reissner–Nordström was carried out by Gajic in [38]. The results of [38] illustrate a remarkably *delicate* dependence of the qualitative behaviour at the inner horizon in the black hole interior on the *precise* late-time behaviour of the solution to (1.7.1) along the event horizon of extremal Reissner–Nordström. Specifically, Gajic showed the following

- *Solutions  $\psi$  to (1.7.1) on extremal Reissner–Nordström with Type A initial data (which enter the black hole interior) are extendible across the Cauchy horizon as functions in  $C^{0,\alpha} \cap H^1_{\text{loc}}$ , with  $\alpha < 1$ . Furthermore, the spherical mean  $\frac{1}{4\pi} \int_{S^2} \psi d\Omega$  can in fact be extended as a  $C^2$  function.*



Gajic made use of the precise late-time asymptotics including the logarithmic corrections as in (2.3.7). For spherically symmetric data one can construct  $C^2$  extensions of  $\psi$  across the Cauchy horizon that are moreover *classical* solutions to (1.7.1) with respect to a smooth extension of the extremal Reissner–Nordström metric across the inner horizon. These extensions of  $\psi$ , much like the smooth extensions of the metric, are *non-unique*! We remark that the precise second-order asymptotics (2.3.7) are important for deriving this extendibility result. See also [39] for extendibility results in the context of (1.7.1) in the interior of extremal Kerr–Newman spacetimes.

The interior dynamics of ERN differ drastically from the interior dynamics of sub-extremal Reissner–Nordström black holes, for which it is known that solutions to the wave equation are extendible in  $C^0$  across the inner (Cauchy) horizon, but *inextendible* in  $H^1_{\text{loc}}$ , see [40, 41]. See also [42–45] for extendibility results in sub-extremal Kerr.

The study of the wave equation in black hole interiors serves as a linear “toy model” for the analysis of dynamical black hole interiors, which is closely related to the *Strong Cosmic Censorship Conjecture* (SCC). As formulated in [46], SCC states that

- **Strong cosmic censorship conjecture:** “Generic” asymptotically flat initial data for the Einstein vacuum equations have maximal globally hyperbolic developments that are *intextendible* as Lorentzian manifolds with continuous metrics with locally square integrable Christoffel symbols.

Hence, a non-linear theory studying dynamical extremal black holes is needed. This is precisely what was numerically accomplished in [5]. As we discussed in the pre-

vious section, [5] predicted that there is special family of nonlinear perturbations of ERN which evolve into dynamical extremal black holes. Furthermore, the authors predicted that these spacetimes admit a  $C^1$  extension across the Cauchy horizon. Rigorous results were presented in [47] where it was shown that dynamical extremal black holes are extendible across the Cauchy horizon as *weak* solutions to the spherically symmetric Einstein–Maxwell–(charged) scalar field system of equations (in particular, with Christoffel symbols in  $L^2_{\text{loc}}$ ). Hence, *in contrast to the sub-extremal case, dynamical extremal black holes do not conform to the inextendibility properties stated in SCC*. For results for the interior region of sub-extremal black holes we refer to [48] and references there-in.

## References

1. H. Reissner, Über die eigengravitation des elektrischen feldes nach der Einstein’schen theorie. *Annalen der Physik*
2. G. Nordström, On the energy of the gravitational field in Einstein’s theory, in *Verhandl. Koninkl. Ned. Akad. Wetenschap.* (1918), pp. 1201–1208
3. J. Sbierski, The  $C^0$ -inextendibility of the Schwarzschild spacetime and the spacelike diameter in lorentzian geometry (2015), [arXiv:1507.00601](https://arxiv.org/abs/1507.00601)
4. D. Marolf, The danger of extremes. *Gen. Relativ. Gravit.* **42**, 2337–2343 (2010)
5. K. Murata, H.S. Reall, N. Tanahashi, What happens at the horizon(s) of an extreme black hole? *Class. Quantum Gravity* **30**, 235007 (2013)
6. J. Sbierski, Characterisation of the energy of Gaussian beams on Lorentzian manifolds with applications to black hole spacetimes. *Anal. Part. Diff. Eq.* **8**, 1379–1420 (2015)
7. W. Couch, R. Torrence, Conformal invariance under spatial inversion of extreme Reissner–Nordström black holes. *Gen. Rel. Gravity* **16**, 789–792 (1984)
8. H. Godazgar, M. Godazgar, C.N. Pope, Aretakis charges and asymptotic null infinity. *Phys. Rev. D* **96**, 084055 (2017)
9. S. Aretakis, Stability and instability of extreme Reissner–Nordström black hole spacetimes for linear scalar perturbations I. *Commun. Math. Phys.* **307**, 17–63 (2011)
10. S. Aretakis, Stability and instability of extreme Reissner–Nordström black hole spacetimes for linear scalar perturbations II. *Annales Henri Poincaré* **12**, 1491–1538 (2011)
11. S. Aretakis, The wave equation on extreme Reissner–Nordström black hole spacetimes: stability and instability results (2010), [arXiv:1006.0283](https://arxiv.org/abs/1006.0283)
12. Y. Angelopoulos, S. Aretakis, D. Gajic, The trapping effect on degenerate horizons. *Annales Henri Poincaré* **18**(5), 1593–1633 (2017)
13. J. Lucietti, K. Murata, H.S. Reall, N. Tanahashi, On the horizon instability of an extreme Reissner–Nordström black hole. *JHEP* **1303**, 035 (2013), [arXiv:1212.2557](https://arxiv.org/abs/1212.2557)
14. O. Sela, Late-time decay of coupled electromagnetic and gravitational perturbations outside an extremal charged black hole. *Phys. Rev. D* **94**, 084006 (2016)
15. S. Aretakis, On a non-linear instability of extremal black holes. *Phys. Rev. D* **87**, 084052 (2013)
16. P. Bizon, M. Kahl, A Yang–Mills field on the extremal Reissner–Nordström black hole. *Class. Quantum Gravity* **33**, 175013 (2016)
17. Y. Angelopoulos, S. Aretakis, D. Gajic, Asymptotic blow-up for a class of semi-linear wave equations on extremal Reissner–Nordström spacetimes (2016), [arXiv:1612.01562](https://arxiv.org/abs/1612.01562)
18. Y. Angelopoulos, Global spherically symmetric solutions of non-linear wave equations with null condition on extremal Reissner–Nordström spacetimes. *Int. Math. Res. Not.* **11**, 3279–3355 (2016)

19. S. Hadar, H.S. Reall, Is there a breakdown of effective field theory at the horizon of an extremal black hole? *J. High Energy Phys.* **2017**(12), 62 (2017)
20. K. Murata, Instability of higher dimensional extreme black holes. *Class. Quantum Gravity* **30**, 075002 (2013)
21. N. Tsukamoto, M. Kimura, T. Harada, High energy collision of particles in the vicinity of extremal black holes in higher dimensions: Banados–Silk–West process as linear instability of extremal black holes. *Phys. Rev. D* **89**, 024020 (2014)
22. J. Bičák, Gravitational collapse with charge and small asymmetries I: scalar perturbations. *Gen. Relativ. Gravit.* **3**, 331–349 (1972)
23. H. Onozawa, T. Mishima, T. Okamura, H. Ishihara, Quasinormal modes of maximally charged black holes. *Phys. Rev. D* **53**, 7033 (1996)
24. C.J. Blaksley, L.M. Burko, Late-time tails in the Reissner–Nordström spacetime revisited. *Phys. Rev. D* **76**, 104035 (2007)
25. A. Ori, Late-time tails in extremal Reissner–Nordström spacetime (2013), [arXiv:1305.1564](https://arxiv.org/abs/1305.1564)
26. O. Sela, Late-time decay of perturbations outside extremal charged black hole. *Phys. Rev. D* **93**, 024054 (2016)
27. M. Casals, S.E. Gralla, P. Zimmerman, Horizon instability of extremal Kerr black holes: non-axisymmetric modes and enhanced growth rate. *Phys. Rev. D* **94**, 064003 (2016)
28. Y. Angelopoulos, S. Aretakis, D. Gajic, Late-time asymptotics for the wave equation on extremal Reissner–Nordström backgrounds, preprint (2018)
29. J. Bičák, Gravitational collapse with charge and small asymmetries I. Scalar perturbations. *Gen. Relativ. Gravit.* **3**, 331–349 (1972)
30. P. Bizon, H. Friedrich, A remark about the wave equations on the extreme Reissner–Nordström black hole exterior. *Class. Quantum Gravity* **30**, 065001 (2013)
31. S. Aretakis, A note on instabilities of extremal black holes from afar. *Class. Quantum Gravity* **30**, 095010 (2013)
32. H. Koyama, A. Tomimatsu, Asymptotic power-law tails of massive scalar fields in a Reissner–Nordström background. *Phys. Rev. D* **63**, 064032 (2001)
33. S. Bhattacharjee, B. Chakrabarty, D. D. K. Chow, P. Paul, and A. Virmani, On late time tails in an extreme Reissner–Nordström black hole: Frequency domain analysis (2018), [arxiv:1805.10655](https://arxiv.org/abs/1805.10655)
34. J. Lucietti, H. Reall, Gravitational instability of an extreme Kerr black hole. *Phys. Rev. D* **86**, 104030 (2012)
35. L.M. Burko, G. Khanna, Linearized stability of extreme black holes. *Phys. Rev. D* **97**, 061502 (2018)
36. S.E. Gralla, P. Zimmerman, Critical exponents of extremal Kerr perturbations. *Class. Quantum Gravity* **35**(9) (2018)
37. Y. Angelopoulos, S. Aretakis, D. Gajic, Horizon hair of extremal black holes and measurements at null infinity. *Phys. Rev. Lett.* **121**, 131102 (2018)
38. D. Gajic, Linear waves in the interior of extremal black holes I. *Commun. Math. Phys.* **353**, 717–770 (2017)
39. D. Gajic, Linear waves in the interior of extremal black holes II. *Annales Henri Poincaré* **18**, 4005–4081 (2017)
40. A. Franzen, Boundedness of massless scalar waves on Reissner–Nordström interior backgrounds. *Commun. Math. Phys.* **343**, 601–650 (2014)
41. J. Luk, S.-J. Oh, Proof of linear instability of the Reissner–Nordström Cauchy horizon under scalar perturbations. *Duke Math. J.* **166**(3), 437–493 (2017)
42. P. Hintz, Boundedness and decay of scalar waves at the Cauchy horizon of the Kerr spacetime (2015), [arXiv:1512.08003](https://arxiv.org/abs/1512.08003)
43. J. Luk, J. Sbierski, Instability results for the wave equation in the interior of Kerr black holes. *J. Funct. Anal.* **271**(7), 1948–1995 (2016)
44. M. Dafermos, Y. Shlapentokh-Rothman, Time-translation invariance of scattering maps and blue-shift instabilities on Kerr black hole spacetimes. *Commun. Math. Phys.* **350**, 985–1016 (2016)

45. G. Fournodavlos, J. Sbierski, Generic blow-up results for the wave equation in the interior of a Schwarzschild black hole (2018), [arXiv:1804.01941](#)
46. D. Christodoulou, *The Formation of Black Holes in General Relativity* (European Mathematical Society Publishing House, 2009)
47. D. Gajic, J. Luk, The interior of dynamical extremal black holes in spherical symmetry (2017), [arXiv:1709.09137](#)
48. M. Dafermos, J. Luk, The interior of dynamical vacuum black holes I: the  $C^0$ -stability of the Kerr Cauchy horizon (2017), [arXiv:1710.01722](#)

# Chapter 3

## Extremal Kerr Black Holes



In this chapter we present results for the dynamics of extremal Kerr (EK). This family of black holes model maximally rotating black holes and hence are more physically relevant than ERN. On the other hand, they are more complicated. They are stationary and axisymmetric. As we shall see, axisymmetric perturbations behave very much like the perturbations on ERN (hence the relevance of ERN perturbations). However, non-axisymmetric perturbations introduce major new difficulties, and despite intense recent progress, many fundamental questions still remain open.

### 3.1 The Geometry of EK

The extremal Kerr metric with respect to the *Boyer–Lindquist coordinates*  $(t, r, \theta, \varphi)$  is given by

$$g = g_{tt}dt^2 + g_{rr}dr^2 + g_{\varphi\varphi}d\varphi^2 + g_{\theta\theta}d\theta^2 + 2g_{t\varphi}dtd\varphi,$$

where

$$g_{tt} = -\frac{\Delta - M^2 \sin^2 \theta}{\rho^2}, \quad g_{rr} = \frac{\rho^2}{\Delta}, \quad g_{t\varphi} = -\frac{2M^2 r \sin^2 \theta}{\rho^2},$$

$$g_{\varphi\varphi} = \frac{(r^2 + M^2)^2 - M^2 \Delta \sin^2 \theta}{\rho^2} \sin^2 \theta, \quad g_{\theta\theta} = \rho^2$$

with

$$\Delta = (r - M)^2, \quad \rho^2 = r^2 + M^2 \cos^2 \theta. \tag{3.1.1}$$

In these coordinates, the metric component  $g_{rr}$  is singular precisely at the points where  $\Delta = 0$ , that is at  $r = M$ . This singularity is merely a coordinate singularity

and can be overcome by introducing the following functions  $r^*(r)$ ,  $\varphi^*(\varphi, r)$  and  $v(t, r^*)$  such that

$$r^* = \int \frac{r^2 + M^2}{\Delta}, \quad \varphi^* = \varphi + \int \frac{M}{\Delta}, \quad v = t + r^* \quad (3.1.2)$$

Note that

$$r^*(r) = (r - M) + 2M \log(r - M) - \frac{2M^2}{r - M} - 2M \log(\sqrt{2}M).$$

In the *ingoing Eddington–Finkelstein coordinates*  $(v, r, \theta, \varphi^*)$  the metric takes the form

$$g = g_{vv}dv^2 + g_{rr}dr^2 + g_{\varphi^*\varphi^*}(d\varphi^*)^2 + g_{\theta\theta}d\theta^2 + 2g_{vr}dvdr + 2g_{v\varphi^*}dv d\varphi^* + 2g_{r\varphi^*}dr d\varphi^*,$$

where

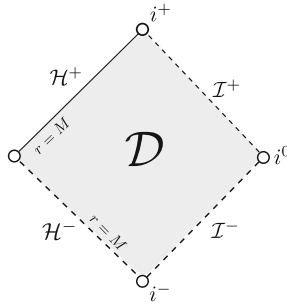
$$\begin{aligned} g_{vv} &= -\left(1 - \frac{2Mr}{\rho^2}\right), & g_{rr} &= 0, & g_{\varphi^*\varphi^*} &= g_{\varphi\varphi}, & g_{\theta\theta} &= \rho^2 \\ g_{vr} &= 1, & g_{v\varphi^*} &= -\frac{2M^2r \sin^2\theta}{\rho^2}, & g_{r\varphi^*} &= -M \sin^2\theta. \end{aligned} \quad (3.1.3)$$

Clearly, the metric (3.1.3) does not break down anymore at the points where  $\Delta = 0$ . We can therefore consider the following manifold

$$\mathcal{M} = \left\{ (v, r, \theta, \varphi^*) \in \left\{ \mathbb{R} \times [M, \infty) \times \mathbb{S}^2 \right\} \right\}$$

equipped with the metric (3.1.3). Note that  $\partial_v$  and  $\partial_{\varphi^*}$  are Killing fields. We will refer to  $\partial_v$  as the stationary vector field and to  $\partial_{\varphi^*}$  as the axisymmetric vector field. Note that  $\partial_v$  fails to be causal everywhere. In particular, the region where  $\partial_v$  is spacelike is known as the *ergoregion* and its boundary is called the *ergosphere*. The ergoregion is well-known for enabling the extraction of energy out of a black hole. This “process” was discovered first by Penrose [1] and remains the subject of intense research in the high energy physics community.

One obtains a global causal Penrose diagram for an appropriate quotient of  $\mathcal{M}$  (see [2]).

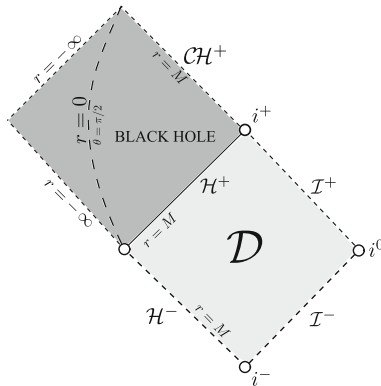


Extremal Kerr admits a complete future null infinity  $\mathcal{I}^+$  and a complete past null infinity  $\mathcal{I}^-$ . The domain of outer communications corresponds to  $\{r > M\}$ . It also admits a future event horizon  $\mathcal{H}^+$  located precisely at  $\{r = M\}$ . The event horizon is a Killing hypersurface, its normal being the vector field  $V = \partial_v + \frac{1}{2M}\partial_{\varphi^*}$ . It is easy to see that  $\nabla_V V = 0$  and hence the surface gravity of  $\mathcal{H}^+$  vanishes.

The past event horizon is not part of the spacetime covered by the  $(v, r, \theta, \varphi^*)$  coordinate system. On the other hand, the interior of the black hole region can be covered by  $(v, r, \theta, \varphi^*)$ . How far inside the black hole can we go? The curvature would blow-up at  $\rho^2 = 0$ , i.e. the equatorial points  $\theta = \pi/2$  of  $r = 0$ . On the other hand, it turns out (see [2]) that the metric (3.1.3) is regular even for negative values  $r < 0$ . This motivates the following definition of the underlying differential structure of the Kerr spacetime:

$$\mathcal{M}_{\text{ext}} = \left\{ (v, r, \theta, \varphi^*) \in \left\{ \left\{ \mathbb{R} \times \mathbb{R} \times \mathbb{S}^2 \right\} \setminus \left\{ \mathbb{R} \times \{0\} \times S_{\text{eq}} \right\} \right\} \right\}.$$

The Penrose representation of this manifold is



### 3.2 Stability and Instability of EK for Scalar Perturbations

First of all, we write the wave equation in  $(v, r, \theta, \varphi^*)$  coordinates:

$$\begin{aligned} \square_g \psi = & \frac{M^2}{\rho^2} \sin^2 \theta (\partial_v \partial_v \psi) + \frac{2(r^2 + M^2)}{\rho^2} (\partial_v \partial_r \psi) + \frac{\Delta}{\rho^2} (\partial_r \partial_r \psi) \\ & + \frac{2M^2}{\rho^2} (\partial_v \partial_{\varphi^*} \psi) + \frac{2M}{\rho^2} (\partial_r \partial_{\varphi^*} \psi) + \frac{2r}{\rho^2} (\partial_v \psi) + \frac{\Delta'}{\rho^2} (\partial_r \psi) + \frac{1}{\rho^2} \mathbb{A}_{(\theta, \varphi^*)} \psi, \end{aligned} \quad (3.2.1)$$

where  $\mathbb{A}_{(\theta, \varphi^*)} \psi$  denotes the standard Laplacian on  $\mathbb{S}^2$  with respect to  $(\theta, \varphi^*)$ .

As in the ERN case, we consider an axisymmetric initial hypersurface  $\Sigma_0$  which crosses the event horizon and terminate at null infinity. We assume that  $\Sigma_0 \cap \mathcal{H}^+ = \{v = 0\} \cap \mathcal{H}^+$ . We also define  $\Sigma_\tau = F_\tau^T(\Sigma_0)$  be the foliation generated by  $\Sigma_0$  under the flow of the stationary field  $\partial_v$ . In this section, we will present stability and instability results for axisymmetric solutions to the wave equation (3.2.1). Let's first start with the stability results (see [3]):

**Stability results for EK:** Consider axisymmetric smooth compactly supported initial data for the wave equation on EK. Then the following decay estimates were rigorously proved in [3] for the (axisymmetric) solution  $\psi$ :

1. **Pointwise decay for  $\psi$ :**

$$\|\psi\|_{L^\infty(\Sigma_\tau)} + \|\partial_v \psi\|_{L^\infty(\Sigma_\tau)} \leq C \cdot E_0[\psi] \cdot \frac{1}{\sqrt{\tau}}.$$

Here  $E_0[\psi]$  is an appropriate weighted norm of the initial data of  $\psi$ .

2. **Decay of degenerate (at  $\mathcal{H}^+$ ) energy of  $\psi$ :** The degenerate energy flux decays likes  $\tau^{-2}$ . The (local observer's) non-degenerate energy is uniformly bounded.

The decay rates are far from sharp, however they are sufficient to yield instability results. Before we present the precise instability results, we review the instability mechanism, namely the conservation laws along the event horizon. If we denote the section of the event horizon by

$$S_\tau = \Sigma_\tau \cap \mathcal{H}^+,$$

then we immediately arrive by restricting  $\rho^2 \cdot \square_g \psi = 0$  on  $r = M$ , where  $\Delta = \Delta' = 0$ , at the following

• **Conservation law along  $\mathcal{H}^+$ :** For all solutions  $\psi$ , the surface integrals

$$H_0^{\text{Kerr}}[\psi](\tau) = \int_{S_\tau} \left( M^2 \sin^2 \theta (\partial_v \psi) + 4M^2 (\partial_r \psi) + 2M\psi \right) d\Omega \quad (3.2.2)$$

are independent of  $\tau$  and hence are conserved along  $\mathcal{H}^+$ .

In fact, we can also obtain a *hierarchy* of conservation laws analogous to that of ERN. We next demonstrate how to derive this hierarchy. Let  $Y_{\ell m} = Y_{\ell m}(\theta, \varphi^*)$  be the standard spherical harmonic with angular number  $\ell$  and azimuthal frequency  $m$ . By restricting  $\partial_r(\rho^2 \square_g \psi) = 0$  on  $\mathcal{H}^+$  and projecting on  $Y_{\ell 0}$  with  $m = 0$  (in order to remove the  $\partial_{\varphi^*}$  derivatives) we obtain

$$\int_{S_\tau} \left[ M^2 \sin^2 \theta (\partial_v \partial_v \partial_r \psi) + 4M^2 (\partial_v \partial_r \partial_r \psi) + 2M (\partial_v \partial_r \psi) + 2(\partial_r \psi) + \mathbb{A} \partial_r \psi \right] \cdot Y_{\ell 0} d\Omega = 0.$$

Taking  $\ell = 1$  and  $m = 0$ , in which case the corresponding eigenvalue is  $-2$ , and using Stokes' theorem for the last term yields that the quantity

$$H_1^{\text{Kerr}}[\psi](\tau) = \int_{S_\tau} \left( \left[ 4M^2 (\partial_r \partial_r \psi) + M^2 \sin^2 \theta (\partial_v \partial_r \psi) + 2M (\partial_r \psi) \right] \cdot Y_{10} \right) d\Omega$$

is conserved along  $\mathcal{H}^+$ . Similarly, we obtain the following

- **Hierarchy of conservation laws for all solutions to the wave equation on EK:**  
For each  $\ell \geq 1$  there is a conservation law involving the projection of the derivative  $\partial_r^\ell \psi$  on the spherical harmonic  $Y_{\ell 0}$ .

See also the next section for a more general approach to conservation laws on EK. The above stability results in conjunction with the conservation laws yield the following (see [4]):

**Instability results for EK:** Generic solutions to the wave equation on EK satisfy

1. **Non-decay:**

$$\sup_{S_\tau} |\partial_r \psi| \not\rightarrow 0,$$

along  $\mathcal{H}^+$ .

2. **Pointwise blow-up:**

$$\sup_{S_\tau} |\partial_r^k \psi| \rightarrow \infty$$

asymptotically along  $\mathcal{H}^+$  for all  $k \geq 2$ .

3. **Energy blow-up:** for any  $\epsilon > 0$  we have

$$\int_{\Sigma_\tau \cap \{r \leq M + \epsilon\}} |\partial_r^k \psi|^2 \rightarrow +\infty,$$

for all  $k \geq 2$ , as  $\tau \rightarrow +\infty$ .

Clearly, the genericity assumption corresponds to the condition  $H_0^{\text{Kerr}}[\psi] \neq 0$ . Let's comment more on how we arrive to these results. Recall the wave equation:

$$\begin{aligned} \rho^2 \square_g \psi &= M^2 \sin^2 \theta (\partial_v \partial_v \psi) + 2(r^2 + M^2) (\partial_v \partial_r \psi) + \Delta (\partial_r \psi) \\ &\quad + 2M^2 (\partial_v \partial_{\varphi^*} \psi) + 2M (\partial_r \partial_{\varphi^*} \psi) + 2r (\partial_v \psi) + \Delta' (\partial_r \psi) + \mathbb{A}_{(\theta, \varphi^*)} \psi, \end{aligned} \tag{3.2.3}$$

The non-decay result for  $\partial_r \psi$  is obtained by integrating in  $v$  along the horizon the red term in (3.2.3) (whose coefficient is constant on  $\mathcal{H}^+$ ) and using that the coefficient of the blue term vanishes (and that all the other terms actually decay). Having obtained non-decay for (the spherical mean of)  $\partial_r \psi$ , we can then obtain blow-up for  $\partial_r \partial_r \psi$  along the horizon. We differentiate (3.2.3) in  $r$ . Again it is the (differentiated) red and the blue terms that play the crucial role. The blue term now appears since its differentiated coefficient is  $\Delta'' = 2$ . The red term, after integrating in  $v$  along the horizon, gives us the derivative  $\partial_r \partial_r \psi$ . It is very important to remark that the coefficient of the red term and the differentiated coefficient  $\Delta'' = 2$  of the blue term are non-zero constants! This is precisely what allows us to derive the blow-up results from the conservation laws. This property has been shown to hold for a general class of extremal black holes by Lucietti and Reall [5]. See also the discussion about general extremal black holes in Chap. 6.

### 3.3 The Lucietti–Reall Gravitational Instability of EK

Lucietti and Reall [5] examined the effects of the horizon instability for scalar perturbations to (linearized) electromagnetic and gravitational perturbations. We will next provide a summary of their results. Let's recall a few standard things first. The Weyl tensor can be decomposed in 5 complex valued components  $\Psi_i$  with  $i = 0, 1, 2, 3, 4$ . The linearized gravity is expressed by five linearized Weyl components  $\check{\Psi}_i$  with  $i = 0, 1, 2, 3, 4$ . The extreme components  $\check{\Psi}_0$  and  $\check{\Psi}_4$  are gauge-invariant with spin weights  $s = 2$  and  $s = -2$ , respectively. Each of them satisfies a second order wave equation known as the  $s$  spin-weighted Teukolsky equation ( $s \in \mathbb{Z}$ ) which schematically reads

$$\partial_v \left( 2(r^2 + M^2) \partial_r \psi + \dots \right) = {}_s \Delta \psi - 2(r - M)(1 - s) \partial_r \psi + \dots \quad (3.3.1)$$

Here  ${}_s \Delta$  denotes the standard  $s$  spin-weighted spherical Laplacian (for  $s = 0$  it reduces to  $-\Delta$ ). This operator is self-adjoint. The (complex) eigenfunctions of  ${}_s \Delta$  are the standard spin-weighted spherical harmonics  ${}_s Y_{\ell m}$ . These are defined for  $\ell \geq |s|$  and  $-\ell \leq m \leq \ell$  and the corresponding eigenvalues are

$${}_s \lambda_{\ell m} = (\ell + s)(\ell + 1 - s). \quad (3.3.2)$$

Note that this eigenvalue is zero only for  $\ell = -s \leq 0$ . Then let's first consider that  $s \leq 0$ . By restricting (3.3.1) on the horizon  $r = M$  and by projecting on the kernel  ${}_s Y_{-s0}$ , with  $\ell = -s$  and  $m = 0$  (the restriction  $m = 0$  allows us to remove  $\partial_{\varphi^*}$  derivatives which are hidden from our schematic notation) we conclude that the quantity

$${}_s I_0[\psi] = \int_{S_r} \left( 4M^2 \partial_r \psi + \dots \right) \cdot {}_s \bar{Y}_{-s0} d\Omega$$

is independent of  $\tau$ . Note that the angular term on the right hand side of (3.3.2) disappears precisely because we projected on the kernel of the (self-adjoint) angular operator. Assuming that the terms hidden above decay, we conclude that  $\partial_r \psi$  generically does not decay and in fact the weighted mean

$$\int_{S_\tau} 4M^2 \partial_r \psi \cdot {}_s \bar{Y}_{-s0} d\Omega$$

generically converges to a non-zero constant. We can derive blow-up results for the same “angular frequencies”  $\ell = -s$ ,  $m = 0$  as follows: Differentiate (3.3.1) with respect to  $\partial_r$ , restrict to  $r = M$  and again project on  ${}_s \bar{Y}_{-s0}$  to obtain that:

$$\partial_v \int_{S_\tau} \left( 4M^2 \partial_r \partial_r \psi + \dots \right) \cdot {}_s \bar{Y}_{-s0} d\Omega = \int_{S_\tau} \left( -2(1-s) \partial_r \psi + \dots \right) \cdot {}_s \bar{Y}_{-s0} d\Omega$$

We can now integrate the above identity in  $v$  and use the fact that the non-decaying weighted mean appears above (note the role of the constant coefficients of the blue and the red terms!) to conclude that the weighted mean of  $\partial_r \partial_r \psi$  grows linearly (and hence asymptotically blows up). In this way, Lucietti and Reall derived similar results for spins  $s \leq 0$ , as for the wave equation ( $s = 0$ ). What about  $s > 0$ ? In this case, Lucietti and Reall observed that one needs to first commute (3.3.1) with  $\partial_r^k$ , for some appropriate  $k$ , in order to derive a conservation law. We need to include one more term that we hid before (the purple term below):

$$\partial_v \left( 2(r^2 + M^2) \partial_r \psi + \dots \right) = {}_s \Delta \psi - (r - M)^2 \partial_r \partial_r \psi - 2(r - M)(1 - s) \partial_r \psi + \dots$$

Note that the purple term played no role for the analysis above. However now it will play a crucial role. Differentiating with respect to  $\partial_r^k$  and restricting on  $r = M$  yields

$$\partial_v \left( 2(r^2 + M^2) \partial_r^{k+1} \psi + \dots \right) = {}_s \Delta \partial_r^k \psi - k(k-1) \partial_r^k \psi - 2k(1-s) \partial_r^k \psi + \dots$$

Projecting on  ${}_s \bar{Y}_{\ell 0}$  for some  $\ell \geq s$  yields

$$\begin{aligned} & \partial_v \int_{S_\tau} \left( 2(r^2 + M^2) \partial_r^{k+1} \psi + \dots \right) \cdot {}_s \bar{Y}_{\ell 0} d\Omega \\ &= \int_{S_\tau} \left( {}_s \Delta \partial_r^k \psi - k(k-1) \partial_r^k \psi - 2k(1-s) \partial_r^k \psi + \dots \right) \cdot {}_s \bar{Y}_{\ell 0} d\Omega \\ &= \int_{S_\tau} \left( (\ell + s)(\ell + 1 - s) - k(k-1) - 2k(1-s) \right) \cdot \partial_r^k \psi \cdot {}_s \bar{Y}_{\ell 0} d\Omega \\ &= \int_{S_\tau} (\ell + s - k)(\ell - s + k + 1) \cdot \partial_r^k \psi \cdot {}_s \bar{Y}_{\ell 0} d\Omega \end{aligned} \tag{3.3.3}$$

and hence the right hand side vanishes for  $k = \ell + s \geq 2s$ . In other words, in order to obtain a conservation law when  $s > 0$  we must first consider at least  $2s$  derivatives. So, for any  $\ell \geq s$  we have a conservation law for a weighted spherical mean of  $\partial_r^{k+1}\psi$  if we take  $k = \ell + s$ . We can use this conservation law to derive blow up for  $\partial_r^{k+2}\psi$ . Indeed, all we have to do is to use (3.3.3) with  $\ell = k + 2$  but where  $k$  is replaced by  $k + 1$  and use the conservation for the weighted spherical mean for  $\partial_r^{k+1}\psi$  which now appears in right hand side. Integrating in  $v$  gives the desired result assuming that all the remaining terms decay or are bounded. Decay results for linearized curvature components were numerically derived by Burko and Khanna [6].

Using the above theory for the components  $\dot{\Psi}_0$  (with  $s = 2$ ) and  $\dot{\Psi}_4$  (with  $s = -2$ ) Lucietti and Reall concluded the following: The second-order derivative  $\partial_r^2\dot{\Psi}_4$  and the sixth-order derivative  $\partial_r^5\dot{\Psi}_0$  blow up along  $\mathcal{H}^+$ . This yields a *genuine linearized gravitational instability for EK*. We remark that the above analysis applies only to axisymmetric perturbations (in view of the fact we projected on  $m = 0$  eigenspaces). A more general and systematic approach to deriving the asymptotic behavior for perturbations of EK was presented in [7] where the authors exploit the asymptotic self-similarity of the perturbations under the near-horizon, late-time scaling symmetry of the background metric. The critical (self-similar) exponent corresponds to the decay rate of the associated perturbation.

### 3.4 The Casals–Gralla–Zimmerman Work on EK

The problem of understanding the evolution of non-axisymmetric solutions to the wave equation on EK has recently attracted a lot of interest in the mathematics and physics communities. Heuristic and numerical work strongly suggests that non-axisymmetric solutions exhibit stronger instability properties compared to the axisymmetric solutions. Andersson and Glampedakis [8], following earlier work of Detweiler [9], argued that the dominant temporal frequencies  $\omega$  for scalar fields  $\psi_m$  with *fixed azimuthal frequencies*  $m$  occur for  $\omega \sim \frac{1}{2M}m$ , instead of  $\omega \sim 0$  in other settings. Specifically, [8] suggested that away from horizon on  $r = r_0 > M$  the following sharp rate holds:

$$|\psi_m|_{\{r=r_0\}} \text{ decays like } \frac{1}{\tau}. \quad (3.4.1)$$

Important subsequent studies of the distribution of quasi-normal modes on EK were presented in [10, 11] and their findings are consistent with (3.4.1). For a more detailed discussion on quasi-normal modes see Sect. 1.9.

Casals, Gralla and Zimmerman [12] were the first to derive the late-time asymptotics along the event horizon for  $\psi_m$ . Their semi-analytic work, which is based on the mode decomposition method of Leaver [13], yielded the following asymptotic behavior along the horizon

$$|\psi_m|_{\mathcal{H}^+} \text{ decays like } \frac{1}{\sqrt{\tau}}. \quad (3.4.2)$$

Reference [12] considered initial data which are compactly supported and *supported away from the event horizon* (and hence they are not horizon-penetrating). Clearly, the rate of (3.4.2) is much slower than the sharp decay rates in all other previously discussed settings. Moreover, Casals, Gralla and Zimmerman argued that the instability is further amplified for the first-order transversal to  $\mathcal{H}^+$  derivative

$$|\partial_r \psi_m|_{\mathcal{H}^+} \text{ decays like } \sqrt{\tau}. \quad (3.4.3)$$

In other words, reference [12] suggested that for data supported *away* from the horizon the first-order derivative **grows** along the horizon. One would naturally expect that the growth is even more severe in the case where the initial data are horizon-penetrating. Hadar and Reall [14] performed a near-horizon analysis which indicates that (3.4.2) and (3.4.3) (surprisingly!) also hold for scalar fields with horizon-penetrating Type A data. Zimmerman [15] obtained the same rates as (3.4.2) and (3.4.3) for charged perturbations on ERN. This agreement is due to common near-horizon symmetries in the two cases. Further extensions have been provided in [7, 16, 17]. A numerical confirmation of (3.4.2) and (3.4.3), as well as stability results for curvature scalars, was presented by Burko and Khanna [6]. Further extensions to supersymmetric quantum mechanics were presented in [18].

## 3.5 Open Problems

We next state several open problems on the dynamics of EK.

### 1. Scalar Perturbations

There are many aspects of the linear wave equation on EK that have not been understood. Let  $m$  be the azimuthal frequency and let  $\psi_m$  denote a solution to the wave equation on EK supported on this frequency, as before.

#### A. Axisymmetric Solutions

Axisymmetric solutions  $\psi_0$  are expected to satisfy similar asymptotic behavior as in the Table 2.1 for general solutions on ERN. A rigorous proof of this is an open problem.

#### B. Fixed $m \neq 0$ Solutions

Another very interesting open problem would be to obtain a rigorous proof of the asymptotic statements (3.4.1), (3.4.2) and (3.4.3). In particular, it would be very nice to find a physical space mechanism that gives rise to these asymptotics. We remark that *precise* late-time asymptotics for  $\psi_m$  on EK are not known. A relevant problem is to describe the distribution of quasinormal modes for exactly extremal Kerr.

### C. General Solutions

The most challenging problem is of course to derive the generic asymptotic behavior for general (summed!) solutions to the wave equation on EK

$$\psi_{\text{total}} = \sum_{m=0}^{\infty} \psi_m.$$

No (rigorous, numerical or heuristic) results are known for  $\psi_{\text{total}}$ . In particular, it is not even known if  $\psi_{\text{total}}$  is uniformly bounded on or away from the event horizon. The main difficulty of this problem stems from the coupling of superradiance and trapping.

## 2. Gravitational and Electromagnetic Perturbations

It would be very interesting to obtain a rigorous proof of the Lucietti–Reall linearized gravitational instability of extremal Kerr. In fact, it would be very interesting to obtain the late-time asymptotics for general (axisymmetric or non-axisymmetric) gravitational and electromagnetic perturbations of EK in the spirit of [19].

## 3. Non-linear Wave Equations

No results are known for non-linear wave equations on EK. As a first step towards the fully non-linear EK instability problem (see below) one would like to study the long time existence of semi-linear and quasi-linear wave equations satisfying appropriate versions of the null condition. This problem is very hard even for the much simpler ERN metric.

## 4. Fully Non-linear Instability of EK

The ultimate goal is to investigate the Cauchy developments in the context of the Cauchy problem for the Einstein equations, without symmetry assumptions, of initial data nearby the initial data of exactly EK. What is the impact of the linear instabilities in the non-linear theory? Do perturbations diverge from EK and asymptotically converge to a sub-extremal Kerr? Do perturbations grow indefinitely leading to asymptotic singularities? Do perturbations form singularities in finite time?

## References

1. R. Penrose, Gravitational collapse: the role of general relativity. *Riv. del Nuovo Cimento* **1**, 272–276 (1969)
2. S. Hawking, G.F.R. Ellis, *The Large Scale Structure of Spacetime* (Cambridge University Press, Cambridge, 1973)
3. S. Aretakis, Decay of axisymmetric solutions of the wave equation on extreme Kerr backgrounds. *J. Funct. Anal.* **263**, 2770–2831 (2012)
4. S. Aretakis, Horizon instability of extremal black holes. *Adv. Theor. Math. Phys.* **19**, 507–530 (2015)

5. J. Lucietti, H. Reall, Gravitational instability of an extreme Kerr black hole. *Phys. Rev. D* **86**, 104030 (2012)
6. L.M. Burko, G. Khanna, Linearized stability of extreme black holes. *Phys. Rev. D* **97**, 061502 (2018)
7. S.E. Gralla, P. Zimmerman, Critical exponents of extremal Kerr perturbations. *Class. Quantum Gravity* **35**(9) (2018)
8. N. Andersson, K. Glampedakis, A superradiance resonance cavity outside rapidly rotating black holes. *Phys. Rev. Lett.* **84**, 4537–4540 (2000)
9. S. Detweiler, Black holes and gravitational waves III. The resonant frequencies of rotating holes. *Astrophys. J.* **239**, 292–295 (1980)
10. H. Yang, A. Zimmerman, A. Zenginoglu, F. Zhang, E. Berti, Y. Chen, Quasinormal modes of nearly extremal Kerr spacetimes: spectrum bifurcation and power-law ringdown. *Phys. Rev. D* **88**, 044047 (2013)
11. M. Richartz, C.A.R. Herdeiro, E. Berti, Synchronous frequencies of extremal Kerr black holes: resonances, scattering, and stability. *Phys. Rev. D* **96**, 044034 (2017)
12. M. Casals, S.E. Gralla, P. Zimmerman, Horizon instability of extremal Kerr black holes: non-axisymmetric modes and enhanced growth rate. *Phys. Rev. D* **94**, 064003 (2016)
13. E.W. Leaver, Spectral decomposition of the perturbation response of the Schwarzschild geometry. *Phys. Rev. D* **34**, 384–408 (1986)
14. S. Hadar, H.S. Reall, Is there a breakdown of effective field theory at the horizon of an extremal black hole? *J. High Energy Phys.* **2017**(12), 62 (2017)
15. P. Zimmerman, Horizon instability of extremal Reissner–Nordström black holes to charged perturbations. *Phys. Rev. D* **95**, 124032 (2017)
16. S.E. Gralla, A. Zimmerman, P. Zimmerman, Transient instability of rapidly rotating black holes. *Phys. Rev. D* **94**, 084017 (2016)
17. M. Casals, P. Zimmerman, Perturbations of extremal Kerr spacetime: analytic framework and late-time tails (2018), [arXiv:1801.05830](https://arxiv.org/abs/1801.05830)
18. V. Cardoso, T. Houri, M. Kimura, Mass ladder operators from spacetime conformal symmetry. *Phys. Rev. D* **96**, 024044 (2017)
19. M. Dafermos, G. Holzegel, I. Rodnianski, The linear stability of the Schwarzschild solution to gravitational perturbations (2016), [arXiv:1601.06467](https://arxiv.org/abs/1601.06467)

**Part II**  
**An Overview of the Proofs**

# Chapter 4

## Asymptotics for Extremal Reissner–Nordström



In this Chapter we present the main estimates for scalar perturbations on extremal Reissner–Nordström backgrounds and provide an overview of the proof of the precise asymptotics.

### 4.1 Introduction to the Vector Field Method

The vector field method is a robust geometric approach to study solutions to, in particular, hyperbolic PDEs on Lorentzian manifolds  $(\mathcal{M}, g)$ . Recall the energy-momentum tensor  $\mathbf{T}[\psi]$ , given by (1.2.6), for scalar perturbations  $\psi$ . Its divergence satisfies  $\text{div}\mathbf{T}[\psi] = \square_g\psi \cdot d\psi$ . Let  $V$  be a general vector field. The *energy  $V$ -current* is given by the 1-form

$$J_\mu^V[\psi] = \mathbf{T}_{\mu\nu}[\psi] \cdot V^\nu.$$

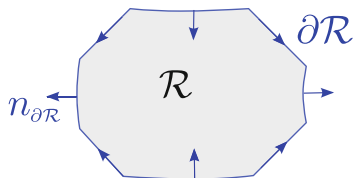
Two fundamentally important properties of the energy currents are:

1. If  $V, W$  are future-directed timelike then  $J_\mu^V[\psi] \cdot W^\mu \sim \sum_\alpha |\partial_\alpha\psi|^2$ ,
2. The divergence of the energy current satisfies

$$\text{div}J^V[\psi] = K^V[\psi] + \square_g\psi \cdot V(\psi)$$

for all functions  $\psi$ . Here  $K^V[\psi] = \mathbf{T}_{\mu\nu}[\psi] \cdot \pi^{\mu\nu}(V)$ , where  $\pi^{\mu\nu}(V) = \frac{1}{2}(\mathcal{L}_Vg)^{\mu\nu}$  is the deformation tensor of  $V$ .

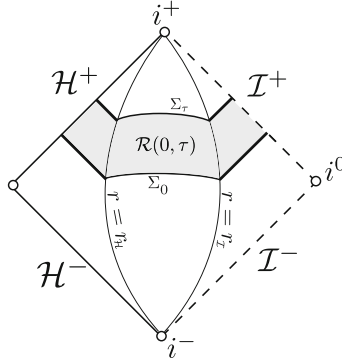
The main idea to derive estimates is to use the divergence identity for the current  $J^V[\psi]$  for appropriate vector fields  $V$  which we will call the *multiplier* vector fields.

$$\int_{\mathcal{R}} \nabla^\mu J_\mu^V = \int_{\partial\mathcal{R}} J^V \cdot n_{\partial\mathcal{R}}$$


Convention: When the volume form is omitted then the induced volume form is being used. In order to obtain higher order estimates, we will apply the above identity for  $X\psi$  in place of  $\psi$ . In this case  $X$  will be called the *commutator* vector field.

## 4.2 Conservation of the $J^T$ -Flux

The vector field  $T = \partial_v$  is Killing and hence its deformation tensor vanishes. Therefore, by applying the divergence theorem for the  $T$ -current  $J^T$  in the shaded region below (between the hypersurfaces  $\Sigma_0$  and  $\Sigma_\tau$  which are defined in Sect. 2.1.4), we obtain a conservation law.



Since  $T$  is globally causal, the boundary terms at  $\mathcal{H}^+$  and  $\mathcal{I}^+$  are non-negative definite. Hence, if we denote

$$J_{\Sigma_\tau}^T[\psi] = \int_{\Sigma_\tau} J_\mu^T[\psi] n_{\Sigma_\tau}^\mu, \quad (4.2.1)$$

then we obtain

$$J_{\Sigma_\tau}^T[\psi] \leq J_{\Sigma_0}^T[\psi].$$

Since  $T$  is null at the horizon, the  $T$ -flux  $J_{\Sigma_\tau}^T[\psi]$  along  $\Sigma_\tau$  *degenerates* at the horizon. This degeneracy schematically looks like

$$J_\mu^T[\psi] n_{\Sigma_\tau}^\mu \sim \left(1 - \frac{M}{r}\right)^2 \cdot |\partial_r \psi|^2 + |\nabla \psi|^2$$

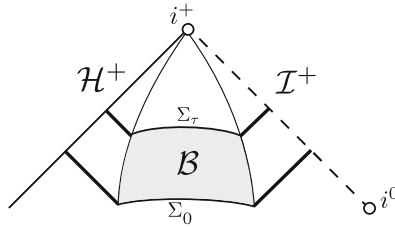
close to the horizon. Here  $\partial_r$  is taken with respect to the coordinate system  $(v, r)$  and  $\nabla$  is the induced gradient on the spheres of symmetry. The above estimate was also used in [1, 2] where various boundedness results were shown for the wave equation on ERN away from the event horizon. Removing the degeneracy is non-trivial in view of the degeneracy of the redshift effect. See Sect. 4.4.

### 4.3 The Morawetz Estimate

The energy current of an appropriate modification of the vector field  $\partial_{r^*}$  (with respect to the  $(t, r^*)$  system) has non-negative definite divergence, and boundary terms which are bounded by the  $T$ -flux. This construction in particular yields the following *degenerate Morawetz estimate* (see [1] for the details)

$$\int_{\mathcal{B}} \psi^2 + \int_{\mathcal{B}} \left(1 - \frac{2M}{r}\right)^2 \sum_{\alpha} |\partial_{\alpha} \psi|^2 \leq C J_{\Sigma_0}^T[\psi]. \tag{4.3.1}$$

The region  $\mathcal{B} = \{r_{\mathcal{H}} \leq r \leq r_{\mathcal{I}}\}$  is depicted below



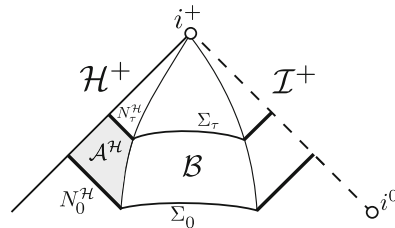
The degeneracy at the photon sphere  $r = 2M$  is due to the presence of trapped null geodesics on that radius (see Sect. 2.1.3) and can be removed by commuting with  $T$ :

$$\int_{\mathcal{B}} \psi^2 + \int_{\mathcal{B}} \sum_{\alpha} |\partial_{\alpha} \psi|^2 \leq C J_{\Sigma_0}^T[\psi] + C J_{\Sigma_0}^T[T\psi]. \tag{4.3.2}$$

### 4.4 The $T, P, N$ Hierarchical Vector Fields

We define

$$\mathcal{A}^{\mathcal{H}^t} = \{r \leq r_{\mathcal{H}^t}\}, \quad N_{\tau}^{\mathcal{H}^t} = \Sigma_{\tau} \cap \mathcal{A}^{\mathcal{H}^t}.$$



In this section we will present the obstructions to proving non-degenerate estimates in the region  $\mathcal{A}^{\mathcal{H}^t}$ . Starting with the general ansatz  $N = f_v(r) \partial_v + f_r(r) \partial_r$  we have that  $N$  is future-directed timelike at the horizon if  $f_v(M) > 0$  and  $f_r(M) < 0$ . Moreover, introducing the energy current  $J_{\mu}^N[\psi]$  we obtain

$$K^N[\psi] = F_{vv}(\partial_v\psi)^2 + F_{rr}(\partial_r\psi)^2 + F_{vr}(\partial_v\psi)(\partial_r\psi) + F_{\mathbb{V}}|\mathbb{V}\psi|^2,$$

where the coefficients are given by

$$\begin{aligned} F_{rr} &= D \left[ \frac{(\partial_r f_r)}{2} - \frac{f_r}{r} \right] - \frac{f_r D'}{2}, \\ F_{vv} &= (\partial_r f_v), \quad F_{\mathbb{V}} = -\frac{1}{2}(\partial_r f_r), \quad F_{vr} = D(\partial_r f_v) - \frac{2f_r}{r}. \end{aligned} \quad (4.4.1)$$

Recall that  $D = (1 - \frac{M}{r})^2$ . We see that the coefficient of  $(\partial_r\psi)^2$  (in bold) vanishes on the horizon  $\mathcal{H}^+$ . This is a manifestation of the degeneracy of the redshift effect (see Sect. 1.5.4). On the other hand, the coefficient of  $\partial_v\psi\partial_r\psi$  is equal to  $-\frac{2f_r(M)}{M}$  which is not zero. Therefore,  $K^N[\psi]$  is not non-negative definite. To overcome this, we introduce the following *modified Lagrangian current*

$$\tilde{J}_\mu^N[\psi] = J_\mu^N[\psi] - \frac{1}{2}\psi\nabla_\mu\psi. \quad (4.4.2)$$

Then, since  $\nabla^\mu\psi \cdot \nabla_\mu\psi = D(\partial_r\psi)^2 + 2\partial_r\psi\partial_v\psi + |\mathbb{V}\psi|^2$ , we have

$$\begin{aligned} \operatorname{div}\tilde{J}^N[\psi] &= F_{vv}(\partial_v\psi)^2 + \left[ F_{rr} - \frac{D}{2} \right] (\partial_r\psi)^2 - \frac{\partial_r f_r + 1}{2} |\mathbb{V}\psi|^2 \\ &\quad + [F_{vr} - 1](\partial_v\psi\partial_r\psi). \end{aligned} \quad (4.4.3)$$

Choosing  $f_v(r) = 16r$ ,  $f_r(r) = -\frac{3}{2}r + M$  then  $N$  is timelike and hence

$$J_\mu^N[\psi]n_{\Sigma_r}^\mu \sim |\partial_r\psi|^2 + |\mathbb{V}\psi|^2$$

close to the horizon. In view of the  $T$ -invariance of  $N$ , the constants in  $\sim$  depend only on  $M$ . Note that the coefficient of  $\partial_r\psi$  is non-degenerate. Most importantly, the (modified) coefficient of the mixed term  $\partial_v\psi\partial_r\psi$  vanishes on the horizon. In fact, we can easily see that in  $\{M \leq r \leq \frac{9M}{8}\}$  we have

$$\operatorname{div}\tilde{J}^N[\psi] \sim \left( (T\psi)^2 + \sqrt{D}(\partial_r\psi)^2 + |\mathbb{V}\psi|^2 \right). \quad (4.4.4)$$

Hence we will take  $r_{\mathcal{H}} \leq \frac{9M}{8}$ . We smoothly extend  $N$  in  $\{r \geq \frac{9M}{8}\}$  so that  $N = T$  for  $r \geq \frac{3M}{2}$  and such that  $N$  is globally timelike and translation-invariant  $[T, N] = 0$ . The idea is of course to apply the divergence theorem for the modified current  $\tilde{J}_\mu^N[\psi]$  in the region  $\mathcal{R}(0, \tau)$ . The divergence has the good sign in region  $\mathcal{A}^{\mathcal{H}}$  and can be bounded by (4.3.1) in the region  $\mathcal{B}$ . What about the boundary terms? Since  $N$  is timelike the  $N$ -fluxes are positive-definite. However, here we consider the modified  $N$ -current which introduces additional boundary zeroth order terms. These additional terms can be bounded using appropriate Hardy inequalities, such as

$$\int_{\Sigma_r \cap \mathcal{A}^{\mathcal{H}^+}} \frac{1}{r^2} \psi^2 \leq C \int_{\Sigma_r} J_\mu^T[\psi] n_\Sigma^\mu \quad (4.4.5)$$

which allows us to bound the local  $L^2$  norm of  $\psi$  via the (conserved)  $T$ -flux. We finally obtain the following flux estimates

$$\begin{aligned} \int_{\Sigma_r} J_\mu^N[\psi] n^\mu &\leq 2 \int_{\Sigma_r} \tilde{J}_\mu^N[\psi] n^\mu + C \int_{\Sigma_r} J_\mu^T[\psi] n^\mu, \\ c \int_{\mathcal{H}^+} J_\mu^N[\psi] n_{\mathcal{H}^+}^\mu &\leq \int_{\mathcal{H}^+} \tilde{J}_\mu^N[\psi] n_{\mathcal{H}^+}^\mu + C_\epsilon \int_{\Sigma_r} J_\mu^T[\psi] n_{\Sigma_r}^\mu + \epsilon \int_{\Sigma_r} J_\mu^N[\psi] n_{\Sigma_r}^\mu, \end{aligned}$$

which yield

$$\int_{\Sigma_r} J_\mu^N[\psi] n_{\Sigma_r}^\mu + \int_{\mathcal{H}^+} J_\mu^N[\psi] n_{\mathcal{H}^+}^\mu + \int_{\mathcal{A}^{\mathcal{H}^+}} \operatorname{div} \tilde{J}^N[\psi] \leq C \int_{\Sigma_0} J_\mu^N[\psi] n_{\Sigma_0}^\mu. \quad (4.4.6)$$

We next introduce yet another important vector field, which as we shall see, lies in some sense “between”  $T$  and  $N$ . Consider the ansatz

$$P = P_v \partial_v - \sqrt{D} \partial_r$$

close to the horizon. Then, by virtue of (4.4.1), we have

$$F_{rr} = D \left[ -\frac{D'}{4\sqrt{D}} + \frac{\sqrt{D}}{r} \right] + \frac{\sqrt{D} D'}{2} \sim D.$$

Furthermore,

$$F_{vr} = \sqrt{D} \left[ \sqrt{D} (\partial_r f_v) + \frac{2}{r} \right] \leq \epsilon D + \frac{1}{\epsilon} \left[ \sqrt{D} (\partial_r f_v) + \frac{2}{r} \right]^2.$$

Hence, choosing  $P_v > 0$  such that

$$\frac{1}{\epsilon} \left[ \sqrt{D} (\partial_r P_v) + \frac{2}{r} \right]^2 < \partial_r P_v,$$

close to the horizon, gives rise to a causal vector field  $P$  (which is null on the horizon) such that

$$K^P[\psi] \sim ((\partial_v \psi)^2 + D(\partial_r \psi)^2 + |\nabla \psi|^2) \sim J_\mu^T n_\Sigma^\mu \quad (4.4.7)$$

close to the horizon. Note that, unlike the  $N$ -current, no modification was needed for  $J^P$ . We conclude that the following  $T - P - N$  hierarchy holds

$$\operatorname{div} J_\mu^T[\psi] = 0, \quad \operatorname{div} J_\mu^P[\psi] \sim J^T[\psi], \quad \operatorname{div} J_\mu^N[\psi] \sim J^P[\psi] \quad (4.4.8)$$

in the region  $\mathcal{A}^{\mathcal{H}}$ .

## 4.5 The Trapping Effect on the Event Horizon

Note that the spacetime integral obtained by the  $N$ -current degenerates at the horizon in view of (4.4.4). We will address this degeneracy in this section. The  $N$ -energy

$$E_\gamma(s) = g(\dot{\gamma}(s), N)$$

of affinely-parametrized null generators  $\gamma(s)$  of the event horizon of ERN is **constant** for all  $s$ . This is of course related to the vanishing of the surface gravity on ERN and is in stark contrast with sub-extremal horizons where the energy of the null generators decays in  $s$ . Sbierski [3] used the Gaussian beam approximation to show that there are solutions to the wave equation on ERN that are localized in a neighborhood of  $\mathcal{H}^+$  with almost constant  $N$ -energy on  $\Sigma_\tau$  for arbitrarily large  $\tau$ . This result immediately yields an obstruction to bounding the following integral

$$\Gamma_1[\psi] = \int_0^\infty \left( \int_{\Sigma_\tau \cap \{r \leq M + \epsilon\}} |\partial_\rho \psi|^2 \right) d\tau$$

for (any) arbitrarily small  $\epsilon > 0$ . Specifically, Sbierski's result shows that the above integral cannot be bounded purely in terms of the  $N$ -initial energy of  $\psi$  on  $\Sigma_0$ . A Morawetz estimate bounding  $\Gamma_1[\psi]$  was established in [4] where it was shown that such an estimate requires

1. *the finiteness of a weighted higher-order norm of the initial data, and*
2. *the vanishing of the conserved charge  $H_0[\psi]$ .*

Furthermore, it was shown that *for smooth and compactly supported initial data,  $\Gamma_1[\psi]$  is infinite if and only if  $H_0[\psi] \neq 0$ .*

The first requirement above is reminiscent to that of the Morawetz estimates on the photon sphere. On the other hand, the second requirement is a global (low-frequency) condition on all of the event horizon, that is on all the null generators of the event horizon. This shows that *the event horizon on ERN exhibits a global trapping effect.*

Another characteristic feature of the event horizon on ERN is the following *stable higher-order trapping effect: For generic smooth and compactly supported initial data with support away from the event horizon, the following higher-order integral*

$$\Gamma_k[\psi] = \int_0^\infty \left( \int_{\Sigma_\tau \cap \{r \leq M + \epsilon\}} |\partial^k \psi|^2 \right) d\tau$$

is infinite, for all  $k \geq 2$ .

## 4.6 Horizon Localized and Infinity Localized Hierarchies

The following global Morawetz estimate extending (4.3.2) holds on ERN (see [5])

$$\int_{\tau_1}^{\tau_2} \left( \int_{\Sigma_\tau} (r - M)^{\sigma_1} \cdot \frac{1}{r^{\sigma_2}} \cdot J^T[\psi] \right) d\tau \lesssim \int_{\Sigma_{\tau_1}} J^T[\psi] + J^T[T\psi], \quad (4.6.1)$$

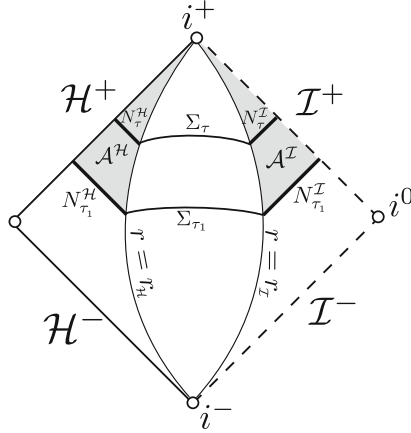
with  $\sigma_1, \sigma_2 > 2$  sufficient large constants. Here,  $J^T[\psi]$  denotes the standard  $T$ -energy flux through  $\Sigma_\tau$ . The higher-order terms on the right hand side account for *the high-frequency trapping effect on the photon sphere* at  $\{r = 2M\}$ . The  $r^{-\sigma_2}$  degenerate (at infinity) coefficient is related to the asymptotical flatness of the spacetime and is present in the analogous estimate for Minkowski spacetime. On the other hand, the degenerate factor  $(r - M)^{\sigma_1}$  is related to the degeneracy of the redshift effect (see also Sect. 4.5). In order to prove decay of the energy flux (4.2.1), we need to remove the degenerate factors from (4.6.1). Dafermos and Rodnianski [6] and subsequently Moschidis [7] showed that the weight at infinity  $r^{-\sigma_2}$  can be removed for general asymptotically flat spacetimes by introducing appropriate *growing*  $r$  weights on the right hand side yielding *a hierarchy of two  $r$ -weighted estimates*.

The strategy of [8] for obtaining precise late-time asymptotics on ERN, which we outline in the remaining of this chapter, is based on the integrated  $r^p$ -weighted energy decay approach of Dafermos–Rodnianski [6] and its extension presented in [9].

### 4.6.1 The Conformal Fluxes $C_{N_\tau^{\mathcal{H}}}$ and $C_{N_\tau^{\mathcal{I}}}$

In view of the degenerate factors both at the horizon and at infinity in the Morawetz estimate (4.6.1) on ERN, one needs to obtain *an analogue of the Dafermos–Rodnianski hierarchy at both the near-infinity region  $\mathcal{A}^{\mathcal{I}} = \{r \geq r_{\mathcal{I}}\}$  and the near-horizon region  $\mathcal{A}^{\mathcal{H}} = \{r \leq r_{\mathcal{H}}\}$* . We define

$$N_\tau^{\mathcal{H}} = \Sigma_\tau \cap \mathcal{A}^{\mathcal{H}}, \quad N_\tau^{\mathcal{I}} = \Sigma_\tau \cap \mathcal{A}^{\mathcal{I}}.$$



In the remaining of this chapter we will use the double null coordinate system  $(u, v)$ , unless otherwise stated. The  $T - P - N$  hierarchy (4.4.8) yields the following  $\mathcal{H}^+$ –**localized hierarchy** in  $\mathcal{A}^{\mathcal{H}}$  for all  $\tau_2 \geq \tau_1 \geq 0$

$$\int_{\tau_1}^{\tau_2} \left[ \int_{N_{\tau_1}^{\mathcal{H}}} J^T[\psi] \right] d\tau \lesssim \int_{N_{\tau_1}^{\mathcal{H}}} (r - M)^{-1} \cdot (\partial_u(r\psi))^2 d\Omega du + \text{l.o.t.},$$

$$\int_{\tau_1}^{\tau_2} \left[ \int_{N_{\tau_1}^{\mathcal{H}}} (r - M)^{-1} \cdot (\partial_u(r\psi))^2 d\Omega du \right] d\tau \lesssim \int_{N_{\tau_1}^{\mathcal{H}}} (r - M)^{-2} \cdot (\partial_u(r\psi))^2 d\Omega du + \text{l.o.t.} \quad (4.6.2)$$

Moreover, the following  $\mathcal{I}^+$ –**localized hierarchy** holds in  $\mathcal{A}^{\mathcal{I}}$  (see [5])

$$\int_{\tau_1}^{\tau_2} \left[ \int_{N_{\tau_1}^{\mathcal{I}}} J^T[\psi] \right] d\tau \lesssim \int_{N_{\tau_1}^{\mathcal{I}}} r \cdot (\partial_v(r\psi))^2 d\Omega dv + \text{l.o.t.},$$

$$\int_{\tau_1}^{\tau_2} \left[ \int_{N_{\tau_1}^{\mathcal{I}}} r \cdot (\partial_v(r\psi))^2 d\Omega dv \right] d\tau \lesssim \int_{N_{\tau_1}^{\mathcal{I}}} r^2 \cdot (\partial_v(r\psi))^2 d\Omega dv + \text{l.o.t.} \quad (4.6.3)$$

The integral on the right hand side of the second estimate of the  $\mathcal{I}^+$ –localized hierarchy corresponds to *the conformal energy near  $\mathcal{I}^+$* . Similarly, the integral on the right hand side of the second estimate of the  $\mathcal{H}^+$ –localized hierarchy corresponds to *the conformal energy near  $\mathcal{H}^+$* . We denote

$$\text{Conformal energy near } \mathcal{I}^+ : C_{N_{\tau}^{\mathcal{I}}}[\psi] = \int_{N_{\tau}^{\mathcal{I}}} r^2 \cdot (\partial_v(r\psi))^2 d\Omega dv \quad (4.6.4)$$

and

$$\text{Conformal energy near } \mathcal{H}^+ : C_{N_{\tau}^{\mathcal{H}}}[\psi] = \int_{N_{\tau}^{\mathcal{H}}} (r - M)^{-2} \cdot (\partial_u(r\psi))^2 d\Omega du. \quad (4.6.5)$$

Note that  $du = -2 \left(1 - \frac{M}{r}\right)^{-2} dr$  on  $\Sigma_\tau$  and  $\partial_u = -\frac{1}{2} \left(1 - \frac{M}{r}\right)^2 Y$ , where  $Y = \partial_r$  –with respect to the system  $(v, r)$ – is regular at the horizon. Hence, the conformal flux near  $\mathcal{H}^+$   $C_{N_\tau^+}[\psi] \sim \int_{N_\tau^+} (Y\psi)^2$  is at the level of the *non-degenerate* energy.

If both of the energies (4.6.4) and (4.6.5) are initially finite, then by a standard application of the mean value theorem on dyadic time intervals and the boundedness of the  $T$ -energy flux, we obtain the decay rate  $\tau^{-2}$  for the  $T$ -energy flux  $J_{\Sigma_\tau}^T[\psi]$ . This decay rate however is not sharp. Faster decay rates for the higher order flux  $J_{\Sigma_\tau}^T[T\psi]$  were obtained for sub-extremal black holes by Schlue [10] and Moschidis [7]. Their method used  $\partial_v, r\partial_v$  as commutator vector fields in the near-infinity region. Nonetheless, their approach does not yield faster decay for the  $T$ -flux  $J_{\Sigma_\tau}^T[\psi]$  itself.

### 4.6.2 Commuted Hierarchies in the Regions $\mathcal{A}^{\mathcal{H}}$ and $\mathcal{A}^{\mathcal{I}}$

The strategy for obtaining further decay for  $J_{\Sigma_\tau}^T[\psi]$  on ERN is to establish *integrated decay estimates for the conformal fluxes*<sup>1</sup>  $C_{N_\tau^+}[\psi]$  and  $C_{N_\tau^+}[\psi]$ , extending thereby the  $\mathcal{I}^+$ –localized and  $\mathcal{H}^+$ –localized hierarchies (4.6.3) and (4.6.2). However, it is not possible to further extend of (4.6.3) and (4.6.2) by considering larger powers of  $r$  and  $(r - M)^{-1}$ , respectively. Instead, motivated by the following Hardy inequality (see also Sect. 4.7.2)

$$\int_0^\infty x^2 \cdot (\partial_x f)^2 \lesssim \int_0^\infty \left( \partial_x (x^2 \partial_x f) \right)^2 \quad (4.6.6)$$

applied to  $f = r\psi$  with  $x = r$  in  $\mathcal{A}^{\mathcal{I}}$  and  $x = (r - M)^{-1}$  in  $\mathcal{A}^{\mathcal{H}}$ , we introduce the following *n-commuted* quantities:

$$\Phi_{(n)} := (r^2 \partial_v)^n (r\psi), \quad \underline{\Phi}_{(n)} := Y^n (r\psi) \sim \left( - (r - M)^{-2} \partial_u \right)^n (r\psi),$$

where  $n \in \mathbb{N}_0$ . Note that the weights are of second-order in  $r$  and  $(r - M)^{-1}$ . The idea, therefore, is to derive  $\mathcal{I}^+$ –localized and  $\mathcal{H}^+$ –localized *commuted* hierarchies which yield decay for weighted fluxes of the commuted functions  $\Phi_{(n)}$  and  $\underline{\Phi}_{(n)}$ . If  $\psi$  solves the wave equation (1.7.1) on ERN then for all  $n \geq 0$  and for all  $p \in \mathbb{R}$  the commuted quantities  $\Phi_{(n)}$  and  $\underline{\Phi}_{(n)}$  satisfy the following *key identities* in  $\mathcal{A}^{\mathcal{I}}$  and  $\mathcal{A}^{\mathcal{H}}$  regions, respectively: **Near-infinity identity**:

$$\begin{aligned} & \int_{\mathbb{S}^2} \partial_u \left( r^p (\partial_v \Phi_{(n)})^2 \right) + \partial_v \left( r^{p-2} |\nabla_{\mathbb{S}^2} \Phi_{(n)}|^2 - n(n+1) r^{p-2} \Phi_{(n)}^2 \right) d\Omega \\ & + \int_{\mathbb{S}^2} (p+4n) r^{p-1} (\partial_v \Phi_{(n)})^2 + (2-p) r^{p-3} \left( |\nabla_{\mathbb{S}^2} \Phi|^2 - n(n+1) \Phi_{(n)}^2 \right) d\Omega \quad (4.6.7) \\ & = n \cdot \sum_{k=0}^{\max(0, n-1)} \int_{\mathbb{S}^2} \mathcal{O}(r^{p-2}) \cdot \Phi_{(k)} \cdot \partial_v \Phi_{(n)} d\Omega + \text{l.o.t.}, \end{aligned}$$

<sup>1</sup>Note that (non-degenerate) integrated decay estimates for the fluxes  $C_{N_\tau^+}[\psi]$  and  $C_{N_\tau^+}[\psi]$  on ERN are closely related to the *trapping effect* at  $\mathcal{I}^+$  and at  $\mathcal{H}^+$ .

**Near-horizon identity:**

$$\begin{aligned}
& \int_{\mathbb{S}^2} \partial_v \left( (r-M)^{-p} (\partial_u \Phi_{(n)})^2 \right) + \partial_u \left( (r-M)^{-p+2} |\nabla_{\mathbb{S}^2} \Phi_{(n)}|^2 - n(n+1)(r-M)^{-p+2} \Phi_{(n)}^2 \right) d\Omega \\
& + \int_{\mathbb{S}^2} (p+4n)(r-M)^{-p+1} (\partial_u \Phi_{(n)})^2 + (2-p)(r-M)^{-p+3} \left( |\nabla_{\mathbb{S}^2} \Phi_{(n)}|^2 - n(n+1)\Phi_{(n)}^2 \right) d\Omega \\
& = n \cdot \sum_{k=0}^{\max\{0, n-1\}} \int_{\mathbb{S}^2} O((r-M)^{-p+2}) \cdot \Phi_{(k)} \cdot \partial_u \Phi_{(n)} d\Omega + \text{l.o.t.}
\end{aligned} \tag{4.6.8}$$

Note that (4.6.8) is of the same form as (4.6.7), but with  $u$  and  $v$  reversed and  $r$  replaced by  $(r-M)^{-1}$ . This is of course related to the existence of the Couch–Torrence conformal inversion of ERN. After integrating in  $u$  and  $v$ , the (red) “error” terms in the derived spacetime identities can be controlled via *Morawetz and Hardy inequalities* for the following range of weights<sup>2</sup>:

$$-4n < p \leq 2. \tag{4.6.9}$$

We arrive at the following inequalities

$\mathcal{I}^+$ –**localized  $n$ –commuted  $p$ –weighted inequalities for  $\Phi_{(n)}$ :**

$$\begin{aligned}
& \int_{N_2^I} r^p (\partial_v \Phi_{(n)})^2 d\Omega dv \\
& + \int_{\tau_1}^{\tau_2} \int_{N_1^I} (p+4n)r^{p-1} (\partial_v \Phi_{(n)})^2 d\Omega dv d\tau \\
& + (2-p) \int_{\tau_1}^{\tau_2} \int_{N_1^I} r^{p-3} (|\nabla_{\mathbb{S}^2} \Phi_{(n)}|^2 - n(n+1)\Phi_{(n)}^2) d\Omega dv d\tau \\
& \lesssim_p \int_{N_1^I} r^p (\partial_v \Phi_{(n)})^2 d\Omega dv + \dots,
\end{aligned} \tag{4.6.10}$$

$\mathcal{H}^+$ –**localized  $n$ –commuted  $p$ –weighted inequalities for  $\Phi_{(n)}$ :**

$$\begin{aligned}
& \int_{N_2^H} (r-M)^{-p} (\partial_u \Phi_{(n)})^2 d\Omega du \\
& + \int_{\tau_1}^{\tau_2} \int_{N_1^H} (p+4n)(r-M)^{-p+1} (\partial_u \Phi_{(n)})^2 d\Omega du d\tau \\
& + (2-p) \int_{\tau_1}^{\tau_2} \int_{N_1^H} (r-M)^{-p+3} (|\nabla_{\mathbb{S}^2} \Phi_{(n)}|^2 - n(n+1)\Phi_{(n)}^2) d\Omega du d\tau \\
& \lesssim_p \int_{N_1^H} (r-M)^{-p} (\partial_u \Phi_{(n)})^2 d\Omega du + \dots
\end{aligned} \tag{4.6.11}$$

---

<sup>2</sup>For spherically symmetric solutions (with harmonic mode number  $\ell = 0$ ) we only take  $n = 0$ .

These inequalities hold for **all**  $n$ , as long as  $p$  satisfies (4.6.9). In order to turn these inequalities into actual estimates we need to guarantee the non-negativity of the terms  $|\nabla_{\mathbb{S}^2} \Phi_{(n)}|^2 - n(n + 1)\Phi_{(n)}^2$  and  $|\nabla_{\mathbb{S}^2} \underline{\Phi}_{(n)}|^2 - n(n + 1)\underline{\Phi}_{(n)}^2$ . In view of the *Poincaré inequality* on  $\mathbb{S}^2$ , these terms are non-negative if  $\psi$  is supported on angular frequencies  $\ell$  such that

$$\ell \geq n. \tag{4.6.12}$$

In other words, we can commute the wave equation  $n$  times and obtain two estimates for  $\Phi_{(n)}$  and two estimates for  $\underline{\Phi}_{(n)}$  as long as  $n$  is less or equal than the lowest harmonic mode that is present in a harmonic mode expansion of  $\psi$ . The two estimates correspond to the values  $p = 1$  and  $p = 2$ .

It is worth mentioning that the estimates (4.6.11) can be thought of as *degenerate remnants* of the red shift estimates. Note that the degeneracy of the red shift effect is manifested in the additional factor of  $(r - M)$  that appears in the spacetime integral of  $(\partial_u \underline{\Phi}_{(n)})^2$  on the left-hand side of (4.6.11).

The Table 4.1 summarizes the number of the  $\mathcal{H}^+$ -localized  $n$ -commuted estimates and the  $\mathcal{I}^+$ -localized  $n$ -commuted estimates for each fixed  $n$  as well as the total number of estimates available in the **total hierarchy** over all admissible values of  $n$ .

**Definition:** We define the **length of a hierarchy** to be equal to the number of available and useful integrated estimates in the hierarchy. Useful here means that the exponents  $p$  of the weights increase by an integer number or by an almost (modulo  $\epsilon > 0$ ) integer number.

**Table 4.1** The length of the commuted hierarchies for  $\ell = 0$ ,  $\ell = 1$  and  $\ell \geq 2$

Harmonic mode	Commuted hierarchies		
	Fixed $n$ commuted		Total hierarchy
	$n$	Length	Length
$\ell = 0$	0	2	2
$\ell = 1$	0	2	4
	1	2	
$\ell \geq 2$	0	2	6
	1	2	
	2	2	

### 4.6.3 Improved Hierarchies for $\ell = 0, 1$

The harmonic projections  $\psi_{\ell=0}$  and  $\psi_{\ell=1}$  of  $\psi$  satisfy only two and four estimates in the total hierarchy, respectively, as in Table 4.1. When dealing with  $\ell = 0$  (and hence  $n = 0$ ) separately, we can show that the range of  $p$  can actually be *extended* to  $0 < p < 3$  for both the  $\mathcal{H}^+$ -localized and the  $\mathcal{I}^+$ -localized hierarchies. Note

that even though we cannot take  $p = 3$  exactly, we can (and will) take  $p = 3 - \epsilon$  for sufficiently small  $\epsilon > 0$ . Additionally, we can show that

- if  $I_0[\psi] = 0$  then we can take  $0 < p < 5$  in the  $\mathcal{I}^+$ -localized hierarchy, and
- if  $H_0[\psi] = 0$  then we can take  $0 < p < 5$  in the  $\mathcal{H}^+$ -localized hierarchy.

Similarly as above, even though we cannot take  $p = 5$  exactly, we will take  $p = 5 - \epsilon$  for  $\epsilon > 0$ . In this sense, the lengths of the above hierarchies (under the vanishing assumptions) is five. Moreover, these hierarchies are *inextendible* (consistent with the horizon instability results of Sect. 2.2) and hence their length is sharp. It is important to observe that, based on the above result, the lengths of the total hierarchies depend on the type of data. These are summarized in the Table 4.2.

**Convention:** By  $\mathcal{R}$ -**global hierarchy** we mean the hierarchy that arises from weighted fluxes on  $\Sigma_\tau$  by adding the  $\mathcal{H}^+$ -localized hierarchy (in region  $\mathcal{A}^{\mathcal{H}}$ ), the  $\mathcal{I}^+$ -localized hierarchy (in region  $\mathcal{A}^{\mathcal{I}}$ ) and the higher-order Morawetz estimates in region  $\mathcal{B}$  (that is, higher order analogues of (4.3.2)). Recall that  $\mathcal{R} = \mathcal{A}^{\mathcal{H}} \cup \mathcal{A}^{\mathcal{I}} \cup \mathcal{B}$ .

**Table 4.2** Lengths of improved hierarchies for  $\ell = 0$

Data	Improved hierarchies for $\ell = 0$ with $n = 0$		
	$\mathcal{H}^+$ -localized	$\mathcal{I}^+$ -localized	$\mathcal{R}$ -global
Type A	3	5	3
Type B	5	5	5
Type C	3	3	3
Type D	5	3	3

In order to extend the length of the hierarchies for  $\ell = 1$  we introduce the following “modified” variants of  $\Phi_{(1)}$  and  $\underline{\Phi}_{(1)}$  (with  $n = 1$ ):

$$\tilde{\Phi} = \tilde{\Phi}_{(1)} := r(r - M)\partial_v(r\psi_{\ell=1}), \quad \tilde{\underline{\Phi}} = \tilde{\underline{\Phi}}_{(1)} := r \cdot Y(r\psi_{\ell=1}).$$

The following identities hold for  $\psi_{\ell=1}$ :

$$\begin{aligned} & \int_{\mathbb{S}^2} \partial_u (r^p (\partial_v \tilde{\Phi})^2) d\Omega + \int_{\mathbb{S}^2} (p + 4n)r^{p-1} (\partial_v \tilde{\Phi})^2 d\Omega \\ &= \int_{\mathbb{S}^2} \mathbf{O}(r^{p-3}) \cdot r\psi \cdot \partial_v \tilde{\Phi} d\Omega + \text{l.o.t} \end{aligned} \quad (4.6.13)$$

and

$$\begin{aligned} & \int_{\mathbb{S}^2} \partial_v ((r - M)^{-p} (\partial_u \tilde{\underline{\Phi}})^2) + \int_{\mathbb{S}^2} (p + 4n)(r - M)^{-p+1} (\partial_u \tilde{\underline{\Phi}})^2 d\Omega \\ &= \int_{\mathbb{S}^2} \mathbf{O}((r - M)^{-p+3}) \cdot r\psi \cdot \partial_u \tilde{\underline{\Phi}} d\Omega + \text{l.o.t} \end{aligned} \quad (4.6.14)$$

Note that the (red) error terms are now of lower order compared to the error terms in (4.6.7) and (4.6.8). This allows us to obtain versions of (4.6.10) and (4.6.11) with  $\Phi_{(1)}$  and  $\underline{\Phi}_{(1)}$  replaced by  $\tilde{\Phi}$  and  $\tilde{\underline{\Phi}}$ , respectively, where the range of  $p$  can be extended to  $0 < p < 3$ . We further obtain that:

- the range of the  $\mathcal{I}^+$ -localized hierarchy can be further extended to  $0 < p < 4$  if  $\Phi$  decays sufficiently fast towards  $\mathcal{I}^+$ , and
- the range of the  $\mathcal{H}^+$ -localized hierarchy can be further extended to  $0 < p < 4$  if  $\underline{\Phi}$  decays sufficiently fast towards  $\mathcal{H}^+$ .

Again, we cannot take  $p = 44$ , but we will take  $p = 4 - \epsilon$ .

The results for  $\ell = 1$  are summarized in the Tables 4.3 and 4.4.

**Table 4.3** Lengths of improved hierarchies for  $\ell = 1$

Data	Improved hierarchies for $\ell = 1$						
	$\mathcal{H}^+$ -localized			$\mathcal{I}^+$ -localized			$\mathcal{R}$ -global
	$n$ -commuted		Total length	$n$ -commuted		Total length	Total length
	$n$	Length		$n$	Length		
Type A	0	2	5	0	2	6	5
	1	3		1	4		
Type B	0	2	6	0	2	6	6
	1	4		1	4		
Type C	0	2	5	0	2	5	5
	1	3		1	3		
Type D	0	2	6	0	2	5	5
	1	4		1	3		

**Table 4.4** Final table with improved hierarchies

Data	Harmonic mode	Length of total hierarchy		
		$\mathcal{H}^+$ -localized	$\mathcal{I}^+$ -localized	$\mathcal{R}$ -global
Type A	$\ell = 0$	3	5	3
	$\ell = 1$	5	6	5
	$\ell \geq 2$	6	6	6
Type B	$\ell = 0$	5	5	5
	$\ell = 1$	6	6	6
	$\ell \geq 2$	6	6	6
Type C	$\ell = 0$	3	3	3
	$\ell = 1$	5	5	5
	$\ell \geq 2$	6	6	6
Type D	$\ell = 0$	5	3	3
	$\ell = 1$	6	5	5
	$\ell \geq 2$	6	6	6

*Remark: additionally extended hierarchies for time-derivatives*

Schluë [10] and Moschidis [7] obtained improved energy decay estimates for the time derivative  $T\psi$  by considering  $r$ -weighted estimates for the quantities  $\partial_v(r\psi)$  or  $r\partial_v(r\psi)$ . Their approach can be generalized by establishing estimates for  $\partial_v^k\Phi_{(n)}$  in the near-infinity region  $\mathcal{A}^{\mathcal{I}}$  and for  $\partial_u^k\Phi_{(n)}$  in the near-horizon region  $\mathcal{A}^{\mathcal{H}}$  (with  $n$  as above), where  $k \in \mathbb{N}$  takes *any* positive value  $k \geq 1$ . This yields the following: **for each time derivative that we take, we gain two more estimates in the  $\mathcal{I}^+$ –localized hierarchy and two more estimates in the  $\mathcal{H}^+$ –localized hierarchy.** These improvements play an important role in the subsequent subsections.

## 4.7 Energy and Pointwise Decay

### 4.7.1 Decay for the Fluxes $J_{\Sigma_\tau}^T$ , $C_{N_\tau^{\mathcal{H}}}$ and $C_{N_\tau^{\mathcal{I}}}$

The total  $\mathcal{I}^+$ –localized and  $\mathcal{H}^+$ –localized hierarchies (over all admissible  $n$ ) give quantitative decay rates for the conformal fluxes  $C_{N_\tau^{\mathcal{I}}}[\psi]$ , given by (4.6.4), and  $C_{N_\tau^{\mathcal{H}}}[\psi]$ , given by (4.6.5). This is easily obtained via successive application of the mean value theorem in dyadic intervals and of the Hardy inequality (4.6.6). The rule is the following:

*decay rate of the conformal flux  $C_{N_\tau^{\mathcal{I}}}[\psi] = \text{length}(\mathcal{I}^+ \text{–loc. hierarchy}) - 2 - \epsilon$ ,*

and

*decay rate of the conformal flux  $C_{N_\tau^{\mathcal{H}}}[\psi] = \text{length}(\mathcal{H}^+ \text{–loc. hierarchy}) - 2 - \epsilon$*

for any sufficiently small  $\epsilon > 0$ . The  $\epsilon$  loss here has to do with the fact that the maximum value of  $p$  in the extended improved hierarchies for  $\ell = 0$  and  $\ell = 1$  is not an exact integer.

Having obtained the decay rate for the conformal fluxes we can proceed to obtain the decay rate for the global  $T$ -flux  $J_{\Sigma_\tau}^T[\psi]$ . We revisit the  $\mathcal{H}^+$ –localized and  $\mathcal{I}^+$ –localized hierarchies; we add the  $\mathcal{H}^+$ –localized hierarchy (in region  $\mathcal{A}^{\mathcal{H}}$ ), the  $\mathcal{I}^+$ –localized hierarchy (in region  $\mathcal{A}^{\mathcal{I}}$ ) and the higher-order Morawetz estimates (in region  $\mathcal{B}$ ). Using again successively the mean value theorem in dyadic intervals and appropriate Hardy inequalities we obtain decay estimates for the  $T$ -energy flux. The rule here is the following

*decay rate  $T$  – flux  $J_{\Sigma_\tau}^T[\psi] = \text{decay rate of slowest conformal flux} + 2$ .*

Unlike the sub-extremal case, there are **two** independent conformal fluxes that contribute to the decay rate for the energy flux on ERN. This feature of ERN creates further complications later in the derivation of the precise asymptotics.

As an illustration of the method, let us consider initial data for  $\psi$  of Type **A**. As we can see in Table 4.2, the length of the total  $\mathcal{I}^+$ -localized hierarchy and total  $\mathcal{H}^+$ -localized hierarchy for  $\ell = 0$  is 5 and 3, respectively. Hence, we obtain the following schematic decay estimates for the conformal fluxes:

$$\begin{aligned} C_{N\tau^\ell}[\psi_{\ell=0}] &\lesssim E_{\ell=0} \cdot \tau^{-1+\epsilon}, \\ C_{N\tau^\ell}[\psi_{\ell=0}] &\lesssim E_{\ell=0} \cdot \tau^{-3+\epsilon}. \end{aligned}$$

Furthermore, from Tables 4.1 and 4.3 we have that the length of the total  $\mathcal{I}^+$ -localized hierarchy and total  $\mathcal{H}^+$ -localized hierarchy for  $\ell \geq 1$  is 6 and 5, respectively. Hence,

$$\begin{aligned} C_{N\tau^\ell}[\psi_{\ell \geq 1}] &\lesssim E_{\ell \geq 1} \cdot \tau^{-3+\epsilon}, \\ C_{N\tau^\ell}[\psi_{\ell \geq 1}] &\lesssim E_{\ell \geq 1} \cdot \tau^{-4+\epsilon}. \end{aligned}$$

We conclude the following decay estimate for the  $T$ -energy flux:

$$\begin{aligned} J_{\Sigma_\tau}^T[\psi_{\ell=0}] &\lesssim E_{\ell=0} \cdot \tau^{-3+\epsilon}, \\ J_{\Sigma_\tau}^T[\psi_{\ell \geq 1}] &\lesssim E_{\ell \geq 1} \cdot \tau^{-5+\epsilon}, \end{aligned}$$

where  $E_{\ell=0}$  and  $E_{\ell \geq 1}$  denote (higher-order, weighted) initial data energy norms. Furthermore,

$$\begin{aligned} J_{\Sigma_\tau}^T[T^k \psi_{\ell=0}] &\lesssim E_{\ell=0} \cdot \tau^{-3-2k+\epsilon}, \\ J_{\Sigma_\tau}^T[T^k \psi_{\ell \geq 1}] &\lesssim E_{\ell \geq 1} \cdot \tau^{-5-2k+\epsilon}, \end{aligned}$$

for all  $k \geq 1$ . See also Table 4.8.

## 4.7.2 Hardy Inequalities

We next proceed with deriving pointwise decay estimates. We will use the following Hardy estimates

$$\begin{aligned} \int_{\mathbb{S}^2} (r\psi)^2 d\Omega &\lesssim \sqrt{C_{N\tau^\ell}[\psi]} \cdot \sqrt{J_{\Sigma_\tau}^T[\psi]} \quad \text{in } \mathcal{A}^{\mathcal{H}}, \\ \int_{\mathbb{S}^2} (r\psi)^2 d\Omega &\lesssim \sqrt{C_{N\tau^\ell}[\psi]} \cdot \sqrt{J_{\Sigma_\tau}^T[\psi]} \quad \text{in } \mathcal{A}^{\mathcal{I}}, \\ \int_{\mathbb{S}^2} (r-M) \cdot \psi^2 d\Omega &\lesssim \sqrt{J_{\Sigma_\tau}^T[\psi]} \quad \text{on } \Sigma_\tau. \end{aligned} \tag{4.7.1}$$

For initial data of Type **A**, using the above decay estimates for the conformal energies and the  $T$ -energy flux, we obtain

$$\begin{aligned} \int_{\mathbb{S}^2} (r\psi_{\ell=0})^2 d\Omega &\lesssim E_{\ell=0} \cdot \tau^{-2+\epsilon} && \text{in } \mathcal{A}^{\mathcal{H}}, \\ \int_{\mathbb{S}^2} (r\psi_{\ell=0})^2 d\Omega &\lesssim E_{\ell=0} \cdot \tau^{-3+\epsilon} && \text{in } \mathcal{A}^{\mathcal{I}}, \\ \int_{\mathbb{S}^2} (r - M) \cdot (\psi_{\ell=0})^2 d\Omega &\lesssim E_{\ell=0} \cdot \tau^{-3+\epsilon} && \text{on } \Sigma_\tau. \end{aligned}$$

Using the standard Sobolev estimates on  $\mathcal{S}^2$  we immediately obtain  $L^\infty$  decay estimates for  $r\psi_{\ell=0}$  in  $\mathcal{A}^H$ ,  $r\psi_{\ell=0}$  in  $\mathcal{A}^I$  and  $\sqrt{r - M} \cdot \psi_{\ell=0}$  on  $\Sigma_\tau$ , with the decaying factors  $\tau^{-1+\epsilon}$ ,  $\tau^{-\frac{3}{2}+\epsilon}$  and  $\tau^{-\frac{3}{2}+\epsilon}$ , respectively. Similarly,

$$\begin{aligned} \int_{\mathbb{S}^2} (r\psi_{\ell \geq 1})^2 d\Omega &\lesssim E_{\ell=0} \cdot \tau^{-4+\epsilon} && \text{in } \mathcal{A}^{\mathcal{H}}, \\ \int_{\mathbb{S}^2} (r\psi_{\ell \geq 1})^2 d\Omega &\lesssim E_{\ell=0} \cdot \tau^{-\frac{9}{2}+\epsilon} && \text{in } \mathcal{A}^{\mathcal{I}}, \\ \int_{\mathbb{S}^2} (r - M) \cdot (\psi_{\ell \geq 1})^2 d\Omega &\lesssim E_{\ell=0} \cdot \tau^{-5+\epsilon} && \text{on } \Sigma_\tau. \end{aligned}$$

As above,  $L^\infty$  decay estimates for  $r\psi_{\ell \geq 1}$  in  $\mathcal{A}^H$ ,  $r\psi_{\ell \geq 1}$  in  $\mathcal{A}^I$  and  $\sqrt{r - M} \cdot \psi_{\ell \geq 1}$  on  $\Sigma_\tau$ , with the decaying factors  $\tau^{-2+\epsilon}$ ,  $\tau^{-\frac{9}{4}+\epsilon}$  and  $\tau^{-\frac{5}{2}+\epsilon}$ , respectively.

The above estimates illustrate another deviation from the sub-extremal analysis in [9, 11]: for Type **A** initial data, the decay rate of  $r\psi_{\ell=0}$  in  $\mathcal{A}^{\mathcal{I}}$  is a power  $\frac{1}{2} + \epsilon$  away from the sharp decay rate, whereas in the sub-extremal case, the analogous estimate results in a decay rate that is almost sharp, in other words only  $\epsilon$  away from the sharp decay rate. In the extremal case it is the non-vanishing of  $H_0$  and hence the slow decay for the conformal energy in the near-horizon region that forms the “bottleneck” for the maximal length of the global hierarchy of weighted estimates for  $\psi_{\ell=0}$ . Nonetheless, note that the improved decay for the conformal flux gives an *improvement for the decay rate of the radiation field for Type A data*. The energy and pointwise decay rates are summarized in the two Tables 4.5 and 4.6.

**Table 4.5** Decay rates for  $\ell = 0$ . All are almost sharp except the bold rates

Data	Decay rates for $\ell = 0$					
	Energy flux decay			Pointwise decay		
	$J_{\Sigma_\tau}^{\mathcal{I}}[\psi]$	$C_{N_\tau^{\mathcal{H}}}[\psi]$	$C_{N_\tau^{\mathcal{I}}}[\psi]$	$r\psi _{\mathcal{H}^+}$	$\psi _{\{r=r_0\}}$	$r\psi _{\mathcal{I}^+}$
Type <b>A</b>	$\tau^{-3+\epsilon}$	$\tau^{-1+\epsilon}$	$\tau^{-3+\epsilon}$	$\tau^{-1+\epsilon}$	$\tau^{-\frac{3}{2}+\epsilon}$	$\tau^{-\frac{3}{2}+\epsilon}$
Type <b>B</b>	$\tau^{-5+\epsilon}$	$\tau^{-3+\epsilon}$	$\tau^{-3+\epsilon}$	$\tau^{-2+\epsilon}$	$\tau^{-\frac{5}{2}+\epsilon}$	$\tau^{-2+\epsilon}$
Type <b>C</b>	$\tau^{-3+\epsilon}$	$\tau^{-1+\epsilon}$	$\tau^{-1+\epsilon}$	$\tau^{-1+\epsilon}$	$\tau^{-\frac{3}{2}+\epsilon}$	$\tau^{-1+\epsilon}$
Type <b>D</b>	$\tau^{-3+\epsilon}$	$\tau^{-3+\epsilon}$	$\tau^{-1+\epsilon}$	$\tau^{-\frac{3}{2}+\epsilon}$	$\tau^{-\frac{3}{2}+\epsilon}$	$\tau^{-1+\epsilon}$

**Table 4.6** Decay rates for  $\ell \geq 1$ . All are sub-leading except the one in the shaded cell

Data	Decay rates for $\ell \geq 1$					
	Energy flux decay			Pointwise decay		
	$J_{\Sigma_\tau}^T[\psi]$	$C_{N_\tau^{\mathcal{H}}}[\psi]$	$C_{N_\tau^{\mathcal{I}}}[\psi]$	$r\psi _{\mathcal{H}^+}$	$\psi _{\{r=r_0\}}$	$r\psi _{\mathcal{I}^+}$
Type A	$\tau^{-5+\epsilon}$	$\tau^{-3+\epsilon}$	$\tau^{-4+\epsilon}$	$\tau^{-2+\epsilon}$	$\tau^{-\frac{5}{2}+\epsilon}$	$\tau^{-\frac{9}{4}+\epsilon}$
Type B	$\tau^{-6+\epsilon}$	$\tau^{-4+\epsilon}$	$\tau^{-4+\epsilon}$	$\tau^{-\frac{5}{2}+\epsilon}$	$\tau^{-3+\epsilon}$	$\tau^{-\frac{5}{2}+\epsilon}$
Type C	$\tau^{-5+\epsilon}$	$\tau^{-3+\epsilon}$	$\tau^{-3+\epsilon}$	$\tau^{-2+\epsilon}$	$\tau^{-\frac{5}{2}+\epsilon}$	$\tau^{-2+\epsilon}$
Type D	$\tau^{-5+\epsilon}$	$\tau^{-4+\epsilon}$	$\tau^{-3+\epsilon}$	$\tau^{-\frac{5}{2}+\epsilon}$	$\tau^{-\frac{5}{2}+\epsilon}$	$\tau^{-2+\epsilon}$

Note that the decay rates for  $\psi|_{\{r=r_0\}}$  apply for  $\sqrt{r-M}\psi$  for all  $r > M$ .

### 4.7.3 An Elliptic Estimate for $\ell \geq 1$ and Improved Decay

The decay rate for  $\psi|_{\{r=r_0\}}$ , in the  $\ell \geq 1$  case, as in Table 4.6, is *slower* than the corresponding expected sharp rate for the  $\ell = 0$  case. The latter rate must be improved before we obtain late-time asymptotics. We use the following degenerate elliptic estimate for  $\ell \geq 1$  obtained in [8]:

$$\int_{\Sigma_\tau} D^2 \cdot (\partial_\rho \psi_{\ell \geq 1})^2 \cdot r^{-2} d\mu_{\Sigma_\tau} \lesssim \int_{\Sigma_\tau} D \cdot (\partial_\rho T \psi_{\ell \geq 1})^2 d\mu_{\Sigma_\tau}, \quad (4.7.2)$$

where  $\partial_\rho$  denotes the radial vector field tangent to  $\Sigma_\tau$  such that  $\partial_\rho r = 1$  and  $D = (1 - \frac{M}{r})^2$ . Note that we need a degenerate elliptic estimate in view of the fact that the decaying global energy flux  $J_{\Sigma_\tau}^T$  is *degenerate* at the event horizon. Using a standard Hardy inequality and the improved energy decay estimates for  $T\psi$  we obtain for Type B data (see Table 4.8) we obtain:

$$\begin{aligned} \int_{\mathbb{S}^2} (\psi_{\ell \geq 1})^2 d\Omega &\lesssim \frac{1}{D} \sqrt{\int_{\Sigma_\tau} D^2 \cdot (\partial_\rho \psi_{\ell \geq 1})^2 \cdot r^{-2} d\mu_{\Sigma_\tau}} \cdot \sqrt{\int_{\Sigma_\tau} \psi_{\ell \geq 1}^2 \cdot r^{-2} d\mu_{\Sigma_\tau}} \\ &\stackrel{(4.7.2)}{\lesssim} \frac{1}{D} \sqrt{\int_{\Sigma_\tau} D \cdot (\partial_\rho T \psi_{\ell \geq 1})^2 d\mu_{\Sigma_\tau}} \cdot \sqrt{\int_{\Sigma_\tau} D \cdot (\partial_\rho \psi_{\ell \geq 1})^2 d\mu_{\Sigma_\tau}} \\ &= \frac{1}{D} \sqrt{J_{\Sigma_\tau}^T[T\psi_{\ell \geq 1}]} \cdot \sqrt{J_{\Sigma_\tau}^T[\psi_{\ell \geq 1}]} \\ &\lesssim \frac{1}{D} \sqrt{E_{\ell \geq 1; 1}} \cdot \sqrt{E_{\ell \geq 1}} \cdot \tau^{-7+\epsilon}. \end{aligned}$$

This yields that  $(1 - \frac{M}{r}) \cdot \psi_{\ell \geq 1}$  decays with a rate  $\tau^{-\frac{7}{2}+\frac{\epsilon}{2}}$ . This rate is now sub-leading. We summarize our findings in the Table 4.7:

**Table 4.7** Decay in shaded cell is sub-leading after applying elliptic estimate

Data	Decay rates for $\ell \geq 1$					
	Energy flux decay			Pointwise decay		
	$J_{\Sigma_r}^T[\psi]$	$C_{N_r^{\mathcal{H}}}[\psi]$	$C_{N_r^{\mathcal{I}}}[\psi]$	$r\psi _{\mathcal{H}^+}$	$\psi _{\{r=r_0\}}$	$r\psi _{\mathcal{I}^+}$
Type A	$\tau^{-5+\epsilon}$	$\tau^{-3+\epsilon}$	$\tau^{-4+\epsilon}$	$\tau^{-2+\epsilon}$	$\tau^{-\frac{5}{2}+\epsilon}$	$\tau^{-\frac{9}{4}+\epsilon}$
Type B	$\tau^{-6+\epsilon}$	$\tau^{-4+\epsilon}$	$\tau^{-4+\epsilon}$	$\tau^{-\frac{5}{2}+\epsilon}$	$\tau^{-\frac{7}{2}+\epsilon}$	$\tau^{-\frac{5}{2}+\epsilon}$
Type C	$\tau^{-5+\epsilon}$	$\tau^{-3+\epsilon}$	$\tau^{-3+\epsilon}$	$\tau^{-2+\epsilon}$	$\tau^{-\frac{5}{2}+\epsilon}$	$\tau^{-2+\epsilon}$
Type D	$\tau^{-5+\epsilon}$	$\tau^{-4+\epsilon}$	$\tau^{-3+\epsilon}$	$\tau^{-\frac{5}{2}+\epsilon}$	$\tau^{-\frac{5}{2}+\epsilon}$	$\tau^{-2+\epsilon}$

### 4.7.4 Summary of Energy and Pointwise Decay Rates

We summarize the decay rates for  $T^k\psi$  in the Tables 4.8 and 4.9.

**Table 4.8** Energy decay rates for  $T^k\psi$

Data	Energy decay rates for $T^k\psi$ with $k \geq 0$		
	$J_{\Sigma_r}^T[T^k\psi]$	$C_{N_r^{\mathcal{H}}}[T^k\psi]$	$C_{N_r^{\mathcal{I}}}[T^k\psi]$
Type A	$\tau^{-3-2k+\epsilon}$	$\tau^{-1-2k+\epsilon}$	$\tau^{-3-2k+\epsilon}$
Type B	$\tau^{-5-2k+\epsilon}$	$\tau^{-3-2k+\epsilon}$	$\tau^{-3-2k+\epsilon}$
Type C	$\tau^{-3-2k+\epsilon}$	$\tau^{-1-2k+\epsilon}$	$\tau^{-1-2k+\epsilon}$
Type D	$\tau^{-3-2k+\epsilon}$	$\tau^{-3-2k+\epsilon}$	$\tau^{-1-2k+\epsilon}$

**Table 4.9** Pointwise decay rates for  $T^k\psi$

Data	Pointwise decay rates for $T^k\psi$ with $k \geq 0$		
	$rT^k\psi _{\mathcal{H}^+}$	$T^k\psi _{\{r=r_0\}}$	$rT^k\psi _{\mathcal{I}^+}$
Type A	$\tau^{-1-k+\epsilon}$	$\tau^{-\frac{3}{2}-k+\epsilon}$	$\tau^{-\frac{3}{2}-k+\epsilon}$
Type B	$\tau^{-2-k+\epsilon}$	$\tau^{-\frac{5}{2}-k+\epsilon}$	$\tau^{-2-k+\epsilon}$
Type C	$\tau^{-1-k+\epsilon}$	$\tau^{-\frac{3}{2}-k+\epsilon}$	$\tau^{-1-k+\epsilon}$
Type D	$\tau^{-\frac{3}{2}-k+\epsilon}$	$\tau^{-\frac{3}{2}-k+\epsilon}$	$\tau^{-1-k+\epsilon}$

## 4.8 Late-Time Asymptotics

We have so far outlined how to obtain energy and pointwise decay estimates. In this section, we will see how to obtain the late-time asymptotics. Let’s first make a few a priori comments about the coefficients of the precise asymptotics.

### 4.8.1 *A Priori Remarks*

In view of the vanishing of the scalar curvature of ERN, the wave equation (1.7.1) on ERN is conformally invariant. Hence, we can use the Couch–Torrence conformal symmetry  $\Phi$  (see Sect. 2.1.4) to make various a priori remarks for the late-time asymptotics. Recall from Sect. 2.3.3 that  $\psi$  solves the wave equation on ERN if and only if its dual  $\tilde{\psi} = \frac{M}{r-M}\psi \circ \Phi$  solves the wave equation. As before, we denote by  $\partial_\rho$  the radial derivative tangential to  $\Sigma_\tau$  such that  $\partial_\rho r = 1$ . Note that  $\Sigma_\tau$  here is the  $\Phi$ -invariant hypersurface introduced in Sect. 2.1.4. Recall that  $\Phi(\tau, r) = (\tau, r')$  where  $r'$  is given by (2.1.18). First of all note that (see [12])

$$H_0[\psi] = I_0[\tilde{\psi}], \quad I_0[\psi] = H_0[\tilde{\psi}].$$

Assume that  $\psi$  is a Type C perturbation. Then,  $\tilde{\psi}$  is also of Type C. For simplicity, we will here use the notation  $C^\infty[\psi]$  for the coefficient of the late-time asymptotics

$$\psi \rightarrow C^\infty[\psi] \cdot \tau^{-2} + O(\tau^{-2-\eta}).$$

Let's impose the following *ansatz* for the asymptotic coefficient  $C^\infty[\psi]$  of  $\psi$  in the region  $r_{\mathcal{H}} \leq r \leq r_{\mathcal{I}}$ :

$$C^\infty[\psi] = A(r) \cdot H_0[\psi] + B(r) \cdot I_0[\psi]$$

as  $\tau \rightarrow \infty$ . We will investigate any possible conditions that  $A(r)$  and  $B(r)$  have to satisfy independently of  $\psi$  (as long as  $\psi$  is of Type C). Let's consider the asymptotics of  $\tilde{\psi}$  in two ways:

$$C^\infty[\tilde{\psi}] = A(r) \cdot H_0[\tilde{\psi}] + B(r) \cdot I_0[\tilde{\psi}] \tag{4.8.1}$$

and

$$\begin{aligned} C^\infty[\tilde{\psi}] &= C^\infty \left[ \frac{M}{r-M} \cdot \psi \circ \Phi \right] = \frac{M}{r-M} \cdot C^\infty[\psi \circ \Phi] \\ &= \frac{M}{r-M} \cdot \left( A(r') \cdot H_0[\psi] + B(r') \cdot I_0[\psi] \right) \\ &= \frac{M}{r-M} \cdot B(r') \cdot H_0[\tilde{\psi}] + \frac{M}{r-M} \cdot A(r') \cdot I_0[\tilde{\psi}]. \end{aligned} \tag{4.8.2}$$

Combining (4.8.1) and (4.8.2) we conclude that  $A, B$  must satisfy

$$A(r) = \frac{M}{r-M} \cdot B(r'), \quad B(r) = \frac{M}{r-M} \cdot A(r')$$

It is very easy to see that these are equivalent. Two important corollaries of the above are the following:

- the coefficient functions  $A(r)$  and  $B(r)$  are **not** both constants,

- *the derivative  $\partial_\rho\psi$  does not decay faster than  $\tau^2$* . Indeed, we would expect that  $C^\infty[\partial_\rho\psi] = \partial_r A(r) \cdot H_0[\psi] + \partial_r B(r) \cdot I_0[\psi]$ .

Given the above analysis, one would expect that both  $A(r)$  and  $B(r)$  are non-constant functions of  $r$ . *There is no reason a priori why **exactly** one of them would be constant*. If that were the case then the asymptotics for  $\partial_\rho\psi$  would depend **only** on either  $H_0$  or  $I_0$ . However, we will show that

$$B(r) = 4, \quad A(r) = \frac{4M}{r - M}.$$

See also Table 2.1. This implies that the asymptotics of  $\partial_\rho\psi$  in region  $\mathcal{B}$  depend only on  $H_0$ . In other words, we see that there is here a special feature of the horizon that dominates over null infinity.

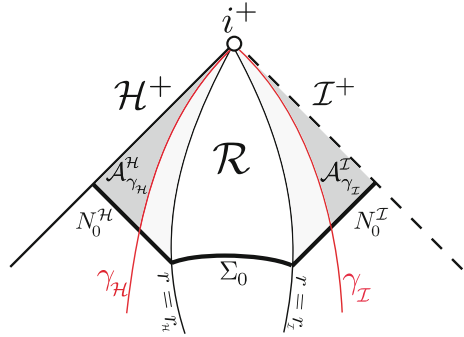
### 4.8.2 The Main Difficulties

We will next provide a summary of the mechanism that gives rise to the precise leading-order asymptotics for  $\psi$ . The decay rates for  $\psi_{\ell \geq 1}$  as in Table 4.7 are faster than the (expected) sharp decay rates for  $\psi_{\ell=0}$ . For this reason, we will derive the precise late-time asymptotics (and hence the sharp rates) for  $\psi_{\ell=0}$ . We will thus assume in the rest of this section that  $\psi$  is a spherically symmetric (and hence supported only on  $\ell = 0$ ) solution to the wave equation (1.7.1) on ERN. We need to overcome the following difficulties.

- **Difficulty 1:** Find spacetime regions in which asymptotics can be derived *independently* of their complement. An obstruction here is that the decay rates that we have already obtained (as summarized in the previous subsections) are a power  $\frac{1}{2} + \epsilon$  from the sharp values in the region  $\mathcal{B} = \{r_{\mathcal{H}} \leq r \leq r_{\mathcal{I}}\}$ . Compare the rates in Tables 2.1 and 4.5.
- **Difficulty 2:** Propagate the above asymptotics *globally* in the region  $\mathcal{R}$ . The main obstruction here is that for data of Type **A**, **B** and **C** the radial (tangential to  $\Sigma_\tau$ ) derivative  $\partial_\rho\psi$  decays only as fast as  $\psi$  itself. Hence, one needs to derive the precise asymptotics for  $\partial_\rho\psi$  before propagating asymptotics of  $\psi$ . Recall the discussion in Sect. 4.8.1 Compare the rates in Tables 2.1 and 2.3. We remark that this is not the case in sub-extremal black holes where radial derivatives decay faster than the scalar field itself.

We consider the timelike hypersurfaces  $\gamma_{\mathcal{I}}$  and  $\gamma_{\mathcal{H}}$  such that  $(v - u)|_{\gamma_{\mathcal{I}}} \sim u^\alpha$  and  $(u - v)|_{\gamma_{\mathcal{H}}} \sim v^\alpha$  where  $0 < \alpha < 1$  is a constant, and we define the following subsets of the near-infinity region  $\mathcal{A}^{\mathcal{I}}$  and the near-horizon region  $\mathcal{A}^{\mathcal{H}}$ :  $\mathcal{A}_{\gamma_{\mathcal{I}}}^{\mathcal{I}} := \mathcal{A}^{\mathcal{I}} \cap \{r \geq r|_{\gamma_{\mathcal{I}}}\}$  and  $\mathcal{A}_{\gamma_{\mathcal{H}}}^{\mathcal{H}} := \mathcal{A}^{\mathcal{H}} \cap \{r \leq r|_{\gamma_{\mathcal{H}}}\}$ . See Fig. 4.1. Note that  $(r - M)|_{\gamma_{\mathcal{H}}} \sim r|_{\gamma_{\mathcal{I}}} \sim \tau^\alpha$ .

**Fig. 4.1** The curves  $\gamma_{\mathcal{H}}$ ,  $\gamma_{\mathcal{I}}$  and the regions  $\mathcal{A}_{\gamma_{\mathcal{H}}}^{\mathcal{H}}$ ,  $\mathcal{A}_{\gamma_{\mathcal{I}}}^{\mathcal{I}}$



We will below summarize the resolutions to the above difficulties for each of the four types of initial data. For the complete details we refer to [8].

### 4.8.3 Asymptotics for Type C Perturbations

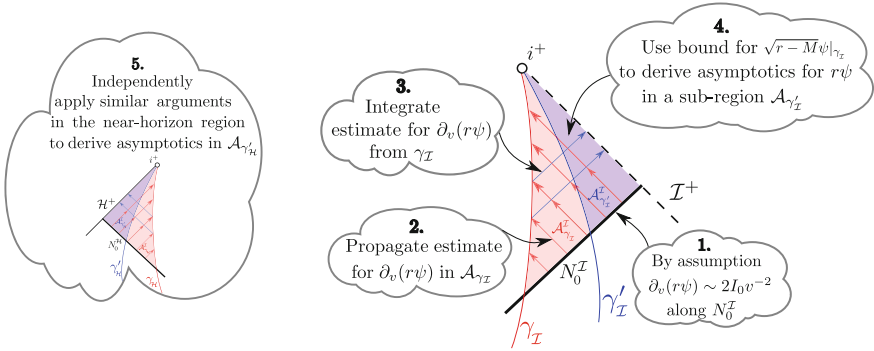
#### Resolution of Difficulty 1

For Type C data we derive the leading-order asymptotics of  $\psi$  in the near-horizon region  $\mathcal{A}_{\gamma_{\mathcal{H}}}^{\mathcal{H}}$  and separately and independently in the near-infinity region  $\mathcal{A}_{\gamma_{\mathcal{I}}}^{\mathcal{I}}$ . This derivation distinguishes the extremal case from the sub-extremal case treated in [11], where the asymptotics at the near-infinity region can be propagated all the way to the event horizon using that the radial derivative  $\partial_{\rho}\psi$  decays faster than  $\psi$ . The reason we can independently derive the asymptotics in the regions  $\mathcal{A}_{\gamma_{\mathcal{H}}}^{\mathcal{H}}$  and  $\mathcal{A}_{\gamma_{\mathcal{I}}}^{\mathcal{I}}$  in the extremal case has to do with the existence of the two (independent) conserved charges  $H_0$  and  $I_0$ ; and for Type C data they are both non-zero:  $H_0 \neq 0$  and  $I_0 \neq 0$ . To obtain the precise asymptotics in  $\mathcal{A}_{\gamma_{\mathcal{I}}}^{\mathcal{I}}$  and  $\mathcal{A}_{\gamma_{\mathcal{H}}}^{\mathcal{H}}$  we propagate the following  $v$ -asymptotics and  $u$ -asymptotics of the initial data on  $N_0^{\mathcal{I}}$  and  $N_0^{\mathcal{H}}$ , respectively,

$$\partial_v(r\psi)|_{N_0^{\mathcal{I}}} \sim 2I_0v^{-2}, \quad \partial_u(r\psi)|_{N_0^{\mathcal{H}}} \sim 2H_0u^{-2} \tag{4.8.3}$$

everywhere in  $\mathcal{A}_{\gamma_{\mathcal{I}}}^{\mathcal{I}}$  and  $\mathcal{A}_{\gamma_{\mathcal{H}}}^{\mathcal{H}}$ , respectively. This can be achieved for  $\alpha < 1$ , but sufficiently close to 1. We next integrate the resulting estimates for  $\partial_v(r\psi)$  and  $\partial_u(r\psi)$  starting from  $\gamma_{\mathcal{I}}$  and  $\gamma_{\mathcal{H}}$ , respectively, to obtain the asymptotics for  $r\psi$ , and consequently  $\psi$ , in appropriate sub-regions  $\mathcal{A}_{\gamma_{\mathcal{I}}}^{\mathcal{I}}$  and  $\mathcal{A}_{\gamma_{\mathcal{H}}}^{\mathcal{H}}$  of  $\mathcal{A}_{\gamma_{\mathcal{I}}}^{\mathcal{I}}$  and  $\mathcal{A}_{\gamma_{\mathcal{H}}}^{\mathcal{H}}$  obtained by replacing  $\alpha$  with appropriate  $\alpha'$  such that  $\alpha < \alpha' < 1$ . A crucial observation is that the previously derived decay rates for  $\sqrt{r-M} \cdot \psi|_{\gamma_{\mathcal{I}'}}$  and  $\sqrt{r-M} \cdot \psi|_{\gamma_{\mathcal{H}'}}$  are almost sharp<sup>3</sup> and hence strong enough to close this argument by showing that, as long as  $a < 1$ , the terms  $r\psi|_{\gamma_{\mathcal{I}'}}$  and  $r\psi|_{\gamma_{\mathcal{H}'}}$  decay faster than, say  $r\psi|_{\gamma_{\mathcal{I}'}}$  and  $r\psi|_{\gamma_{\mathcal{H}'}}$ , and hence are lower order terms.

<sup>3</sup>Note that the relevant decay rates for  $\psi$ , without the  $\sqrt{r-M}$  weight, are not sharp, see Table 4.5.



**Resolution of Difficulty 2**

Ideally, we would like to propagate the asymptotics for  $\psi_{\gamma_{\mathcal{I}^*}}$  to the left of  $\gamma_{\mathcal{I}^*}$ . In the sub-extremal case this follows easily once decay rates for the radial derivative  $\partial_\rho\psi$  have been obtained that are faster than that of  $\psi$ . This however breaks down in the extremal case in view of the fact that the expected sharp decay rate for  $\partial_\rho\psi$  is now the same as the expected sharp rate for  $\psi$  (see also the discussion in Sect. 4.8.1).

The way out is to obtain the precise asymptotic behavior of the radial derivative  $\partial_\rho\psi$ . It turns out that this is possible without knowing the asymptotics for  $\psi$ . We commute by  $T$  and reproduce the above argument to derive the precise late-time asymptotics for  $T(r\psi)$  in the near-horizon region  $\mathcal{A}_{\gamma_{\mathcal{H}}^*}^{\mathcal{H}}$ . The crucial observation here is that *the asymptotics for  $\partial_\rho\psi$  in the region  $\{\gamma_{\mathcal{H}} \leq r \leq r_{\mathcal{I}^*}\}$  depend only on the asymptotics of  $T\psi$  along the event horizon, which in turn depend only on  $H_0$ !* Furthermore, we derive sharp decay estimates (with growing  $r$  weights in the error terms) for  $\partial_\rho\psi$  up to the curve  $\gamma_{\mathcal{I}^*}$ , that is in the region  $\{r_{\mathcal{I}^*} \leq r \leq r_{\gamma_{\mathcal{I}^*}}\}$ .

The wave equation schematically takes the form

$$\partial_\rho(Dr^2\partial_\rho\psi + 2r^2T\psi) = O(r)T\psi + O(r^{1-\eta})T^2\psi.$$

Now, we integrate along  $\Sigma_\tau$  from the horizon  $r = M$  to some  $r > M$  to obtain:

$$Dr^2\partial_\rho\psi(r, \tau) = 2M^2T\psi|_{\mathcal{H}^+(\tau)} + \mathbf{r^2T\psi(r, \tau)} + \int_M^r O(r')T\psi + O(r')T^2\psi dr'.$$

The blue horizon term is the leading one:

$$2M^2T\psi|_{\mathcal{H}^+(\tau)} = -4MH_0 \cdot \tau^{-2} + O(\tau^{-2-\epsilon}).$$

We will show that the red terms are of lower order (and that the bold red is the dominant error term). We estimate by using Cauchy–Schwarz and Hardy

$$\int_M^r O(r') \cdot |T\psi| dr' \leq C \sqrt{\int_{\Sigma_\tau} J^T[T\psi] \cdot n_\tau d\mu_\tau} \cdot r^{\frac{3}{2}} \leq C \cdot \tau^{-\frac{5}{2}+\epsilon} \cdot r^{\frac{3}{2}}.$$

Similarly, we can estimate

$$\int_M^r O(r') \cdot |T^2\psi| dr' \leq C \sqrt{\int_{\Sigma_\tau} J^T[T^2\psi] \cdot n_\tau d\mu_\tau} \cdot r^{\frac{3}{2}} \leq C \cdot \tau^{-\frac{7}{2}+\epsilon} \cdot r^{\frac{3}{2}}$$

We can furthermore estimate:

$$|T\psi|(r, \tau) \leq CD^{-\frac{1}{2}}r^{-\frac{1}{2}} \cdot \sqrt{\int_{\Sigma_\tau} J^T[T\psi] \cdot n_\tau d\mu_\tau} \leq CD^{-\frac{1}{2}}r^{-\frac{1}{2}}\tau^{-\frac{5}{2}+\epsilon}.$$

We conclude that for any  $r > M$ :

$$|\partial_\rho\psi(r, \tau) + 4MH_0D^{-1}r^{-2}\tau^{-2}| \leq C\tau^{-\frac{5}{2}+\epsilon} \cdot D^{-\frac{3}{2}}r^{-\frac{1}{2}} + CD^{-1}r^{-2}\tau^{-2-\epsilon}. \quad (4.8.4)$$

This gives the asymptotics for  $\partial_\rho\psi$  along any constant  $r$  hypersurfaces. For regions where  $r \sim \tau$  it just gives an estimate, not asymptotics, in view of the dominant bold red term. Nonetheless it is still good enough to derive the asymptotics for  $\psi$  in  $\{r_{\gamma_{\mathcal{H}}} \leq r \leq r_{\gamma_{\mathcal{I}}}\}$  by integrating the estimate (4.8.4) for  $\partial_\rho\psi$  in this region backwards from  $\gamma_{\mathcal{I}}$ . Indeed, we obtain

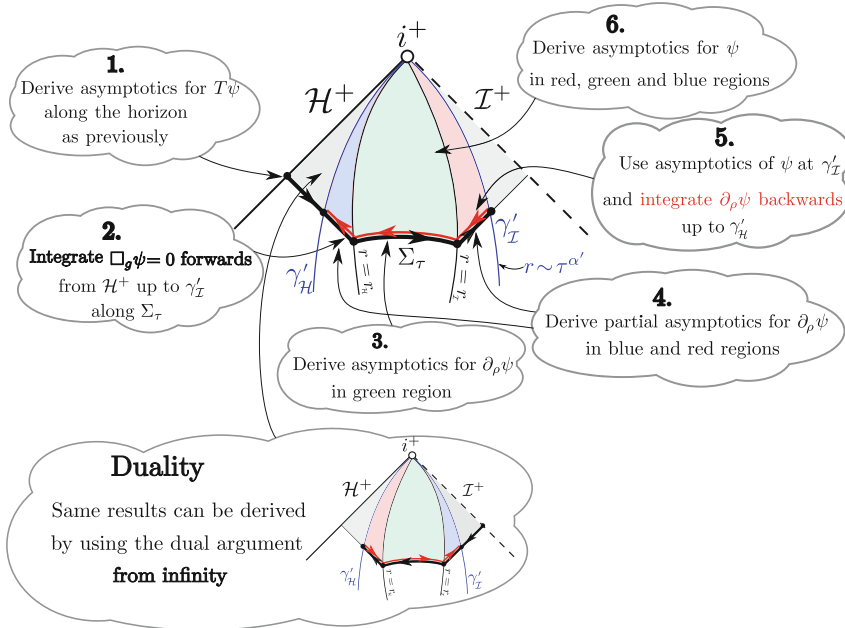
$$\begin{aligned} \psi(r, \tau) &= \psi|_{\gamma_{\mathcal{I}}}(\tau) - \int_r^{\gamma_{\mathcal{I}}} \partial_\rho\psi dr' \\ &= 4 \left( I_0 + \frac{M}{r-M} H_0 \right) \tau^{-2} + D^{-1/2}(r) \cdot O(\tau^{-2-\epsilon}), \end{aligned}$$

where we used the following asymptotics along  $\gamma_{\mathcal{I}}$  from the previous step:

$$\psi|_{\gamma_{\mathcal{I}}} = 4I_0\tau^{-2} + O(\tau^{-2-\epsilon}). \quad (4.8.5)$$

The integral of the red term in the asymptotics for  $\partial_\rho\psi$  can be controlled only up to a region with  $\alpha' < 1$ . This shows the importance of first closing estimates in the region  $\mathcal{A}_{\gamma_{\mathcal{I}}}^{\mathcal{I}}$ .

**Remark:** We can use the (slow) estimate (4.8.4), which **blows up at the horizon**, to propagate the asymptotics of  $\psi|_{r_{\mathcal{H}}} \sim \tau^{-2}$  (fast) to get the asymptotics of  $\psi|_{\gamma_{\mathcal{H}}} \sim \tau^{-2+\alpha'}$  (slow) (in the red direction as in the figure below), but we **cannot** use (4.8.4) to propagate the asymptotics of  $\psi|_{\gamma_{\mathcal{H}}} \sim \tau^{-2+\alpha'}$  (slow) to get the asymptotics of  $\psi|_{r_{\mathcal{H}}} \sim \tau^{-2}$  (fast). In the former case we get: slow=slow+fast (consistent with asymptotics), and in the latter case we get fast=slow+slow (inconsistent with asymptotics). This is the reason we need to go from  $\gamma_{\mathcal{H}}$  all the way to  $\gamma_{\mathcal{I}}$  where  $\psi|_{\gamma_{\mathcal{I}}} \sim \tau^{-2}$  (fast) and retrieve asymptotics coming back! See the figure below.



Another way, which we simply mention for completeness, would be to follow the dual argument (via the Couch–Torrence inversion) where this time we integrate an appropriate rescaled tangential to  $\Sigma_\tau$  derivative of  $\psi$  **from infinity** and use the asymptotics in  $\mathcal{A}_{\gamma'_I}^{\mathcal{I}}$ . See the figure above.

### 4.8.4 Asymptotics for Type A Perturbations

#### Resolution of Difficulty 1

For Type **A** data we can derive the leading-order asymptotics of  $\psi$ , and crucially of  $T\psi$ , in the near-horizon region  $\mathcal{A}_{\gamma'_H}^{\mathcal{H}}$  as in Type **C** case, but in contrast to the Type **C** case, we cannot obtain independently the asymptotics in the near-infinity region  $\mathcal{A}_{\gamma'_I}^{\mathcal{I}}$  since the first equation of (4.8.3) does not provide exact asymptotics given that  $I_0 = 0$ . Estimate (4.8.5) still holds, but does not provide late-time asymptotics anymore.

#### Resolution of Difficulty 2

The estimate (4.8.4) holds for Type **A** data and provides (partial) asymptotics for  $\partial_\rho\psi$  in the region  $\{r_{\mathcal{H}} \leq r \leq r_{\mathcal{I}}\}$ . However, since, the estimate (4.8.4) blows up at the horizon, it cannot be used to push the asymptotics of  $\psi$  away from  $\mathcal{A}_{\gamma'_H}^{\mathcal{H}}$ . The crucial observation is that we can derive the precise asymptotics **exactly** on  $\gamma'_I$  (and not to the right or to the left of  $\gamma'$ ; asymptotics in these regions will only be derived subsequently at a later step). In order to derive asymptotics of  $\psi|_{\gamma'_I}$  we need to analyze

the contributions from the left side (horizon side) and the right side (infinity side) of  $\gamma'_{\mathcal{I}}$ . In order to capture the precise contributions from both sides we will need to make crucial use of  $I_0 = 0$ . It turns out that we can only capture the precise contributions at one level of differentiability higher using the following splitting identity

$$r\psi|_{\gamma'_{\mathcal{I}}} = \underbrace{r\partial_\rho(r\psi)|_{\gamma'_{\mathcal{I}}}}_{\text{contribution from the right side of } \gamma'_{\mathcal{I}}} - \underbrace{r^2\partial_\rho\psi|_{\gamma'_{\mathcal{I}}}}_{\text{contribution from the left side of } \gamma'_{\mathcal{I}}} \quad (4.8.6)$$

**Contribution from the right side of  $\gamma'_{\mathcal{I}}$ :** Recall that we want to show that  $r\psi|_{\gamma'_{\mathcal{I}}}$  decays like  $\tau^{-2}$  (see Table 2.1) and hence all error terms must decay like  $\tau^{-2-\epsilon}$ . Now propagating in  $\mathcal{A}^T_{\gamma'_{\mathcal{I}}}$  the first of (4.8.3) only yields an  $\epsilon$  improvement for  $\partial_\rho(r\psi)|_{\gamma'_{\mathcal{I}}}$ , that is (note that  $\partial_v \sim \partial_\rho$  in this region)

$$r\partial_\rho(r\psi)|_{\gamma'_{\mathcal{I}}} \sim r\tau^{-2-\epsilon} \sim \tau^{-2-\epsilon+\alpha'}, \quad (4.8.7)$$

since  $r \sim \tau^{\alpha'}$  along  $\gamma'_{\mathcal{I}}$ , which is not fast enough since  $\alpha'$  is close to 1 (the expected decay rate for  $r\psi|_{\gamma'_{\mathcal{I}}}$  is  $\tau^{-2}$ ). To circumvent this difficulty and obtain faster decay for  $r\partial_\rho(r\psi)|_{\gamma'_{\mathcal{I}}}$ , a new technique was introduced in [8], which we call **the singular time inversion**. We construct the time integral  $\psi^{(1)}$  of  $\psi$  that solves the wave equation  $\square_g\psi^{(1)} = 0$  and satisfies  $T\psi^{(1)} = \psi$ . Note that if  $H_0[\psi] \neq 0$  then  $\psi^{(1)}$  is *singular* at the horizon. In fact it can be taken so that it satisfies

$$(r - M) \cdot \partial_\rho\psi^{(1)} = -\frac{2}{M} \cdot H_0[\psi]$$

close to the event horizon. Away from the horizon  $\psi^{(1)}$  is smooth and has a well-defined Newman–Penrose constant  $I_0[\psi^{(1)}] < \infty$ . Using appropriate low regularity energy estimates it can be shown that  $\psi^{(1)} \rightarrow 0$  as  $\tau \rightarrow \infty$  to the right of  $\gamma'_{\mathcal{I}}$ . The rates in Table 4.5 then yield in particular  $|r\psi^{(1)}| \lesssim \tau^{-1/2+\epsilon}$ . This rate is good enough to apply previous techniques and propagate (4.8.3) with  $\psi$  replaced by  $\psi^{(1)}$ , using that generically  $I_0[\psi^{(1)}] \neq 0$ , which yields  $\partial_\rho(r\psi^{(1)})|_{\gamma'_{\mathcal{I}}} \sim v^{-2} \sim \tau^{-2}$  since  $v \sim \tau$  and  $r \sim \tau^{\alpha'}$  along  $\gamma'_{\mathcal{I}}$ . Hence, by integrating in time, we obtain  $\partial_\rho(r\psi)|_{\gamma'_{\mathcal{I}}} \sim \tau^{-3}$  and hence

$$r\partial_\rho(r\psi)|_{\gamma'_{\mathcal{I}}} \sim r\tau^{-3} \sim \tau^{-3+\alpha'} \quad (4.8.8)$$

along  $\gamma'_{\mathcal{I}}$ , which significantly improves (4.8.7). We conclude that this term does not contribute to the asymptotics of  $r\psi|_{\gamma'_{\mathcal{I}}}$ .

**Contribution from the left side of  $\gamma'_{\mathcal{I}}$ :** This is the side that fully contributes to the asymptotics of  $r\psi|_{\gamma'_{\mathcal{I}}}$  via the term  $r^2\partial_\rho\psi|_{\gamma'_{\mathcal{I}}}$ . We will derive the precise asymptotics of  $r^2\partial_\rho\psi|_{\gamma'_{\mathcal{I}}}$ . Expressing the wave equation as a transport equation

$$\partial_\rho(Dr^2\partial_\rho\psi) = 2r\partial_\rho(rT\psi)$$

and integrating on  $N_\tau^{\mathcal{I}}$  yields

$$\left| Dr^2 \partial_\rho \psi \Big|_{r_{\mathcal{I}}} - Dr^2 \partial_\rho \psi \Big|_{\gamma_{\mathcal{I}}} \right| \lesssim \int_{r_{\mathcal{I}}}^{r_{\gamma_{\mathcal{I}}}} r |\partial_\rho(rT\psi)| dr. \quad (4.8.9)$$

Using the improved conformal flux estimate  $C_{N_\tau^{\mathcal{I}}}[T\psi]$  (see Table 4.8)

$$\int_{r_{\mathcal{I}}}^{r_{\gamma_{\mathcal{I}}}} r |\partial_\rho(rT\psi)| dr \lesssim \sqrt{\int_{r_{\mathcal{I}}}^{r_{\gamma_{\mathcal{I}}}} 1 dr} \cdot \sqrt{C_{N_\tau^{\mathcal{I}}}[T\psi]} \lesssim \sqrt{r_{\gamma_{\mathcal{I}}} \cdot \tau^{-5+\epsilon}} \sim \tau^{-\frac{5}{2} + \frac{\epsilon'}{2} + \frac{\epsilon}{2}},$$

which implies that the asymptotics for  $r^2 \partial_v \psi|_{\gamma_{\mathcal{I}'}}$  can be derived from the asymptotics of  $\partial_\rho \psi|_{\{r=r_{\mathcal{I}}\}}$ . We can then apply (4.8.4), which holds also for Type **A** data, at  $r = r_{\mathcal{I}}$ . We see therefore that the asymptotics for  $r^2 \partial_v \psi|_{\gamma_{\mathcal{I}'}}$  and  $r\psi|_{\gamma_{\mathcal{I}'}}$  depend only on  $H_0$  and the respective rate is  $\tau^{-2}$ . Finally,

$$r\psi \Big|_{\gamma_{\mathcal{I}'}} \sim -r^2 \partial_\rho \psi \Big|_{\gamma_{\mathcal{I}'}} \sim -Dr^2 \partial_\rho \psi \Big|_{\gamma_{\mathcal{I}'}} \sim -Dr^2 \partial_\rho \psi \Big|_{r_{\mathcal{I}}} \sim 4MH_0 \tau^{-2}$$

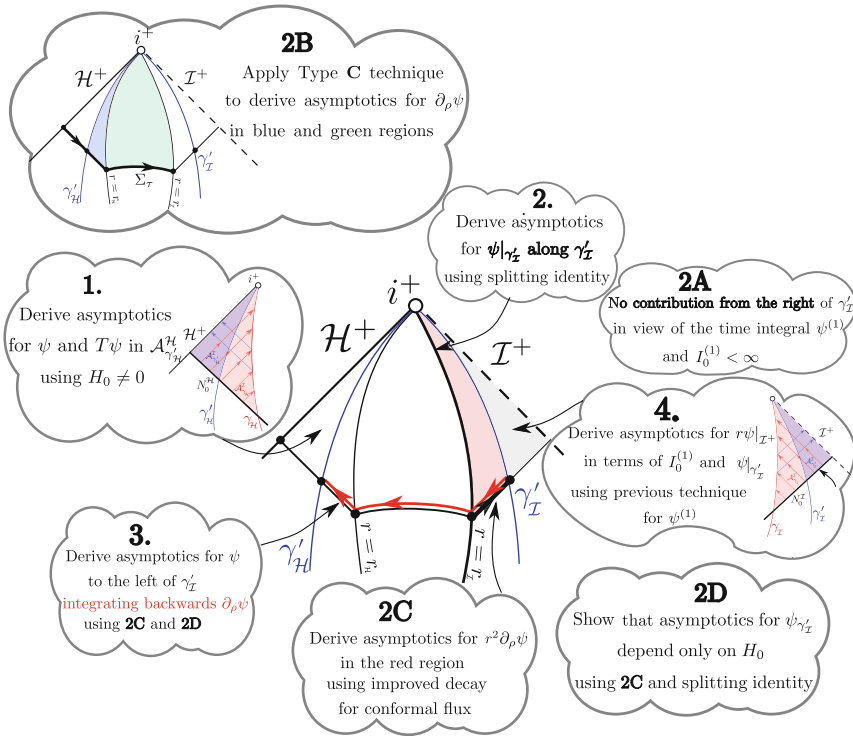
asymptotically as  $\tau \rightarrow \infty$ . Note that  $D \sim 1$  along  $\gamma_{\mathcal{I}'}$ . Concluding, *the precise asymptotics for  $r\psi|_{\gamma_{\mathcal{I}'}}$  depend only on the horizon charge  $H_0[\psi]$* . The decay rate is  $\tau^{-2}$ . The estimate (4.8.9) for the conformal flux, as above, in fact yields partial asymptotics for  $\partial_\rho \psi$  in  $\{r_{\gamma_{\mathcal{H}}} \leq r \leq r_{\gamma_{\mathcal{I}'}}\}$  which we can now integrate **backwards** from  $\gamma_{\mathcal{I}'}$  (using the asymptotics for  $r\psi|_{\gamma_{\mathcal{I}'}}$ !) up to  $r_{\gamma_{\mathcal{H}}}$  to obtain the asymptotics for  $r\psi$  in the region  $\{r_{\gamma_{\mathcal{H}}} \leq r \leq r_{\gamma_{\mathcal{I}'}}\}$ , that is in the complement of  $\mathcal{A}_{\gamma_{\mathcal{I}'}}^{\mathcal{I}} \cup \mathcal{A}_{\gamma_{\mathcal{H}}}^{\mathcal{H}}$ . The asymptotics in  $\mathcal{A}_{\gamma_{\mathcal{H}}}^{\mathcal{H}}$  have been obtained independently in previous steps. *To find the asymptotics of  $r\psi$  to the right of  $\gamma_{\mathcal{I}'}$  all the way up to null infinity we use the construction for the singular time integral  $\psi^{(1)}$  once again.* Specifically, we derive the asymptotics of  $T(r\psi^{(1)}) - T(r\psi^{(1)})|_{\gamma_{\mathcal{I}'}} = r\psi - r\psi|_{\gamma_{\mathcal{I}'}}$  in  $\mathcal{A}_{\gamma_{\mathcal{I}'}}^{\mathcal{I}}$  in terms of  $I_0[\psi^{(1)}]$ :

$$\left| r\psi|_{\mathcal{I}^+}(\tau) - r\psi|_{\gamma_{\mathcal{I}'}}(\tau) + 2I_0^{(1)} \tau^{-2} \right| \lesssim C\tau^{-2-\epsilon}.$$

Unlike for Type **C** data, the term  $r\psi|_{\gamma_{\mathcal{I}'}}$  cannot be neglected above since it decays too slowly (in view of the weak decay of  $\psi^{(1)}$ ). In fact, plugging in the asymptotics of  $r\psi|_{\gamma_{\mathcal{I}'}}$  we obtain the asymptotics of  $r\psi$  in  $\mathcal{A}_{\gamma_{\mathcal{I}'}}^{\mathcal{I}}$ :

$$r\psi|_{\mathcal{I}^+}(\tau) = \left( 4MH_0 - 2I_0^{(1)} \right) \cdot \tau^{-2} + O(\tau^{-2-\epsilon}).$$

Note that both the near-horizon region and the near-infinity region contribute to the asymptotics for the radiation field  $r\psi|_{\mathcal{I}^+}$ . This completes the derivation of the asymptotics for  $\psi$  everywhere in  $\mathcal{R}$ . See figure below for a summary of the steps for Type **A** data.



### 4.8.5 Asymptotics for Type B Perturbations

In the case of Type **B** initial data the time integral  $\psi^{(1)}$  extends smoothly to the horizon. Hence, so we can apply the same methods as for Type **C** data for  $\psi^{(1)}$  and derive the global late-time asymptotics of  $\psi^{(1)}$  and, subsequently, of  $T\psi^{(1)} = \psi$ .

### 4.8.6 Asymptotics for Type D Perturbations

A modified variant of the methods for Type **A** data can be applied for initial data of Type **D**. In this case  $\partial_\rho \psi$  decays faster than  $\psi$  itself. In order to obtain the asymptotics for  $\partial_\rho \psi$  we need to first obtain the asymptotics for the weighted derivative  $\partial_\rho((r - M)\psi)$ , which in fact decays as fast as  $\psi$ , by starting from null infinity and propagating up to  $\gamma_H$ . Once we obtain the asymptotics for  $\psi$  and its time derivatives we then, a posteriori, obtain the asymptotics for  $\partial_\rho \psi$ .

### 4.8.7 Asymptotics for Higher Order Derivatives

In this section we will show how to obtain asymptotics (2.3.19) for  $\partial_r^k T^m \psi$  for all  $k, m \geq 0$  for Type A initial data. The asymptotics for  $\partial_r^k \psi$  can be obtained inductively assuming that

$$\partial_r^k \psi \sim c_k \cdot H_0 \cdot \tau^{k-1}$$

**asymptotically** on  $\mathcal{H}$  for all  $k \geq 1$ . Commuting the wave equation (2.2.1) on ERN with  $\partial_r^k$  with  $k \geq 1$  yields

$$\begin{aligned} \partial_r^k (\square_g \psi) = & D \left( \partial_r^{k+2} \psi \right) + 2\partial_r^{k+1} T \psi + \frac{2}{r} \partial_r^k T \psi + R \partial_r^{k+1} \psi + \partial_r^k \Delta \psi + \\ & + \sum_{i=1}^k \binom{k}{i} \partial_r^i D \cdot \partial_r^{k-i+2} \psi + \sum_{i=1}^k \binom{k}{i} \partial_r^i \frac{2}{r} \cdot \partial_r^{k-i} T \psi + \sum_{i=1}^k \binom{k}{i} \partial_r^i R \cdot \partial_r^{k-i+1} \psi. \end{aligned} \quad (4.8.10)$$

Restricting on  $r = M$  and using the asymptotics for  $T^m \psi$ , for  $m \geq 0$  and solving for  $T \partial_r^{k+1} \psi$  yields

$$T \partial_r^{k+1} \psi \simeq a_{k+1} \cdot \partial_r^k \psi \quad (4.8.11)$$

**asymptotically** on  $\mathcal{H}$  since  $\partial_r^k \psi$  is the only top order term. Here

$$a_{k+1} = \binom{k}{2} D'' + kR' = -\frac{k(k+1)}{2M^2}, \text{ for } k \geq 1 \text{ and } a_1 = \frac{1}{M^2},$$

where  $D = (1 - \frac{M}{r})^2$  and  $R = D' + \frac{2D}{r}$ . Integrating (4.8.11) we obtain

$$c_{k+1} = -c_k \cdot \frac{(k+1)}{2M^2}.$$

We have already proved that  $c_1 = -\frac{1}{M^3}$ . Hence,

$$c_k = (-1)^{k-1} \frac{k!}{(2M^2)^{k-1}} \cdot c_1 = (-1)^k \frac{1}{M^3} \frac{k!}{(2M^2)^{k-1}}.$$

We can also easily obtain the asymptotics for  $\partial_r^{m+j} T^m \psi$  using (4.8.11):

$$\begin{aligned} \partial_r^{m+j} T^m \psi & \sim a_{m+j} \cdot \partial_r^{m+j-1} T^{m-1} \psi \\ & \sim a_{m+j} a_{m+j-1} \cdot \partial_r^{m+j-2} T^{m-2} \psi \\ & \dots \\ & \sim a_{m+j} a_{m+j-1} \dots a_{j+1} \cdot \partial_r^j \psi. \end{aligned}$$

In particular, the bounded non-decaying terms are the following

$$\partial_r^{m+1} T^m \psi \sim \prod_{i=2}^{m+1} a_i \cdot \partial_r \psi \sim -\frac{1}{M^3} \prod_{i=2}^{m+1} a_i \cdot H_0.$$

It is very useful to analyze these terms further

$$\partial_r^{m+1} T^m \psi \sim -\frac{1}{M} \prod_{i=2}^{m+1} a_i \cdot \psi - \frac{1}{M^3} \prod_{i=2}^{m+1} a_i \cdot H_0[\psi].$$

Recall that  $H_0[T\psi] = 0$ . It follows

$$\partial_r^{m+1} T^{m+1} \psi \sim -\frac{1}{M} \prod_{i=2}^{m+1} a_i \cdot T\psi \sim \frac{2}{M^2} \prod_{i=2}^{m+1} a_i \cdot H_0 \cdot \frac{1}{\tau^2}$$

since it is easy to check that all the other terms in the precise equation for  $\partial_r^{m+1} T^{m+1} \psi$  decay strictly faster than  $T\psi$  and since  $T\psi \sim -\frac{2}{M} H_0 \frac{1}{\tau^2}$ . The asymptotics for  $\partial_r^m T^{m+j} \psi$  follow by differentiating the above with respect to  $\tau$  and using that  $\partial_\tau^j \tau^{-2} = (-1)^j (j+1)! \tau^{-2-j}$ . This concludes the proof of the asymptotics (2.3.19).

## References

1. S. Aretakis, Stability and instability of extreme Reissner–Nordström black hole spacetimes for linear scalar perturbations I. *Commun. Math. Phys.* **307**, 17–63 (2011)
2. S. Dain, G. Dotti, The wave equation on the extreme Reissner–Nordström black hole. *Class. Quantum Gravity* **30**, 055011 (2013)
3. J. Sbierski, Characterisation of the energy of Gaussian beams on Lorentzian manifolds with applications to black hole spacetimes. *Anal. Part. Diff. Eq.* **8**, 1379–1420 (2015)
4. Y. Angelopoulos, S. Aretakis, D. Gajic, The trapping effect on degenerate horizons. *Annales Henri Poincaré* **18**(5), 1593–1633 (2017)
5. S. Aretakis, Stability and instability of extreme Reissner–Nordström black hole spacetimes for linear scalar perturbations II. *Annales Henri Poincaré* **12**, 1491–1538 (2011)
6. M. Dafermos, I. Rodnianski, A new physical-space approach to decay for the wave equation with applications to black hole spacetimes, in *XVIIth International Congress on Mathematical Physics* (2010), pp. 421–432
7. G. Moschidis, The  $r^p$ -weighted energy method of Dafermos and Rodnianski in general asymptotically flat spacetimes and applications. *Ann. PDE* **2**, 6 (2016)
8. Y. Angelopoulos, S. Aretakis, D. Gajic, Late-time asymptotics for the wave equation on extremal Reissner–Nordström backgrounds, preprint (2018)
9. Y. Angelopoulos, S. Aretakis, D. Gajic, A vector field approach to almost sharp decay for the wave equation on spherically symmetric, stationary spacetimes (2016), [arXiv:1612.01565](https://arxiv.org/abs/1612.01565)
10. V. Schlue, Decay of linear waves on higher-dimensional Schwarzschild black holes. *Anal. PDE* **6**(3), 515–600 (2013)
11. Y. Angelopoulos, S. Aretakis, D. Gajic, Late-time asymptotics for the wave equation on spherically symmetric, stationary backgrounds. *Adv. Math.* **323**, 529–621 (2018), [arXiv:1612.01566](https://arxiv.org/abs/1612.01566)
12. J. Lucietti, K. Murata, H.S. Reall, N. Tanahashi, On the horizon instability of an extreme Reissner–Nordström black hole. *JHEP* **1303**, 035 (2013), [arXiv:1212.2557](https://arxiv.org/abs/1212.2557)

# Chapter 5

## Decay Estimates for Extremal Kerr



In this Chapter we review the proof of rigorous decay estimates for axisymmetric solutions to the wave equation on EK.

### 5.1 Axisymmetry Versus Superradiance

Recall that  $T = \partial_v$  is spacelike in the ergoregion, close to the event horizon. This means that the energy flux  $J_\mu^T[\psi]n^\mu$ , where  $n^\mu$  is timelike, fails to be non-negative definite. This implies that, in principle, the energy radiated away to null infinity may be larger than the initial energy. This phenomenon is called *superradiance* and is the main reason that obtaining any boundedness result for the wave equation on Kerr (including EK) (even away from  $\mathcal{H}^+$ ) is very difficult. The first major simplification about axisymmetric solutions has to do with the absence of superradiance in this case. For convenience let's denote  $\Phi = \partial_{\varphi^*}$ . Let  $\Sigma$  be an axisymmetric spacelike hypersurface and  $n_\Sigma$  be its future directed timelike unit normal vector field. Then for all axisymmetric solutions to the wave equation on EK we obtain

$$J_\mu^\Phi[\psi]n_\Sigma^\mu = 0.$$

It follows that the  $T$ -flux along the event horizon is non-negative definite. Indeed, we simply use the above and the expression for the horizon normal  $V = T + \frac{1}{2M}\Phi$ . Hence, the degenerate  $T$ -fluxes  $J_\mu^T[\psi]n_\Sigma^\mu \geq 0$  across  $\Sigma_\tau$  and  $J_\mu^T[\psi]n_{\mathcal{H}^+}^\mu \geq 0$  across  $\mathcal{H}^+$  are non-negative definite and uniformly bounded. It is in this sense that superradiance is absent for axisymmetric<sup>1</sup>  $\psi$ . Boundedness of local non-degenerate energy

---

<sup>1</sup>Note that superradiance is in fact absent for all solutions to the wave equation on ERN. That is why we expect axisymmetric solutions on EK to behave like the general solutions on ERN.

can be proved using the techniques of Sect. 4.4. The main difficulty for proving decay is to derive a Morawetz estimate. In ERN such estimates were relatively easy to obtain using purely physical space techniques. The situation is more complicated for EK. We will need to make use of the frequency localization as explained in the next section.

## 5.2 The Carter Separation and Frequency Localization

### 5.2.1 The Killing Tensor $K$ and the Symmetry Operator $Q$

The Kerr metric has two Killing vector fields, the stationary  $T$  and the axially symmetric  $\Phi$ . Furthermore, Kerr (including EK) admits an irreducible Killing 2-tensor. A Killing 2-tensor is a symmetric 2-tensor  $K$  which satisfies  $\nabla_{(\alpha} K_{\beta\gamma)} = 0$ . For example, the metric is always a Killing tensor. A Killing tensor is called irreducible if it can not be constructed from the metric and other Killing vector fields. There are several important consequences of the existence of  $K_{\alpha\beta}$  on Kerr:

1. The Killing tensor  $K$  yields the conserved quantity  $K_{\alpha\beta}\dot{\gamma}^{\alpha}\dot{\gamma}^{\beta}$  along geodesics  $\gamma$ . This means that the geodesic flow admits three constants of motion (including the constants associated to  $T$  and  $\Phi$ ). This further implies that the geodesic flow on Kerr is *completely integrable* (see [1]).
2. The Killing tensor  $K$  gives rise to a *symmetry operator*  $Q = \nabla_{\alpha}(K^{\alpha\beta}\nabla_{\beta})$  given by

$$Q\psi = \Delta_{\mathbb{S}^2}\psi - \Phi^2\psi + (a^2 \sin^2 \theta) T^2\psi \quad (5.2.1)$$

satisfying  $[K, \square_g] = 0$ . The differential operator  $Q$  was first used in the context of estimating solutions to the wave equation in [2] for slowly rotating Kerr backgrounds. As we shall see, in view of the degeneracy of redshift on EK, commuting with  $Q$  turns out to be useful for deriving pointwise estimates on EK (see Sect. 5.5).

3. The wave equation, as discovered by Carter [3], is *separable*. This makes possible to decompose a solution to the wave equation into modes and perform a *mode analysis*. The separability of the wave equation has been used by Dafermos et al. (see for instance [4]) in their program for solving the Kerr stability conjecture.

### 5.2.2 Carter's Separability for the Wave Equation

The separability of the wave equation on EK was used on [5] to derive decay results for axisymmetric solutions. We next describe the method of [5]. We will use the Boyer–Lindquist coordinates  $(t, r, \theta, \varphi)$  and write solutions  $\psi$  as a superposition of

mode solutions of the form

$$F(t) \cdot F(r) \cdot F(\theta) \cdot F(\varphi).$$

On Kerr, the wave equation in Boyer–Lindquist coordinates takes the form

$$\begin{aligned} & \left[ \partial_r \Delta \partial_r + \frac{1}{\Delta} \left[ \Delta \cdot M^2 - (r^2 + M^2)^2 \right] \partial_t^2 - \frac{1}{\Delta} 4M^2 r \partial_t \partial_\varphi - \frac{1}{\Delta} M^2 \partial_\varphi^2 \right] \psi \\ & + \left[ \Delta_{\mathbb{S}^2} - (M^2 \cos^2 \theta) \partial_t^2 \right] \psi = 0 \end{aligned}$$

Let's assume that we can (at least formally) take the Fourier transform of  $\psi$  in  $t$  and  $\varphi$  (assuming for a moment that  $\psi$  is in  $L^2(dt)$ ):

$$\psi(t, r, \theta, \varphi) = \frac{1}{\sqrt{2\pi}} \int_{\omega \in \mathbb{R}} \sum_{m \in \mathbb{Z}} \widehat{\psi}(\omega, r, m, \theta) e^{im\varphi} e^{-i\omega t} d\omega.$$

Since  $\partial_t, \partial_\varphi$  are Killing, then for each frequency pair  $(\omega, m) \in \mathbb{R} \times \mathbb{Z}$  the projection

$$\psi_{\omega, m}(t, r, \theta, \varphi) = \widehat{\psi}(\omega, m, r, \theta) e^{im\varphi} e^{-i\omega t}$$

(which is manifestly separated in  $t, \varphi$ ) satisfies the wave equation. Since

$$\partial_t \psi_{\omega, m} = -i\omega \cdot \psi_{\omega, m}, \quad \partial_\varphi \psi_{\omega, m} = im \cdot \psi_{\omega, m}$$

the wave equation for each projection  $\psi_{\omega, m}$  reads

$$\mathcal{R}_{\omega, m} \psi_{\omega, m} + \mathcal{A}_\omega \psi_{\omega, m} = 0,$$

where the **radial** operator  $\mathcal{R}_{\omega, m}$  is given by

$$\mathcal{R}_{\omega, m} = \left[ \partial_r \Delta \partial_r - \frac{1}{\Delta} \left[ \Delta M^2 - (r^2 + M^2)^2 \right] \omega^2 - \frac{1}{\Delta} 4M^2 r m \omega + \frac{1}{\Delta} M^2 m^2 \right]$$

and the **angular** (also known as *spheroidal wave*) operator  $\mathcal{A}_\omega$  by

$$\mathcal{A}_{a\omega} = \left[ \Delta_{\mathbb{S}^2} + (M\omega)^2 \cos^2 \theta \right].$$

We can now further separate in the remaining two variables  $r$  and  $\theta$ :

$$\begin{aligned}\psi_{\omega,m}(t, r, \theta, \varphi) &= \widehat{\psi}(\omega, m, r, \theta) e^{im\varphi} e^{-i\omega t} \\ &= R_{\omega,m}(r) \cdot (\Theta_{\omega,m}(\theta) e^{im\varphi}) \cdot e^{-i\omega t} \\ &= R_{\omega,m}(r) \cdot S_{\omega,m}(\theta, \varphi) \cdot e^{-i\omega t},\end{aligned}$$

where the angular part  $S_{\omega,m}(\theta, \varphi) = \Theta_{\omega,m}(\theta) e^{im\varphi}$  is supported on the fixed azimuthal frequency  $m$ . Then,  $\square_g \psi_{\omega,m} = 0$  becomes

$$\frac{\mathcal{R}_{\omega,m} R_{\omega,m}(r)}{R_{\omega,m}(r)} + \frac{\mathcal{A}_{\omega} S_{\omega,m}(\theta, \varphi)}{S_{\omega,m}(\theta, \varphi)} = 0.$$

Hence, there is a separation constant  $\lambda$  such that

$$\mathcal{A}_{\omega} S_{\omega,m}(\theta, \varphi) = -\lambda S_{\omega,m}(\theta, \varphi), \quad \mathcal{R}_{\omega,m} R_{\omega,m}(r) = \lambda R_{\omega,m}(r).$$

The angular functions  $\Theta(\theta)$  are required to be regular at the poles  $\theta = 0$  and  $\theta = \pi$ . These boundary conditions pick out a discrete set of eigenvalues  $\lambda_{\ell m}^{(\omega)}$  with  $\ell \in \mathbb{Z}$ ,  $\ell \geq |m|$ . In view of standard elliptic theory, we can infer the existence of a complete orthonormal system  $S_{\ell m}^{(\omega)}(\theta, \varphi)$  with  $m, \ell \in \mathbb{Z}$ ,  $\ell \geq |m|$  of  $L^2(\mathbb{S}^2)$  of eigenfunctions of  $\mathcal{A}_{\omega}$  with real eigenvalues  $-\lambda_{\ell m}^{(\omega)}$ . The functions  $S_{\ell m}^{(\omega)}$  are known as the *oblate spheroidal harmonics*. For  $\omega = 0$  these reduce to the standard spherical harmonics  $Y_{\ell m}$  and  $\lambda_{\ell m}^{(0)} = \ell(\ell + 1)$ . If we define  $\Lambda_{\ell m}^{(\omega)} = \lambda_{\ell m}^{(\omega)} + (M\omega)^2$  then it follows that  $\Lambda_{\ell m}^{(\omega)} \geq |m|(|m| + 1)$ . Hence, for any fixed  $\omega$  and fixed  $r$  we can decompose

$$\widehat{\psi}(\omega, m, r, \theta) e^{im\varphi} = \sum_{\ell \geq |m|} R_{\omega,m,\ell}(r) \cdot S_{\ell m}^{(a\omega)}(\theta, \varphi)$$

where  $R_{\omega,m,\ell}(r)$  satisfies *Carter's 2nd-order radial equation*

$$\mathcal{R}_{\omega,m} R_{\omega,m,\ell}(r) = \lambda_{\ell m}^{(\omega)} R_{\omega,m,\ell}(r). \quad (5.2.2)$$

As for the angular decomposition, we need to impose boundary conditions for  $R_{\omega,m,\ell}(r)$ . It turns out that the correct boundary conditions associated to the wave equation correspond to those of outgoing waves at infinity  $r = +\infty$  and ingoing waves at the event horizon  $r = M$  as measured by a co-moving observer:

$$R_{\omega,m,\ell}(r) \sim \begin{cases} \frac{1}{r} e^{i\omega r^*} & \text{as } r \rightarrow +\infty \text{ } (r^* \rightarrow +\infty) \\ e^{-i(\omega - \frac{m}{2M})r^*} & \text{as } r \rightarrow r_{\mathcal{H}^+} \text{ } (r^* \rightarrow -\infty). \end{cases} \quad (5.2.3)$$

The oscillatory behavior of  $R_{\omega,m,\ell}$  towards  $\mathcal{H}$  accounts for the regularity of  $\psi$  expressed in terms of a regular local coordinate system such as  $(v, r, \theta, \varphi^*)$ . Indeed, if  $\widehat{\psi}_{v,\varphi^*}(\omega, m, r, \theta)$  denotes the (regular) Fourier transform of (the regu-

lar)  $\psi(v, r, \theta, \varphi^*)$  with respect to  $v$  and  $\varphi^*$  and, as above,  $\widehat{\psi}(\omega, m, r, \theta)$  denotes the Fourier transform of  $\psi(t, r, \theta, \varphi)$  with respect to  $t$  and  $\varphi$ , then

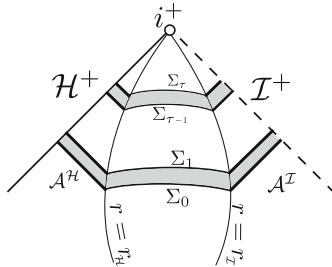
$$\widehat{\psi}(\omega, m, r, \theta) = e^{i\omega(t-v)} \cdot e^{-im(\varphi-\varphi^*)} \cdot \widehat{\psi}_{v,\varphi^*}.$$

The horizon boundary condition follows from (3.1.2) and the relation  $(\varphi^* - \varphi) \sim \frac{1}{2M}r^*$  close to the horizon. Finally, we conclude that solutions  $\psi$  of the wave equation can be formally decomposed as follows

$$\psi(t, r, \theta, \varphi) = \frac{1}{\sqrt{2\pi}} \int_{\omega \in \mathbb{R}} \underbrace{\sum_{m,\ell} \underbrace{R_{\omega,m,\ell}(r)}_{\text{radial wave}} \cdot \underbrace{S_{\ell m}^{(\omega)}(\theta, \varphi)}_{\text{Oblate Spheroidal Expansion}}}_{\text{Fourier Expansion}} \cdot e^{-i\omega t} d\omega.$$

### 5.2.3 The Cut-off $\xi_\tau$ and the Renormalized Carter Equation

Separating the wave equation involves taking the Fourier transform in time. Since, a priori, we do not know that the solution is  $L^2(dt)$  we must first cut off in time. Let  $\xi_\tau$  be a cut-off function such that  $\xi_\tau(\tilde{\tau}) = 0$  for  $\tilde{\tau} \leq 0$  and  $\tilde{\tau} \geq \tau$  and  $\xi_\tau(\tilde{\tau}) = 1$  for  $1 \leq \tilde{\tau} \leq \tau - 1$ . Then the support of  $\nabla \xi_\tau$  is the shaded region  $S_\xi = \{0 \leq \tilde{\tau} \leq 1\} \cup \{\tau - 1 \leq \tilde{\tau} \leq \tau\}$ :



Define  $\psi_{\leq \tau} = \xi_\tau \psi$ . Then,

$$\square_g \psi_{\leq \tau} = F,$$

where

$$F = 2\nabla^\mu \xi_\tau \nabla_\mu \psi + (\square \xi_\tau) \psi. \tag{5.2.4}$$

We will use the separability theory developed in the previous section for  $\psi_{\leq \tau}$ . In fact, instead of working with the radial functions  $R_{\leq \tau}(\omega)_{\ell m}(r)$  we will work with the *renormalized radial functions*

$$u_{\ell m}^{(\omega)}(r^*) = \sqrt{(r^2 + M^2)} \cdot (R_{\leq \tau}(\omega)_{\ell m}(r))$$

These satisfy

$$\boxed{\frac{d^2}{(dr^*)^2} u_{\ell m}^{(\omega)} + \left( \omega^2 - V_{\ell m}^{(\omega)}(r) \right) u_{\ell m}^{(\omega)} = H_{\ell m}^{(\omega)}} \quad (5.2.5)$$

where

$$V_{\ell m}^{(\omega)}(r) = \frac{4M^2 r m \omega - M^2 m^2 + \Delta \cdot \Lambda_{\ell m}^{(\omega)}}{(r^2 + M^2)^2} + \frac{\Delta(3r^2 - 4Mr + M^2)}{(r^2 + M^2)^3} - \frac{3\Delta^2 r^2}{(r^2 + M^2)^4},$$

and

$$H_{\ell m}^{(\omega)}(r) = \frac{\Delta F_{\ell m}^{(\omega)}(r)}{(r^2 + M^2)^{1/2}}.$$

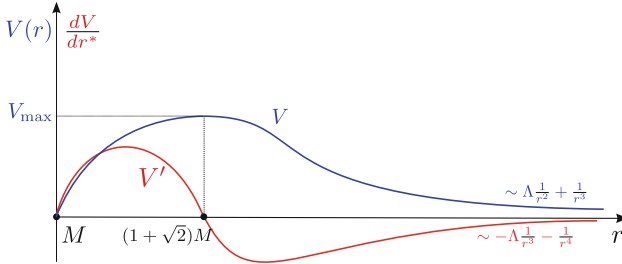
Although  $u$  is a complex-valued function, the potential  $V$  is real. This would not be true if we had separated with respect to  $(v, r, \theta, \varphi^*)$ .

### 5.2.4 Properties of the Potential $V$

Restricting to axisymmetric  $\psi$  (i.e.  $m = 0$ ) and by dropping the indices we obtain

$$V = \frac{(r - M)^2}{(r^2 + M^2)^2} \cdot \Lambda + \frac{(r - M)^3 M}{(r^2 + M^2)^4} (2r^2 + 3rM - M^2).$$

For a detailed analysis of  $V$  we refer to [5]. We next give the graphs of  $V$  and  $\frac{dV}{dr^*}$ .



Two remarks are in order.

1. The potential  $V$  exhibits a symmetric asymptotic behavior towards the event horizon and towards infinity. Indeed,  $V \sim \frac{1}{(r^*)^2} \Lambda - \frac{1}{(r^*)^3}$ , for all  $r \leq r_{\mathcal{H}}$  and  $V \sim \frac{1}{r^2} \Lambda + \frac{1}{r^3}$ , for all  $r \geq r_{\mathcal{I}}$ .
2. For all frequencies  $\Lambda$  (with  $m = 0$ ),  $V'$  vanishes exactly at  $r = M$  and  $r = (1 + \sqrt{2})M$ . This is related to the fact that axisymmetric frequencies effectively see only the trapped null geodesics orthogonal to the axial vector field  $\Phi$ . These geodesics span the hypersurface  $\{r = (1 + \sqrt{2})M\}$  which is known as the “*effective photon sphere*”.

### 5.3 Physical Space–Fourier Space Correspondence

Parseval identity immediately yields the following identities

$$\begin{aligned} \int_{-\infty}^{+\infty} \sum_{m,l} |u|^2 d\omega &= \int_{-\infty}^{+\infty} \int_{\mathbb{S}^2} (\psi_{\geq \omega})^2 \cdot (r^2 + M^2) dt d\Omega, \\ \int_{-\infty}^{+\infty} \sum_{m,l} \omega^2 |u|^2 d\omega &= \int_{-\infty}^{+\infty} \int_{\mathbb{S}^2} (T\psi_{\geq \omega})^2 \cdot (r^2 + M^2) dt d\Omega, \\ \int_{-\infty}^{+\infty} \sum_{m,l} \Lambda |u|^2 d\omega &= \int_{-\infty}^{+\infty} \int_{\mathbb{S}^2} [|\nabla_{\mathbb{S}^2} \psi_{\geq \omega}|^2 + M^2 \sin^2 \theta \cdot (T\psi_{\geq \omega})^2] \cdot (r^2 + M^2) dt d\Omega, \\ \int_{-\infty}^{+\infty} \sum_{m,l} |u'|^2 d\omega &= \int_{-\infty}^{+\infty} \int_{\mathbb{S}^2} \left( \partial_{r^*} \left( \sqrt{r^2 + M^2} \cdot \psi_{\geq \omega} \right) \right)^2 dt d\Omega, \end{aligned}$$

where  $\nabla_{\mathbb{S}^2} \psi$  denotes the gradient of  $\psi$  on the unit sphere with respect to the standard metric and  $d\Omega = \sin \theta d\theta d\varphi$ .

### 5.4 Frequency Localized Morawetz Estimates

The Fourier transform has the advantage that it allows for a clean way to deal with the geometric features of all frequency ranges. The main idea is to modify the energy method so that it is applicable for the radial functions  $u$ . We introduce the *microlocal currents* (see also [4])

$$\begin{aligned} \mathcal{J}_1^y[u] &= y \left[ |u'|^2 + (\omega^2 - V) |u|^2 \right], \\ \mathcal{J}_2^h[u] &= h \operatorname{Re}(u' \bar{u}) - \frac{1}{2} h' |u|^2, \\ \mathcal{J}_3^f[u] &= f \left[ |u'|^2 + (\omega^2 - V) |u|^2 \right] + f' \operatorname{Re}(u' \bar{u}) - \frac{1}{2} f'' |u|^2. \end{aligned} \tag{5.4.1}$$

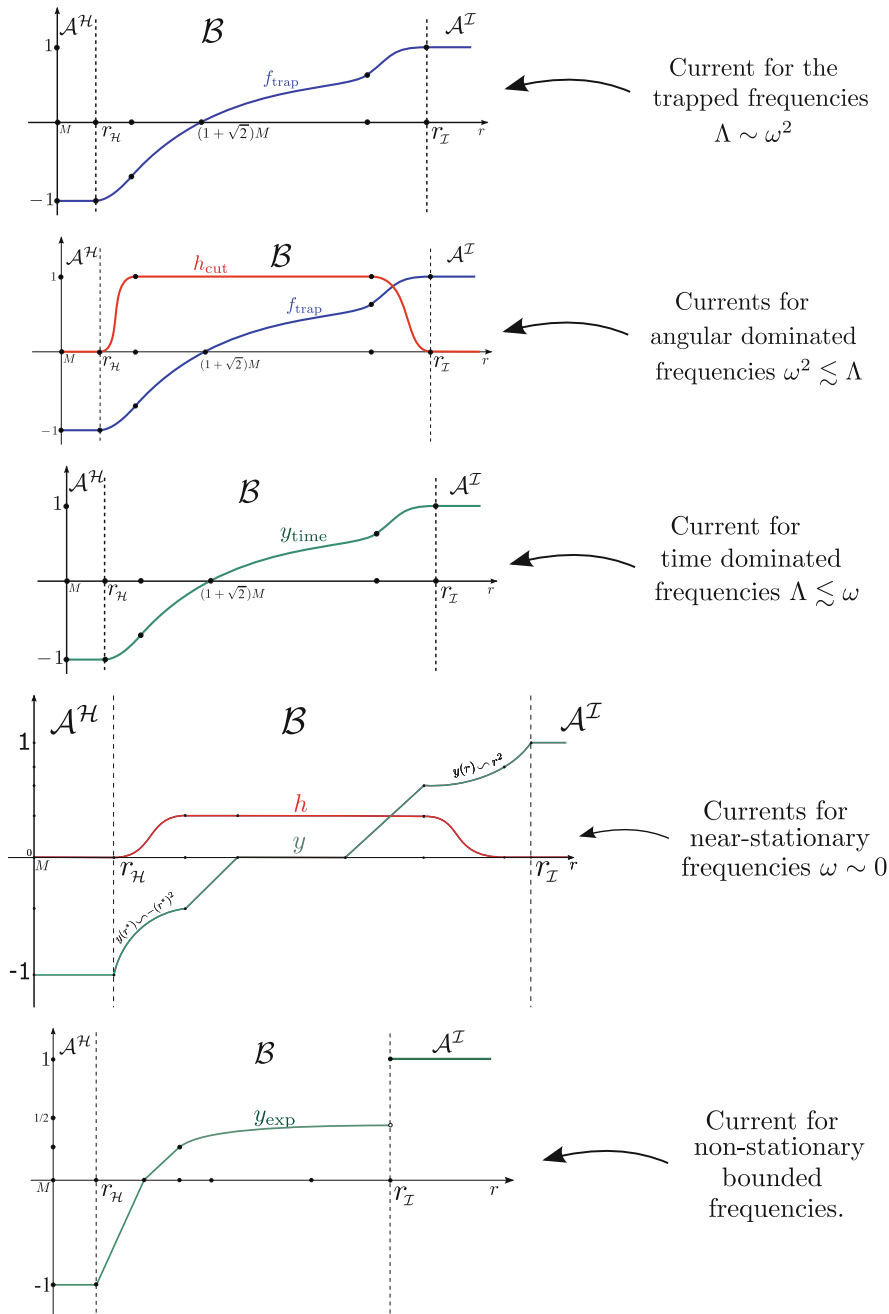
We shall construct several combinations of these currents with appropriate multiplier functions  $y, h, f$  such that the derivatives

$$\begin{aligned} \left( \mathcal{J}_1^y[u] \right)' &= y' \left[ |u'|^2 + (\omega^2 - V) |u|^2 \right] - yV' |u|^2 + 2y \operatorname{Re}(u' \bar{H}), \\ \left( \mathcal{J}_2^h[u] \right)' &= h \left[ |u'|^2 + (V - \omega^2) |u|^2 \right] - \frac{1}{2} h'' |u|^2 + h \operatorname{Re}(u \bar{H}), \\ \left( \mathcal{J}_3^f[u] \right)' &= 2f' |u'|^2 - fV' |u|^2 - \frac{1}{2} f''' |u|^2 + 2f \operatorname{Re}(u' \bar{H}) + f' \operatorname{Re}(u \bar{H}). \end{aligned} \tag{5.4.2}$$

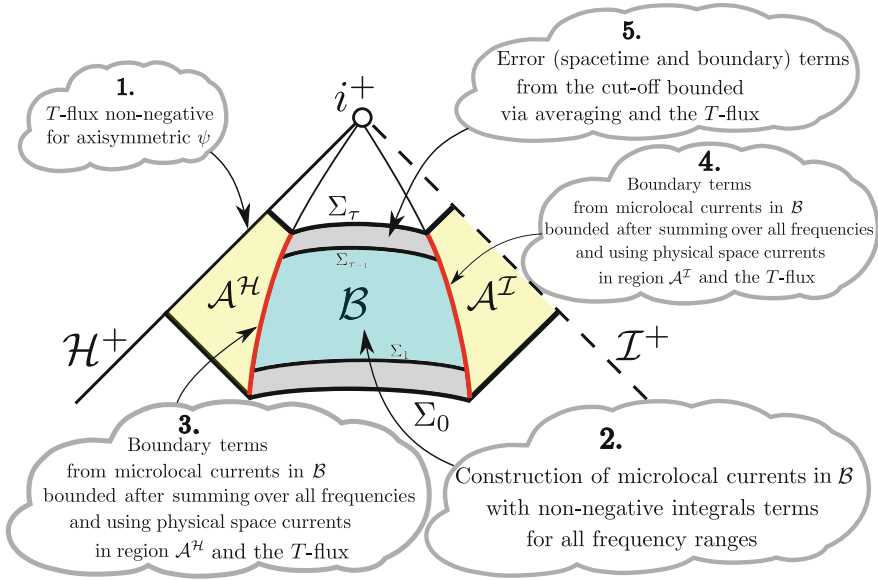
of the combined currents control

$$\int_r \left[ |u'|^2 + |u|^2 + \left( r - (1 + \sqrt{2})M \right)^2 \left[ \Lambda + \omega^2 \right] |u|^2 \right] dr^*.$$

The main constructions are depicted below



Observe that all these currents take the same values for all frequencies at  $r = r_{\mathcal{H}}$  and  $r = r_{\mathcal{I}}$ . The next figure summarizes the main steps in proving a Morawetz estimate using the above microlocal currents.



We finally arrive at the following Morawetz estimate: for all axisymmetric solutions  $\psi$  of the wave equation on EK we have

$$\int_{\{r_{\mathcal{H}} \leq r \leq r_{\mathcal{I}}\}} \left[ (\partial_{r^*} \psi)^2 + \psi^2 + \left( r - (1 + \sqrt{2})M \right)^2 [|\nabla \psi|^2 + (T\psi)^2] \right] \leq C \int_{\Sigma_0} J_{\mu}^T[\psi] n_{\Sigma_0}^{\mu}. \tag{5.4.3}$$

The degeneracy at  $r = (1 + \sqrt{2})M$  can be removed by commuting the above estimate with  $T$ . It is important to note that the above method decouples completely the Morawetz estimate from the redshift estimate (or the  $T - N - P$  hierarchy) near the horizon. This was achieved by (1) having frequency-independent currents at the (red) boundary hypersurfaces  $r = r_{\mathcal{H}}$ ,  $r = r_{\mathcal{I}}$ , (2) summing the currents over all frequencies and using Parseval’s identity, (3) using physical space currents which are controlled purely by the  $T$ -flux.

### 5.5 Energy and Pointwise Decay in Time

The near-horizon  $T - P - N$  hierarchy and the  $r^P$ -weighted hierarchy near infinity can be derived for axisymmetric solutions on EK as in ERN. These hierarchies in conjunction with the above Morawetz estimate yield  $\tau^{-2}$  decay for the  $T$ -flux  $J_{\Sigma_{\tau}}^T[\psi]$  and uniform boundedness for the conformal fluxes  $C_{N_{\mathcal{H}}}[\psi]$  and  $C_{N_{\mathcal{I}}}[\psi]$ . Then, the Hardy inequalities (4.7.1) give us decay for the  $L^2$  norm on the spheres  $S^2(\theta, \varphi^*)$ .

To obtain pointwise bounds we need to commute and apply Sobolev inequalities on the sphere.

In ERN we simply commute with angular momentum operators. However, the only vector fields we can commute with are  $T$  and  $\Phi$  and these are not enough to bound an elliptic operator on the sphere. This difficulty can be overcome by commuting with the 2nd-order symmetry operator  $Q$  given by (5.2.1). Summarizing, the symmetry operators of up to second order on EK are the following

$$\mathbb{S}_0 = \{id\}, \quad \mathbb{S}_1 = \{T, \Phi\} \quad \mathbb{S}_2 = \{T^2, \Phi^2, T\Phi, Q\}.$$

The following estimate allows us to obtain pointwise boundedness and decay bounds for  $\psi$ :

$$|\psi|^2 \leq C \sum_{|k| \leq 2} \int_{\mathbb{S}^2} |S^k \psi|^2,$$

where  $|S^k \psi|^2 = \sum_{S \in \mathbb{S}_k} |S\psi|^2$ . This bound follows from the spherical Sobolev inequality

$$|\psi|^2 \leq C \int_{\mathbb{S}^2} |\psi|^2 + |\mathcal{L}\psi|^2.$$

and the bound on the Laplacian using the Carter symmetry:

$$|\mathcal{L}\psi|^2 \leq C [(Q\psi)^2 + (TT\psi)^2 + (\Phi\Phi\psi)^2].$$

## References

1. R. Penrose, M. Walker, On quadratic first integrals of the geodesic equations for type {22} spacetimes. *Commun. Math. Phys.* **18**, 265–274 (1970)
2. L. Andersson, P. Blue, Hidden symmetries and decay for the wave equation on the Kerr space-time. *Ann. Math.* **182**, 787–853 (2015)
3. B. Carter, Black hole equilibrium states, *Les Houches Lectures* (1972)
4. M. Dafermos, I. Rodnianski, Decay for solutions of the wave equation on Kerr exterior spacetimes I-II: the cases  $|a| \ll m$  or axisymmetry (2010), [arXiv:1010.5132](https://arxiv.org/abs/1010.5132)
5. S. Aretakis, Decay of axisymmetric solutions of the wave equation on extreme Kerr backgrounds. *J. Funct. Anal.* **263**, 2770–2831 (2012)

# Chapter 6

## A Theory of Conservation Laws on Null Hypersurfaces



In this Chapter we present a theory of conservation laws on null hypersurfaces in general Lorentzian manifolds. These conservation laws are a generalization of the conservation laws on extremal event horizons. We also review their relevance to the characteristic gluing problem and provide necessary and sufficient conditions for their existence.

### 6.1 The Geometry of Null Foliations

Let  $\mathcal{H}$  be a regular null hypersurface of a four-dimensional Lorentzian manifold  $(\mathcal{M}, g)$ . A foliation  $\mathcal{S} = (S_v)_{v \in \mathbb{R}}$  with sections  $S_v$  of  $\mathcal{H}$  can be determined by a section  $S_0$ , a function  $\Omega \in C^\infty(\mathcal{H})$  on  $\mathcal{H}$  and a null normal geodesic vector field  $L_{geod}$  satisfying  $\nabla_{L_{geod}} L_{geod} = 0$ . We denote

$$\mathcal{S} = \langle S_0, L_{geod}, \Omega \rangle. \tag{6.1.1}$$

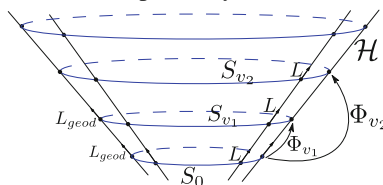
Indeed, if we define the vector field

$$L = \Omega^2 \cdot L_{geod}$$

on  $\mathcal{H}$  and consider the affine parameter  $v$  of  $L$  such that

$$Lv = 1, \text{ with } v = 0 \text{ on } S_0,$$

then the level sets  $S_v$  of  $v$  on  $\mathcal{H}$  are precisely the leaves of the foliation  $\mathcal{S}$ .



We will assume that  $S_v$  are diffeomorphic to  $\mathbb{S}^2$ . The flow of  $L$  on  $\mathcal{H}$  provides a diffeomorphism  $\Phi_v$  between the sections  $S_v$  and  $S_0$ . In addition to the induced metric on  $S_v$ , which we will denote by  $\mathcal{g}$ , we can also equip all sections with the standard metric on the unit sphere  $\mathcal{g}_{\mathbb{S}^2}$  such that it is invariant under  $\Phi_v$ . The volume form on  $S_v$  with respect to  $\mathcal{g}_{\mathbb{S}^2}$  will be denoted by  $d\mu_{\mathbb{S}^2}$ . Given any section  $S_v$ , there is a unique metric  $\hat{g}$  which is conformal to the induced metric  $\mathcal{g}$  such that the volume form  $d\mu_{\hat{g}}$  with respect to  $\hat{g}$  and the volume form  $d\mu_{\mathbb{S}^2}$  with respect to  $\mathcal{g}_{\mathbb{S}^2}$  are equal:

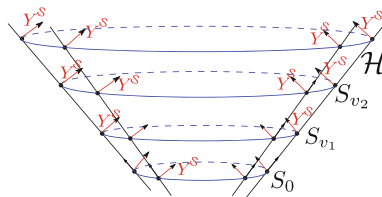
$$d\mu_{\hat{g}} = d\mu_{\mathbb{S}^2}.$$

We denote by  $\phi$  the conformal factor:

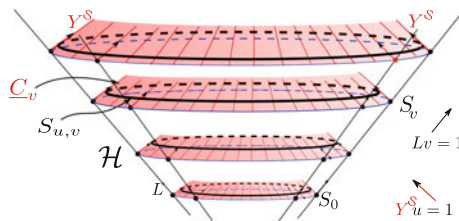
$$\mathcal{g} = \phi^2 \cdot \hat{g}. \tag{6.1.2}$$

Furthermore, given a foliation  $\mathcal{S}$  we denote by  $Y^{\mathcal{S}}$  the unique null vector field which is normal to the sections  $S_v$ , conjugate to  $\mathcal{H}$  and normalized such that

$$g(L_{geod}, Y^{\mathcal{S}}) = -1. \tag{6.1.3}$$



In view of the theory in Sect. 1.1.4, the vector field  $Y^{\mathcal{S}}$  can be seen as the generator of an optical function  $u$  such that  $\mathcal{H} = \{u = 0\}$ . The optical function  $u$  satisfies  $Y^{\mathcal{S}}u = 1$  on  $\mathcal{H}$ . Let's denote by  $C_u$  the level sets of  $u$ . We have  $\mathcal{H} = C_0$ . We further denote by  $\underline{C}_v$  the conjugate null normal geodesic congruence emanating from the sections  $S_v$  of  $\mathcal{H}$ , and define  $S_{u,v} = C_u \cap \underline{C}_v$ . We denote by  $\underline{L}$  the null normal to  $\underline{C}_v$  normalized such that  $\underline{L}u = 1$ . Clearly,  $\underline{L} = Y^{\mathcal{S}}$  on  $\mathcal{H}$ . In order to define the conformal factor  $\phi$  of the sections  $S_{u,v}$ , as above, we need first to equip  $S_{u,v}$  with  $\mathcal{g}_{\mathbb{S}^2}$ . This is done by propagating  $\mathcal{g}_{\mathbb{S}^2}$  on  $S_v$  along  $\underline{C}_v$  via the flow of  $\underline{L}$ .



Finally, if  $X, Y$  are tangential to the sections  $S_v$  on  $\mathcal{H}$  then we define the tensors  $\chi, \underline{\chi}, \zeta$  such that

$$\Omega\chi(X, Y) = g(\nabla_X L, Y), \quad \Omega\underline{\chi}(X, Y) = g(\nabla_X \underline{L}, Y), \quad \Omega\zeta(x) = g\left(\nabla_X \left(\Omega^{-1}L\right), \underline{L}\right). \quad (6.1.4)$$

Note that quantities induced on the sections  $S_v$  will be slashed. That is,  $\not{g}$ ,  $\not{\ell}$ ,  $\not{\nabla}$ ,  $\not{\Delta}$  denote the induced metric, volume form, covariant derivative and Laplacian respectively.

## 6.2 Conservation Laws for the Wave Equation

Consider the linear space  $\mathcal{V}_{\mathcal{H}}$  consisting of all smooth functions on  $\mathcal{H}$  which are constant along the null generators of  $\mathcal{H}$ :

$$\mathcal{V}_{\mathcal{H}} = \left\{ f \in C^\infty(\mathcal{H}) : Lf = 0 \right\}. \quad (6.2.1)$$

Let  $\mathcal{S} = (S_v)_{v \in \mathbb{R}}$  be a foliation of  $\mathcal{H}$  and let  $Y^{\mathcal{S}}$  be the vector field and  $\phi$  the conformal factor defined above. We define the linear space  $\mathcal{W}^{\mathcal{S}}$  to be the subspace of  $\mathcal{V}_{\mathcal{H}}$  such that: If  $\Theta^{\mathcal{S}} \in \mathcal{W}^{\mathcal{S}}$  then for all solutions  $\psi$  to the wave equation  $\square_g \psi = 0$  the integrals

$$\int_{S_v} Y^{\mathcal{S}}(\phi \cdot \psi) \cdot \Theta^{\mathcal{S}} d\mu_{\mathbb{S}^2} \quad (6.2.2)$$

are conserved, i.e. independent of  $v$ . That is,

$$\mathcal{W}^{\mathcal{S}} = \left\{ \Theta^{\mathcal{S}} \in C^\infty(\mathcal{H}) : L\Theta^{\mathcal{S}} = 0, \partial_v \left( \int_{S_v} Y^{\mathcal{S}}(\phi \cdot \psi) \cdot \Theta^{\mathcal{S}} d\mu_{\mathbb{S}^2} \right) = 0 \right\} \subset \mathcal{V}_{\mathcal{H}}. \quad (6.2.3)$$

**Definition 6.2.1** (*Conservation laws on  $\mathcal{H}$* ) We say that a null hypersurface  $\mathcal{H}$  admits (first order) conservation laws with respect to a foliation  $\mathcal{S}$  of  $\mathcal{H}$  if

$$\dim \mathcal{W}^{\mathcal{S}} \geq 1. \quad (6.2.4)$$

If (6.2.4) holds then we will refer to the space  $\mathcal{W}^{\mathcal{S}}$  the *kernel* and the number  $\dim \mathcal{W}^{\mathcal{S}}$  as *the dimension* of the conservation laws. As we shall see in Sect. 6.4, the conservation laws in the sense of Definition 6.2.1 are in fact the **only** type of “first order” conservation laws that a null hypersurface might admit. Important examples of hypersurfaces which admit conservation laws are (1) the standard hypersurfaces in Minkowski spacetime, (2) null infinity with the associated Newman–Penrose constants (see Sect. 1.8.2), (3) ERN and EK. See also Sect. 6.5 for a more general discussion about conservation laws on extremal black holes.

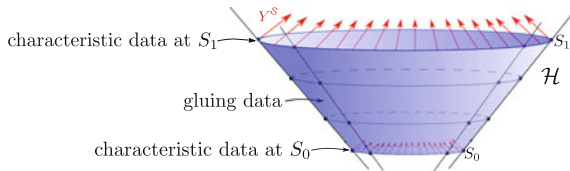
### 6.3 The Characteristic Gluing Problem

The characteristic gluing problem, first introduced in [1], for the wave equation provides a means to formally show that Definition 6.2.1 is the right notion of conservation laws on null hypersurfaces. The problem of gluing of characteristic initial data along a null hypersurface  $\mathcal{H}$  is the following: Let  $\mathcal{S} = (S_v)_{v \in \mathbb{R}}$  be foliation and  $S_0, S_1$  two sections. We define the (reduced) characteristic data on the sections  $S_0$  and  $S_1$  as follows:

$$\begin{aligned} \text{Data}(S_0) &= \{Y^{\mathcal{S}}\psi|_{S_0}, L^n\psi|_{S_0}, n \geq 0\}, \\ \text{Data}(S_1) &= \{Y^{\mathcal{S}}\psi|_{S_1}, L^n\psi|_{S_1}, n \geq 0\}. \end{aligned}$$

Recall that  $L$  is tangential to the null generator of  $\mathcal{H}$ . Our problem is to *smoothly extend  $\psi$  on  $\mathcal{H}$  between  $S_0$  and  $S_1$  such that*

1.  $\psi$  solves the wave equation,
2. the transversal derivative  $Y\psi$  is continuous on  $\mathcal{H} \cap \{0 \leq v \leq 1\}$ .



Clearly, if  $\mathcal{H}$  admits non-trivial conservation laws with respect to the foliation  $\mathcal{S}$  in the sense of Definition 6.2.1, then we cannot perform gluing of general data at  $S_0$  and  $S_1$  since the respective charges at  $S_0$  and  $S_1$  may not be equal. However, it is not a priori clear if these conservation laws are the **only** obstruction to gluing of characteristic data. The following was shown in [1]:

**Conservation laws and gluing of characteristic data:** *One can perform first order gluing constructions on  $\mathcal{H}$  for general characteristic data if and only if there are no first order conservation laws on  $\mathcal{H}$  in the sense of Definition 6.2.1. If  $\mathcal{H}$  admits conservation laws, then we can glue characteristic data if and only if their associated charges are equal.*

This result immediately yields the following

**Classification of conservation laws on null hypersurfaces:** *No conserved (or, more generally, monotonic in  $v$ ) quantities involving the 1-jet of solutions to the wave equation exist on  $\mathcal{H}$  unless they have the form of the conservation laws given precisely by Definition 6.2.1.*

### 6.4 Necessary and Sufficient Conditions

The main result of [1] is the derivation of geometric necessary and sufficient conditions for the existence of conservation laws in the sense of Definition 6.2.1. Let's introduce the following 2nd order operator on  $\mathcal{H}$

$$\begin{aligned} \mathcal{O}^S \psi = & \Omega^2 \cdot \Delta \psi + [\nabla \Omega^2 + 2\Omega^2 \cdot \zeta^\sharp] \cdot \nabla \psi \\ & + \left[ 2\text{div}(\Omega^2 \cdot \zeta^\sharp) + L(\Omega \text{tr} \underline{\chi}) + \frac{1}{2}(\Omega \text{tr} \underline{\chi})(\Omega \text{tr} \chi) \right] \cdot \psi. \end{aligned} \tag{6.4.1}$$

and the linear space

$$\mathcal{U}^S = \left\{ \Theta^S \in C^\infty(\mathcal{H}) : L\Theta^S = 0, \mathcal{O}^S \left( \frac{1}{\phi} \cdot \Theta^S \right) = 0 \text{ on } \mathcal{H} \right\} \subset \mathcal{V}_{\mathcal{H}}, \tag{6.4.2}$$

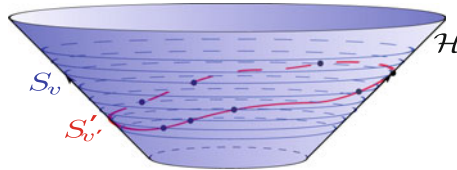
where  $\phi$  denotes the conformal factor of the sections of  $\mathcal{S}$ . The following result was proved in [1]:

**Classification of null hypersurfaces admitting conservation laws:** *A null hypersurface  $\mathcal{H}$  admits first order conservation laws for the wave equation with respect to a foliation  $\mathcal{S}$  in the sense of Definition 6.2.1 if and only if  $\mathcal{U}^S \neq \{0\}$ . Specifically, the kernel of the conservation laws satisfies*

$$\mathcal{W}^S = \mathcal{U}^S.$$

Standard elliptic theory implies that  $\mathcal{H}$  can only admit finitely many linearly independent conservation laws, i.e.  $\dim \mathcal{W}^S < \infty$ .

**Conservation laws and change of foliation:** *If  $\mathcal{H}$  admits a conservation law with respect to the foliation  $\mathcal{S} = \langle S_0, L_{geod}, \Omega \rangle$ , then it also admits a conservation law with respect to **any** other foliation  $\mathcal{S}' = \langle S'_0, L'_{geod}, \Omega' \rangle$ .*



Specifically, the kernels  $\mathcal{W}^S, \mathcal{W}^{S'}$  satisfy  $\mathcal{W}^{S'} = \{ f^2 \cdot \Theta^S, \Theta^S \in \mathcal{W}^S \}$ , where  $f \in \mathcal{V}_{\mathcal{H}}$  such that  $L'_{geod} = f^2 \cdot L_{geod}$ , and so  $\dim \mathcal{W}^{S'} = \dim \mathcal{W}^S$ . See [2].

## 6.5 Conservation Laws on Extremal Black Holes

Let's consider the following geodesic foliation of a general Killing horizon with Killing normal  $V$  and surface gravity  $\kappa \geq 0$ :

$$\mathcal{S} = \left\langle S_0, L_{geod}|_{S_0} = V|_{S_0}, \Omega = 1 \right\rangle. \quad (6.5.1)$$

Here  $S_0$  is a section for which  $tr \underline{\chi}|_{S_0} < 0$ . Then, for this foliation, the operator  $\mathcal{O}^{\mathcal{S}}$  takes the form (see [1])

$$\mathcal{O}^{\mathcal{S}} \psi = \mathbb{A} \psi + \mathbf{div}(2\psi \cdot \zeta) + \left[ tr \underline{\chi}|_{S_0} \cdot \kappa \right] \cdot \psi.$$

Let  $\Psi > 0$  be the unique (up to rescaling) positive principal eigenfunction of  $\mathcal{O}^{\mathcal{S}}$  and let  $\lambda$  be its principal (maximum) eigenvalue. Then, we immediately obtain

$$\int_{S_v} \left( tr \underline{\chi}|_{S_0} \cdot \kappa \right) \cdot \Psi d\mu_{\mathring{g}} = \lambda \cdot \int_{S_v} \Psi d\mu_{\mathring{g}}.$$

The left hand side is manifestly non-positive and forces the maximum eigenvalue  $\lambda$  to be non-positive. This implies that *non-extremal horizons (with  $\kappa > 0$ ) do not admit conservation laws whereas extremal horizons (with  $\kappa = 0$ ) admit a **unique conservation law***. This generalized conservation law was first discovered by Lucietti and Reall [3]. It reduces to the conservation laws for ERN and EK discussed throughout this Brief. Lucietti and Reall went one step further and investigated the impact of the existence of this conservation law for general extremal black holes with the aim to derive asymptotic blow up results for higher order derivatives along the extremal horizon. They found that blow up results can be obtained if a certain function determined purely by the near-horizon geometry is constant. Lucietti and Reall showed that this property holds for a large class of near-horizon geometries. It holds for the near-horizon geometry of extremal Myers–Perry black holes and also for extremal black hole solutions to the Einstein field equations coupled to arbitrarily many abelian vectors and uncharged scalars (see [3] for details and references). In summary, all known extremal black holes satisfy this property. This suggests that *general extremal black holes exhibit some form of the horizon instability*. Understanding this in the context of the Cauchy problem for the Einstein equations remains an open problem.

## References

1. S. Aretakis, The characteristic gluing problem and conservation laws for the wave equation on null hypersurfaces. *Ann. PDE* **3**(1) (2017), [arXiv:1310.1365](https://arxiv.org/abs/1310.1365)
2. S. Aretakis, On a foliation-covariant elliptic operator on null hypersurfaces. *Int. Math. Res. Not.* **15**(15), 6433–6469 (2015)
3. J. Lucietti, H. Reall, Gravitational instability of an extreme Kerr black hole. *Phys. Rev. D* **86**, 104030 (2012)